State-of-the-art Heat Transfer Fluids for Parabolic Trough Collector

Yathin Krishna[1], M.Faizal[1], R. Saidur[2,3], K.C.Ng[5], Navid Aslfattahi[4]

[1]School of Engineering, Taylor's University, Lakeside campus, 47500 Selangor Malaysia.
[2]Research Centre for Nano-Materials and Energy Technology (RCNMET), School of Science and Technology, Sunway University, No. 5, Jalan University, Bandar Sunway, Petaling Jaya, 47500 Selangor Darul Ehsan, Malaysia.
[3]Department of Engineering, Lancaster University, LA1 4YW, UK.
[4]Department of Mechanical Engineering, Faculty of Engineering, University of Malaya, 50603 Kuala Lumpur, Malaysia.
[5]Department of Mechanical Engineering, Materials and Manufacturing Engineering, The University of Nottingham Malaysia Campus, Jalan Broga, 43500 Semenyih, Selangor Darul Ehsan, Malaysia.

Contents

Abstract

Solar thermal energy conversion is gaining more attention among researchers due to the recent development in nanofluids and molten salt technology. Among various solar collectors, parabolic trough collector has received significant attention from researchers due to their operating temperature range (60-240 °C) feasible for power generation. Parabolic trough collector is currently having a higher number of installations compared to other concentrated solar power technology around the globe. Most of the conventional heat transfer fluid used in PTC has poor heat transfer and light to heat conversion properties. Therefore, it is advantageous to enhance the thermophysical properties of heat transfer fluid to improve the overall efficiency of the system. Well-engineered nano-enhanced heat transfer fluid is advantageous because a very low mass fraction of nanoparticles bring considerable enhancement in thermophysical properties. This paper focuses on the most recent advancement in heat transfer fluids, their preparation, and stability issues when doped with nanoparticles. Various heat transfer fluids currently used in parabolic trough collectors and the nano-enhanced heat transfer fluids having the properties better than conventional heat transfer fluids are compared and their preparation methods and properties are discussed. Enhancement of thermophysical properties of molten salts by doping nanoparticles and their enhancement in thermal stability at high temperature, the possibility of using mono and hybrid nanofluid, ionic liquids, gaseous heat transfer fluid, and vegetable oil as the heat transfer fluid in parabolic trough collectors are the key highlights of this review.

Keywords: Parabolic trough collectors, Heat transfer fluids, Nanofluids, Renewable energy.

Abbreviations	
CNT	Carbon nanotube
CPV	Concentrated photovoltaic
CLFR	Compact Linear Fresnel reflector
CSP	Concentrated Solar Power
DASC	Direct Absorption Solar Collector
DI	Deionized water
DLS	Dynamic light scattering
DNI	Direct normal irradiation
DOE	Department of Energy
DSC	Differential scanning calorimetry
DSG	Direct steam generation
EG	Ethylene glycol
EEW	Electrical explosive wire
EO	Engine oil
FPSC	Flat plate solar collector
GHG	Greenhouse gas
GE	Graphene
GNP	Graphene nanoparticles
GO	Graphene oxide
HCE	Heat collecting Elements
HDH	Humidification and Dehumidification
HTF	Heat transfer fluid
IEA	International Energy Agency
LFR	Linear Fresnel reflector
MSBNF	Molten salt based nanofluid
MWCNT	Multi-wall carbon nanotube
PCM	Phase Change Material
PNC	Plasma nano colloid
PSD	Particle size distribution
PTC	Parabolic trough collectors
PV	Photovoltaic
RGO	Reduced graphene oxide
SEGS	Solar energy generating system
SEM	Scanning electron microscope
STA	Simultaneous thermal analysis
SWCNT	Single wall carbon nanotube
TEM	Transmission electron microscopy
TES	Thermal energy storage
TGA	Thermogravimetric analysis
UV-Vis	Ultra Violet-Visible spectrophotometer

Greek Symbols	
η_{th}	Thermal efficiency
λ	Thermal conductivity, W/mK
μ	Fluid dynamic viscosity, Pa.s
ρ	Density, kg/m^3
φ	Volume fraction of nanoparticles, (%)
ε	Emittance

Nomenclature	
A_{area}	Aperture area, m^2
$A_{r,outer}$	Receiver outer area, m^2
$A_{r,inner}$	Receiver inner area, m^2
c_p	Specific heat capacity, kJ/KgK
$D_{r,in}$	Receiver inner diameter, m
G_{beam}	Solar beam radiation, W/m^2
h	Convective heat transfer coefficient, W/m^{2}K
k	Thermal conductivity, W/mK
Nu	Nusselt number,-
Pr	Prandtl number -
Re	Reynolds number -
Q_{solar}	Total available solar radiation, W
T	Temperature ^{o}C or K

1. Introduction

The energy consumption in 2018 is twice the rate of energy consumption since 2010. Figure 1 shows the annual energy demand growth from 2010 to 2018. Due to increased energy consumption, the CO_2 emission rose to a 33.1G tonne in 2018, which is highest in history, as shown in Figure 2. Therefore, there is a need to scale up renewable energy production to meet the energy demands of the rapidly growing economy of the world. Also, due to changing weather conditions resulting from GHG (greenhouse gas) emissions, there is an increasing demand of power for heating and cooling equipment in many parts of the globe [1]. Using renewable and sustainable energy sources, the impact on the environment can be reversed by reducing emissions caused by GHG and fulfill the demands of energy guzzlers. Therefore, there is a need for energy production in a gigawatt power scale to meet the energy demands. Solar, wind, bio-energy, hydropower is well-established power sources that can meet energy demands if the efficiency of the system further investigated and improved [2]. In one hour, energy from sun radiating on earth is 410×10^{15} J, which is more than the total energy consumed worldwide in 2001[3]. Therefore, solar energy is a promising alternative for current challenges to fulfill energy demands.

There are three distinct technological approaches to utilize solar energy: solar photovoltaic, solar thermal, and solar fuel technologies [4]. Currently, PV (photovoltaic) and solar thermal are the leading technologies to utilize solar energy. PV directly converts solar radiation to electricity [5] but, the efficiency of PV decreases with an increase in temperature, production of power during overcast day is not possible; these are the significant challenges in PV solar cells [6]. The solar thermal system employs mirrors or lenses to focus the sun's radiation on an absorber. HTF (Heat transfer fluid) is made to pass through the absorber tube, which converts water to steam and then the steam is made to run the turbine to generate power. Storage of energy after sundown and low heat transfer efficiency of the HTF are the major challenges faced by solar thermal technologies. Researchers around the world have done reviews on heat transfer fluid for CSP (Concentrated solar power). Recently, Vignarooban et al. [7], Akbarzaheh et al.[8], Bonk et al.[9], and Farhana et al. [10] discussed the current state of the art in HTF applicable for the concentrated solar power system. However, in these reviews, less emphasis has been given on the preparation and stability of heat transfer fluids. The current review presents various HTFs suitable for PTC (Parabolic trough collector), their method of preparation to obtain stable HTF, and stability of this HTF at high temperatures.

The choice of HTF is a crucial parameter for the economic effectiveness of solar thermal technology. Numerous parameters can affect the thermodynamics of PTC. The properties such as specific heat capacity, thermal conductivity, viscosity, density, pressure drop, heat transfer coefficients of HTF, and stability at high temperature are the governing parameters in enhancing the thermal efficiency of PTC. The enhancement of heat transfer efficiency and storage property of HTF is possible to achieve by using advanced heat transfer fluids like molten salts and nanofluids, which significantly adds value to make PTC attain grid parity. However, there are few limitations like agglomeration/flocculation of nanofluids in a short time, the stability of HTF at high temperature, high viscosity due to the addition of nanoparticles, low thermal conductivity, and specific heat capacity. Therefore, the current review can improve our understanding of advanced HTFs currently under research which can optimize the thermal performance of PTC. The main objective of the current review is to (1) investigate the present state-of-the-art HTF used in PTC. The HTFs are selected based on the operating temperature of both medium and high-temperature PTC applications. (2) finding the most important and relevant research done to improve the heat transfer efficiency in PTC. (3) Reporting the investigation of preparation techniques to obtain stable nanofluids and enhance their stability at high temperatures. (4) Presenting the historical trends in terms of HTF used in PTC application. The organization of the article is as follows: followed by the introduction, section 2 emphasize on the thermophysical properties of HTF which influence the energy and exergy efficiency of PTC, section 3 gives the comprehensive review on recent research on the enhancement of thermophysical properties of conventional HTF by advanced preparation methods, by doping nanoparticles, and various stabilization techniques of nano-enhanced HTFs and section 4 briefs on the prospects of PTC, and Section 5 concludes the article with a conclusion and future direction.

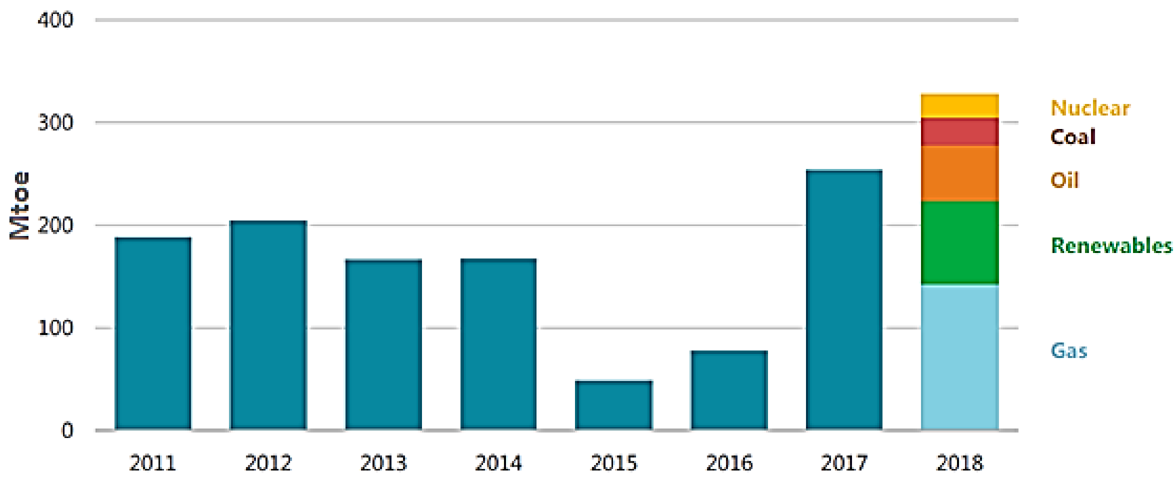

Figure 1: Bar graph shows average global annual energy demand by primary fuel 2011-18[1].

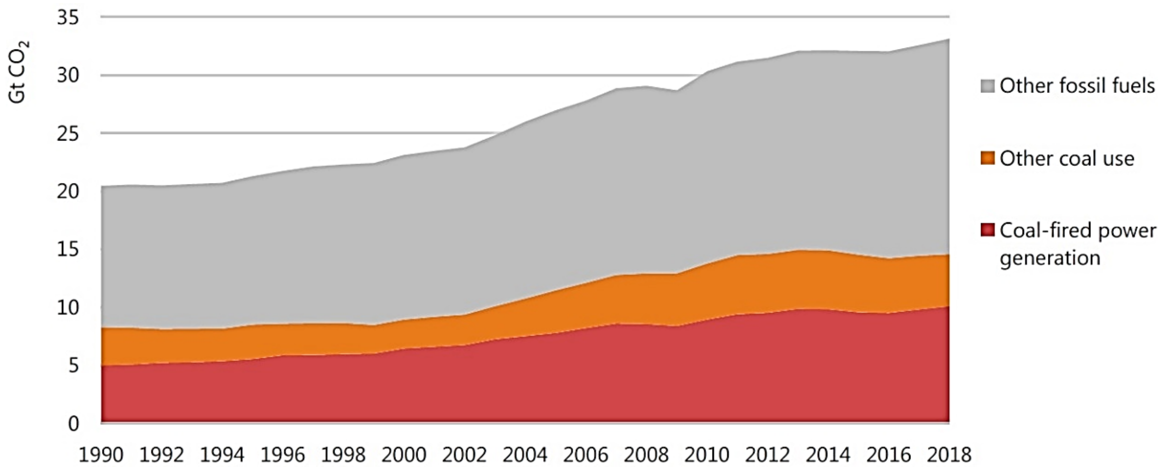

Figure 2: CO_2 emission by fuel source 1990-2018 [1].

2. Concentrating solar power plants

The concentrating solar power technology uses reflective mirrors to concentrate the sun's radiation and produces heat; later, this heat is converted into electricity by running steam turbines. Globally this technology holds promising, particularly in the sunshine region, where abundant sunshine is available (approximately 2,000 kWh/m^2/y or more) [11]. Figure 3 shows the direct sunshine region on the globe suitable for CSP installation. It is the most promising technology, and 10% of the global energy production will be contributed from CSP and CPV (concentrated photovoltaic) by 2050 due to the following reason [11]:

- The bulk installation will bring down the cost (cheaper than solar cell technology)

- Concentrating photovoltaic thermal will increase the efficiency of the combined system.
- Thermal storage can be used to generate electricity even during night time.
- It is suited for sun-belt-region where the intensity of the sun’s radiation is abundant.

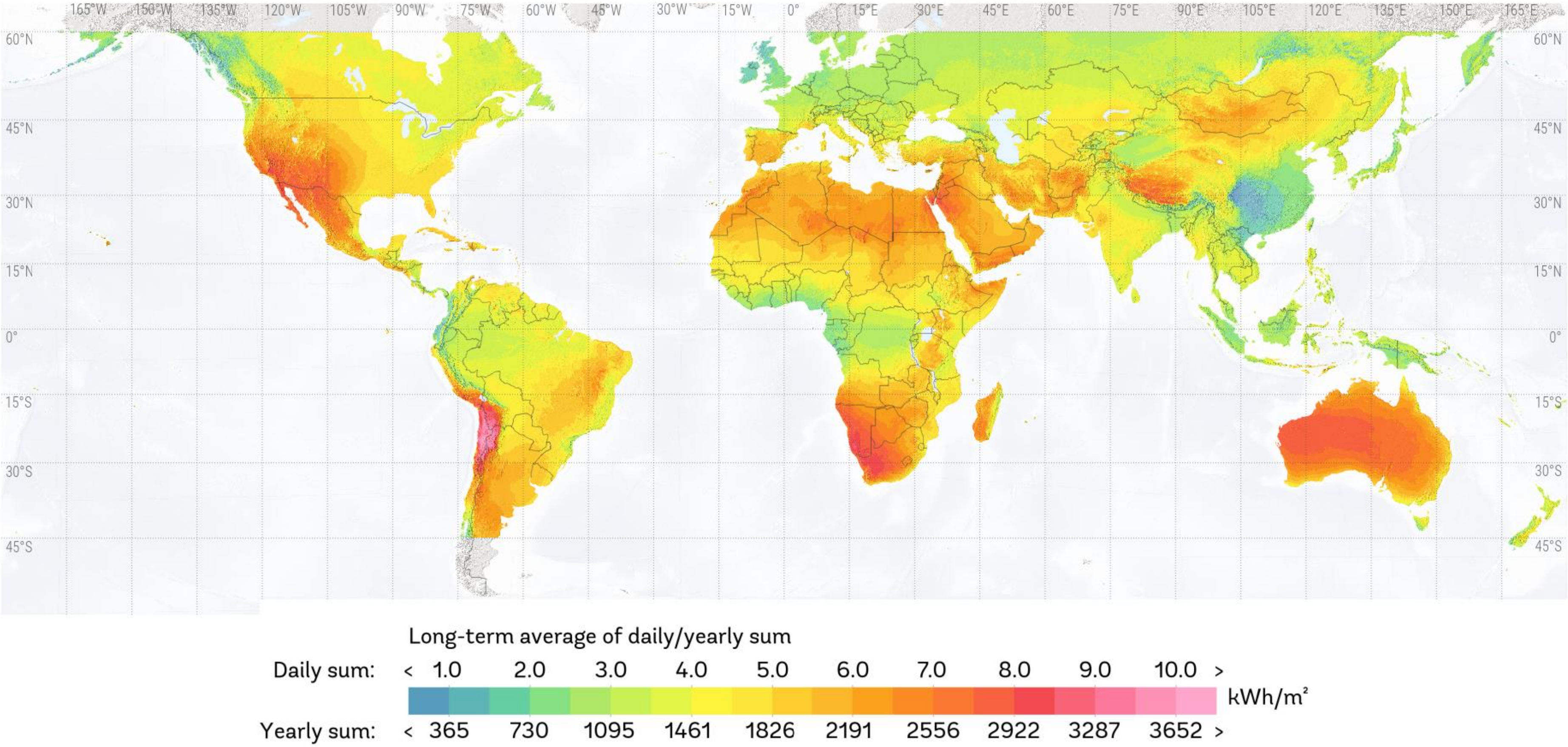

Figure 3: Global direct sunshine region [12]

140

Table **1** shows the probability of production of energy from concentrated solar power technology until 2050, in a different part of the globe depending on the sunlight intensity falling in that region [11]. Table 2 gives the specification of different types of solar thermal technologies, and Table 3 gives a brief history of the progress in CSP technology.

Therefore the potential of CSP is higher in the future, and this technology can also be combined with solar photovoltaic, thermoelectric generators to form a Hybrid concentrated solar photovoltaic thermal system to get higher efficiency [13].

Generally, CSP plants comprise of various components such as solar radiation focusing concentrators and receivers, steam turbines, and electricity generators. Until now, four kinds of CSP power-producing systems are commercialized they are solar parabolic dish collector, Linear Fresnel lenses, Parabolic trough collector, and solar power tower. Figure 4 presents the classification of Concentrated Solar Power (CSP) technologies. In Parabolic dish, the solar collector is a point focusing solar collector where solar radiation is concentrated on a focal point where the receiver is placed. The power conversion using Brayton or Stirling cycle engine is used with an electrical generator. It is possible to obtain a temperature of 700 to 750 °C and the pressure of 2×10^4 kPa with the concentration ratio of 2000 using parabolic dish technology. Linear Fresnel reflector is a line focusing solar collector which uses linear mirror plates for concentrating solar radiation on the absorber tube containing heat transfer fluid. It is possible to attain the operating temperature range of 150 to 400 °C with a concentration ratio of 25 to 170. Whereas, Solar power towers use large mirrors to reflect the sun’s radiation on a tower, placed at the center of the field. Solar power towers can obtain the solar flux of 200 kW/m^2 to 1000kW/m^2 where the sunlight is focused, making it feasible to produce high temperature higher than 1200 °C [14].

Table 1: The probability of production of energy from concentrated solar energy technology until 2050

Group	Country/Region	2020	2030	2040	2050
1	Central Asia, Australia, India (Gujarat, Rajasthan), Chile, Mexico, Middle East, North Africa, South Africa, United States (south-western region), Peru.	5%	12%	30%	40%
2	United States (outside of the south-western region)	3%	6%	13%	20%
3	Turkey and Europe.	3%	6%	10%	15%
4	Argentina, Africa (outside of the northern region),India and Brazil.	1%	5%	8%	15%
5	Worldwide	*	*	*	11%

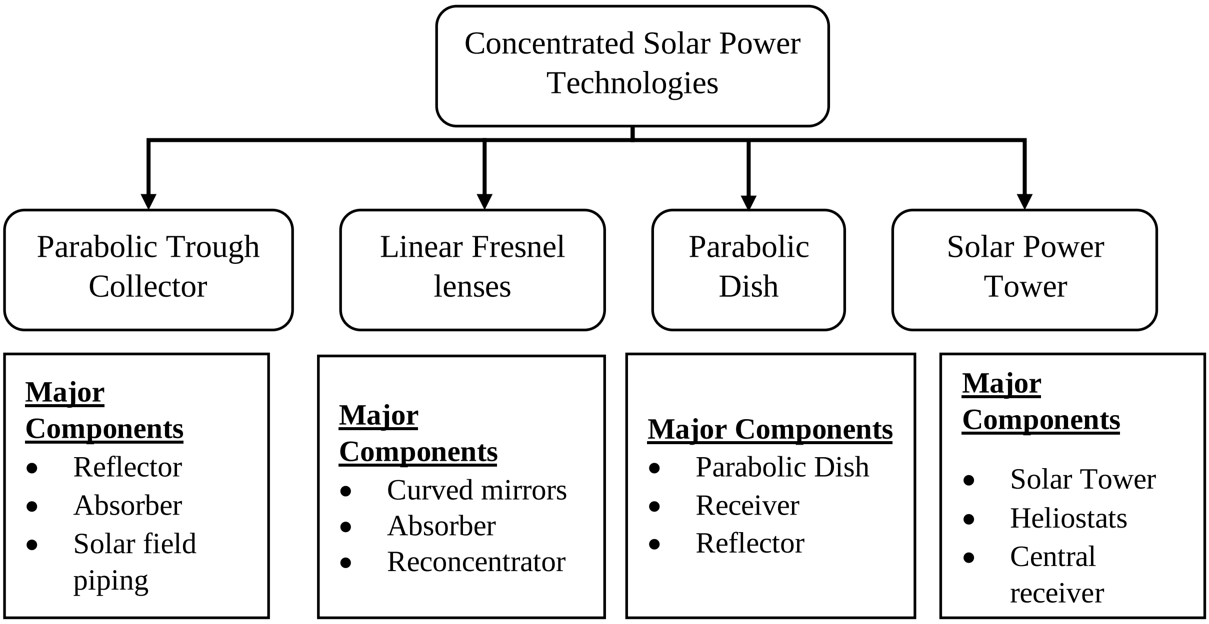

Figure 4: Classification of Concentrated Solar Power technology[14]

Table 2: Specifications of different Solar thermal technologies [15-18]

	Parabolic dish collector	**Linear Fresnel Reflector**	**Parabolic Trough collector**	**Solar Power tower**
Capacity Range (MW)	0.01-1	5-250	10-100	10-100
Operating temperature range (^{0}C)	300-1500	150-400	150-800 (reaches high temperature >700 with gaseous HTF)	300->1200
Solar concentration ratio	<3000	25-170	50-90	600-1000
Solar to electricity conversion efficiency(%)	16-29	8-12	10-16	10-22
Relative cost	Very high	Low	Low	High
Power cycle	Steam Rankine; Sterling Engine; Brayton cycle	Organic Rankine; Steam Rankine;	Steam Rankine	Steam Rankine; Gas turbine Bryton cycle;
Commercial Maturity	Low	Medium	High	Medium
Outlook for improvement	High	Significant	Restricted	Substantial scope for improvement.
Advantages	Suitable for mass production with high efficiency; No need for water cooling	Easy to construct; Compatible with hybrid powerplants running on oil and gas.	Highly durable and reliable; Components are modular; Compatible with hybrid powerplants running on oil and gas.	High efficiency; Compatible with hybrid powerplants running on oil and gas.
Disadvantages	Low commercialization; Lack of TES.	Comparatively Low efficiency; Limited operation temperature range.	Comparatively Low efficiency; Limited operation temperature range; Colling systems are required, and cleaning of the collector is necessary.	High maintenance cost; water is necessary for cooling and cleaning.

Table 3: Past and Present CSP installations in the world

Year	Author/Name	Affiliation	Country	CSP type	Capacity	Energy storage	Remarks
212 BC	Archimedes		Greece	Burning glass[19]	----	----	Archimedes destroyed the Roman fleet from their siege on Syracuse by concentrating the sun’s radiation with the help of a bronze mirror[19].
1866	Auguste Mou Chout		France	Dish type			Invented the first solar-powered steam engine using a concentrated collector[20].
1886	Alessandro Battaglia		Gneo, Italy	Mirrors			Invented a concentrated solar-powered boiler for industrial application[21]
1913	Frank Shumann		Cairo, Egypt	Parabolic			Shumann finished 55HP solar thermal energy station in Maadi[22].
1913	John Ericsson		North America	Parabolic			CSP for irrigation, refrigeration, and locomotion[22].
1929	Dr. RH Goddard	Clark University, USA	USA	Mirror dish			Described as a unique solar steam engine which uses CSP technology [23]
1968	Prof. Giovanni Francia (1911-1980)		Sant'ilarioGenova		1MW[24]		First, the concentrated power plant was designed and implemented [25].
1973	Dr.loannisSakkas		Greece	Metallic mirrors	----	----	Tested Archimedes experiment on the Roman fleet [26].
1981	Solar one power	Department of	Southern	Heliostats	10MW	Molten	Used Heliostats and built at the

	tower	Energy (DOE) led by Sandia National Laboratories in Livermore, California	California,			salt	Mojave Desert, East of Barstow, CA, USA. The first test of large-scale solar thermal power plants [25].
1984	Solar Energy generating system (SEGS)	NextEra Energy Resources	California	Parabolic troughs, along with natural gas to generate electricity.	354MW	Synthetic oil which heats over 400°C.	Largest solar power plant until 2014
1995	Solar two power tower	Department of Energy (DOE) led by Sandia National Laboratories in Livermore, California	Southern California,	Heliostats	10MW	Molten salt	The solar one is converted into solar two projects by adding an extra ring of heliostats totaling 1926 heliostats.
2006	The compact linear Fresnel reflector system	Liddell Power station	Australia	Fresnel reflector	100MW	Water as the Heat transfer fluid	Direct steam generation (DSG) within the solar array has been achieved[27].
2007	Nevada solar one		Eldorado Valley the USA	Parabolic troughs	75MW	Synthetic oil	Has a design efficiency and annual average efficiency of 22.4 and 15.3 %[28]
2009	Kimberlina Solar Thermal Energy	Areva Solar	Bakersfield California	Compact linear Fresnel reflector (CLFR)	5MW	Water	Achieved 750°C superheated steam and is used to run steam turbines [29].

2011	Solar Tree power tower later renamed as a Gemmasolarthermo solar power plant.		Spain	Heliostats	120MW	Molten salt	Attained a temperature of 565°C and had thermal storage [30].
2011	Ivanpah Solar power facility	Bright source Energy, Google, and NRG Energy.	Mojave Desert, Ivanpah Dry Lake, CA	Heliostat, solar tower	392 MW	Molten salt	Till 2014 it was the largest solar thermal power plant. [31]
2014	Dhursar[32]	Reliance Power project,	DhursalJaisalmer district of India	Linear Fresnel Reflector(LFR)	125 MW	Molten salt	___
2018	Kathu Solar Park	A partnership between Building Energy Africa and Old Mutual	Northern Cape South Africa	Fresnel Reflector	81 MW	Molten salt	4.5-hour Molten salt heat storage[33]

2.1. Influence of thermophysical properties of HTF on Parabolic trough efficiency

Thermophysical properties are the essential factor to be considered for the efficient working of solar collectors. In this section thermophysical properties and mathematical modeling of a parabolic trough, the collector is discussed. It is essential to operate the PTC power plant within the proper temperature and pressure limits. Because in water operated parabolic trough power plant, the pressure of approximately 80 bar should be maintained in order to maintain the liquid phase of water at high temperatures. Therminol and Dowtherm synthetic oil can withstand the temperature up to 400 ºC, but the power plant must operate above 12 ºC to avoid crystallization of the synthetic oil. Eutectic Nitrate molten salts (solar salt $NaNO_3$:KNO_3:60:40 wt.%) must operate between 220 ºC and 600 ºC. While liquid metals (Sodium) between 98ºC and 883 ºC. Gaseous HTF (Air, CO_2, S-CO_2, He) has no constrains for temperature and pressure limits; therefore, gaseous HTF is used for very high-temperature applications. Therefore one has to know about the thermophysical properties of HTF before designing the PTC power plant. Table 4 and Table 5 includes the thermophysical properties of HTF for a characteristic temperature range.

2.2. Energy and Exergy Modelling

The fundamental thermodynamics and heat transfer modeling of the PTC is presented in this section. The following equations define the Energy, Exergy efficiencies and thermodynamics of the PTC. PTC utilizes the sun's direct beam radiation (G_{beam}) which is reflected on the receiver by the aperture with area Aarea. The total available radiation (Q_{solar}) in the receiver is calculated by equation (1 [34]:

$$Q_{solar} = A_{area} \cdot G_{beam}, \tag{1}$$

The HTF absorbs a part of this solar energy and increases its temperature from T_{in} to T_{out}. This useful heat energy (Q_{useful}) is expressed in the energy balance equation as follows [35]:

$$Q_{useful} = \dot{m} \cdot c_p \cdot (T_{out} - T_{in}), \tag{2}$$

The collector efficiency is calculated by the ratio of its output, i.e. useful energy gain, to its input, i.e. solar irradiation as indicated in equation (3:

$$\eta_{th} = \frac{Q_{useful}}{Q_{solar}}, \tag{3}$$

Also, by studying the heat transfer phenomenon inside the absorber tube, the useful energy gain can be calculated using equation (4. The equation defines the heat convection from the absorber tube to the HTF.

$$Q_{useful} = h \cdot A_{r,in} \cdot \left(T_{in} - T_{f,av}\right) \tag{4}$$

The heat transfer coefficient h can be calculated using the Nusselt number for the absorber tube flow conditions, the thermal conductivity of HTF ‘k’, and the inner diameter of absorber tube ‘$D_{r,in}$’ as described in equation (5:

$$h = \frac{Nu \cdot k}{D_{r,in}} \tag{5}$$

The Nusselt number has been calculated depending upon the flow conditions inside the absorber tube. For the laminar flow condition (Re<2300), the Nusselt number is assumed to be constant and is equal to 4.36 [36]. If Re> 2300, the flow condition changes to turbulent and for such condition Dittus-Boelter correlation is well suited for determining the value of Nusselt number, which is expressed in equation (6.

$$Nu = 0.023 \cdot Re^{0.8} \cdot Pr^{0.4} \tag{6}$$

For thermal fluids like Liquid sodium, the more accurate value for Nusselt number is obtained by equation (7.

$$Nu = 7 + 0.025 \cdot Re^{0.8} \cdot Pr^{0.8} \tag{7}$$

The Reynolds number (Re) and Prandtl number (Pr) is the function of fluid properties like dynamic viscosity ‘μ’, Specific heat capacity ‘c_p’, thermal conductivity ‘k’ and are expressed in equation (8 and(9 respectively.

$$Re = \frac{4 \cdot \dot{m}}{\pi \cdot D_{r,in} \cdot \mu} \tag{8}$$

$$\mathrm{Pr} = \frac{\mu \cdot c_p}{k} \tag{9}$$

Energy loss analysis is an essential part of thermal analysis. Numerous ways have been used to quantify these losses. The following section presents the equations which determine the exergy losses. The energy absorbed by the receiver is divided into useful energy and losses (Q_{loss}), as shown in equation 10.

$$Q_{solar} \cdot \eta_{optical} = Q_{useful} + Q_{loss,} \tag{10}$$

The calculations of the thermal losses in the receiver are made by understanding the heat transfer phenomenon taking place between the receiver and glass cover, and glass cover with the environment. Equation 11 describes the thermal losses taking place between the receiver and the glass tube. In this equation, radiation loss is considered, and convective losses are neglected because of the vacuum present between the receiver and the glass tube [34].

$$Q_{loss} = \frac{A_{r,outer} \cdot \sigma \cdot (T_r^4 - T_c^4)}{\frac{1}{\varepsilon_c} - \frac{1-\varepsilon_c}{\varepsilon_c} \cdot \left(\frac{A_{r,outer}}{A_{c,inner}}\right)}, \tag{11}$$

Another critical factor is the overall heat transfer coefficient which is presented in equation 12. The exchange of energy between the cover and the ambient takes place in two ways, convection, and radiation. The following equation 13 presents the equation of these losses. In evacuated tubes, since the cover temperature is lower than the receiver temperature, the values closer to ambient temperature is applied.

$$U_L = \frac{Q_{loss}}{A_r \cdot (T_r - T_{amb})} \tag{12}$$

$$Q_{loss} = A_{c,outer} \cdot h_{out} \cdot (T_c - T_{amb}) + A_{c.outer} \cdot \sigma \cdot \varepsilon_c \cdot (T_c^4 - T_{amb}^4), \tag{13}$$

The next critical analysis of PTC is exergy analysis. Exergy analysis or second law analysis is a vital tool to determine the useful energy available after the deduction of losses. The higher the exergetic performance of the system, the lower the irreversibility and leads the system to the ideal condition. For PTC, the exergetic output is the difference between the useful output and the irreversibilities. Equation 14 presents this available energy using the concept of entropy generation [35].

$$\mathrm{E_{useful}} = \mathrm{Q_{useful}} - \mathrm{T_{amb}} \cdot \Delta \mathrm{S_{gen,}} \tag{14}$$

This Equation can also be represented by splitting it into two different losses. The first loss related to the thermal losses to the environment and the second quantity is related to the loss in pressure along the length of the receiver tube. This is an important consideration when gasses like air, He, CO_2 and s-CO_2 is used as HTF because in these particular cases the operating pressure is very high and plays a vital role in exergetic output and is presented in equation 15 [37] :

$$\mathrm{E_{useful}} = \mathrm{Q_{useful}} - \dot{\mathrm{m}} \cdot c_{\mathrm{p}} \cdot \mathrm{T_{amb}} \cdot \ln\left[\frac{\mathrm{T_{out}}}{\mathrm{T_{in}}}\right] - \dot{\mathrm{m}} \cdot \mathrm{T_{amb}} \cdot \frac{\Delta \mathrm{P}}{\rho \cdot \mathrm{T_{fm}}}, \tag{15}$$

This can also be understood by the presence of density term in the denominator of the later part of the equation. The liquids have densities 1000 times greater than gases. Therefore, for liquid cases, equation 15 can be modified into equation 16, and the pressure drop can be calculated using equation 17:

$$\mathrm{E_{useful}} = \mathrm{Q_{useful}} - \dot{\mathrm{m}} \cdot c_{\mathrm{p}} \cdot \mathrm{T_{amb}} \cdot \ln\left[\frac{\mathrm{T_{out}}}{\mathrm{T_{in}}}\right], \tag{16}$$

$$\Delta \mathrm{P} = \mathrm{f_r} \cdot \frac{\mathrm{L}}{\mathrm{D_{r,inner}}} \cdot \left(\frac{1}{2} \cdot \rho \cdot \mathrm{u}^2\right) \tag{17}$$

Where f_r is the friction factor and 'u' is the mass flow rate of the HTF and is given by equations 18 and 19:

$$\mathrm{f_r} = \frac{1}{[0.79 \cdot \ln(\mathrm{Re}) - 1.64]^2}, \tag{18}$$

$$\mathrm{u} = \frac{\dot{\mathrm{m}}}{\rho \cdot \left(\pi \cdot \frac{\mathrm{D_{r,inner}^2}}{4}\right)}, \tag{19}$$

The exergetic performance of the collector is obtained by the exergetic analysis of the solar irradiation. Equation 20 shows the exergetic analysis of solar radiation [38]. The temperature of the sun is assumed as 5770 K for this equation [39].

$$E_{solar} = Q_{solar} \cdot \left[1 - \frac{4}{3} \cdot \left(\frac{T_{amb}}{T_{sun}}\right) + \frac{1}{3} \cdot \left(\frac{T_{amb}}{T_{sun}}\right)^4\right], \tag{20}$$

The exergetic efficiency of the solar collector is presented in equation 21. It is the ratio of exergetic output of the collector to the solar exergy input.

$$\eta_{exergy} = \frac{E_{useful}}{E_{solar}}, \tag{21}$$

2.3. Thermophysical properties required for HTF in PTC

The heat transfer fluid should be classified/characterized based on the thermophysical properties in the working condition of PTC. The thermophysical properties of the HTF are the basis for the characterization of HTF in the working range of the PTC. The significant thermophysical properties required for HTF in PTC are the following: specific heat capacity, enthalpy of phase change, thermal conductivity, viscosity, and melting point. However, the thermophysical properties like density, degradation temperature, thermal expansion coefficient, and thermal stability are necessary while selecting the HTF, designing the operating condition of the PTC plant and TES (thermal energy storage) system. Each thermophysical properties can be either obtained in the literature or can be determined experimentally by various measuring techniques. However, one must evaluate whether the given properties are in the working range of PTC.

Specific heat capacity (c_p) is an important property that decides the suitability of HTF to be used as heat transfer or TES material. Specific heat capacity is the factor that controls the rise in temperature that can be transferred or stored. Enhancing the specific heat capacity increases the thermodynamic cycle efficiency as represented in equation (2) and equation (3). Loading heat transfer fluids with nanoparticles has both pros and cons concerning specific heat capacity. However, doping nanoparticles to base fluids like water, ethylene glycol, and ionic liquids have detrimental results, but, molten salts show positive results. Figure 5 represents the effect on the specific heat capacity of based fluids by doping nanoparticles [40].

Another important property of heat transfer fluid is its melting or freezing point temperature. The melting point is directly related to the operational cost of the power plant because the solar field has to be maintained above the freezing point even after sundown [41]. Differential scanning calorimeter is also used for measuring the melting/freezing temperature of the HTF. The DSC is also used for measuring the enthalpy of fusion or latent heat of fusion if the heat transfer fluid is a PCM using constant heating or cooling rate under the International Energy Agency (IEA) SHC/ECES T42A29 [42]. The T-history technique is yet another technique developed in 1999 to measure the enthalpy of phase changing HTFs [43].

The thermodynamic cycle efficiency of the power plant depends on the operating temperature. It is evident from equation (2) and equation (3), that with the increase in operating temperature the plant efficiency increases. Therefore, the degradation temperature of HTF plays a key role in deciding the efficiency of the plant. The degradation temperature refers to the temperature at which 3% of the initial sample weight is lost when heated [44]. Thermogravimetric analysis (TGA) is used to obtain the thermogram of weight/mass loss as a function of temperature. Thermogravimetric analysis can also be used to understand the thermal behavior of the HTF under different atmospheric conditions like air, oxygen, argon or nitrogen [45].

The thermal conductivity of the HTF is an important thermophysical property that influences the Nusselt number. The steady-state method is the commonly used method used for measuring thermal conductivity (k) [46]. Thermal conductivity can be indirectly measured using the laser-flash technique using equation (22):

$$k = a \cdot \rho \cdot c_{\mathrm{p}} \tag{22}$$

Where k is thermal conductivity, a is thermal diffusivity obtained for LFA and c_{p} is specific heat capacity[45].

Thermal conductivity and density of HTF are very sensitive to temperature. Therefore, it is recommended to measure these parameters in the working temperature range. Density is commonly measured using pycnometers, hydrometers, hydrostatic balances and density meters [47].

The pumping efficiency of the plant depends on the dynamic viscosity of the HTF. A dynamic sheer rheometer is used to measure the viscosity and shear rates of the HTF. The value of viscosity is calculated from the rheological parameters like shear stress, shear rate, deflection angle, torque, speed, and deformation. Another property required for the characterization of HTF is vapor pressure. Usually, in PTCs, low vapor pressure is suitable because it shows the evaporation rate of the liquid. The vapor pressure is calculated using empirical methods like the Antoine equation or Clausius-Clapeyron equation [48]. Also, TGA [49] and Knudsen cell technique [50] is available for the vapor pressure measurement of HTF.

The thermal expansion coefficient is yet another thermophysical property required for the characterization of HTF. The thermal expansion is more predominant in molten salt operated PTC power plants when compared to liquid phase HTF operated power plants. Peng et al. investigated the thermal expansion coefficient of various molten salts using thermal expansion apparatus [47]. It is essential to study the phenomenon of thermal expansion while designing the PTC because of the possibility of damaging the system especially evacuated absorber tubes and field piping. Table 4 presents the thermophysical properties of various HTF suitable for heat transfer applications in PTC.

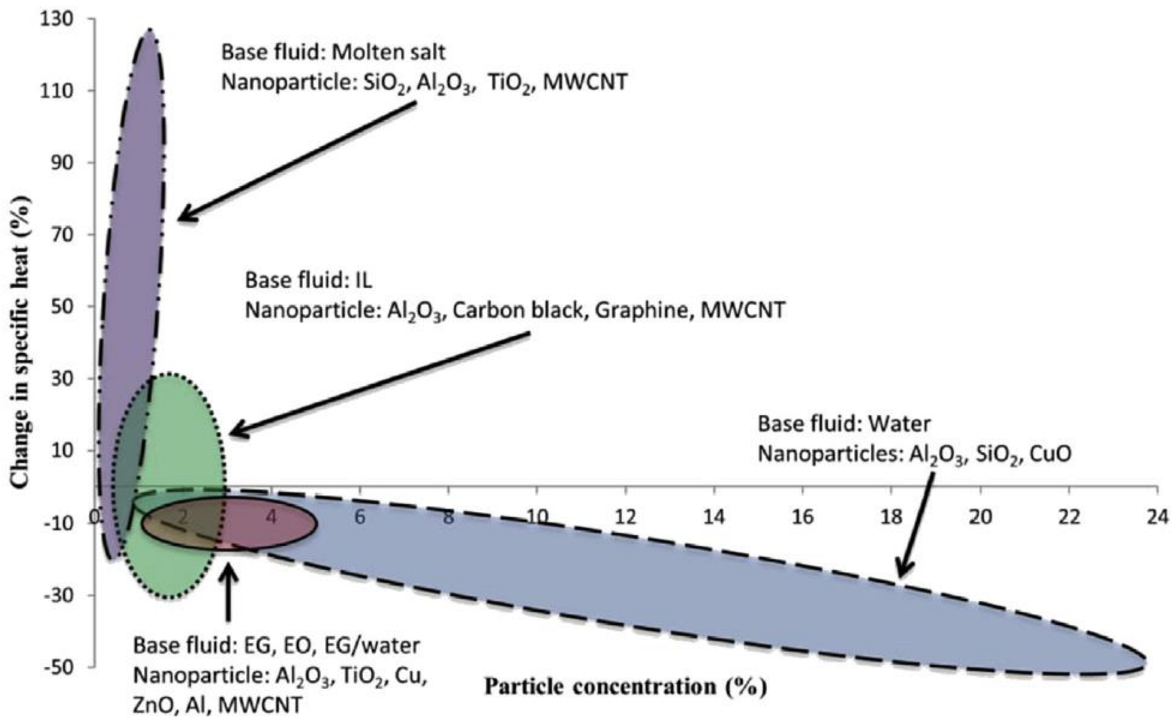

Figure 5: Overview of % change in specific heat capacity by adding nanoparticles to base fluids [40].

3. Recent developments in heat transfer enhancement

Enhancement of thermophysical properties like specific heat, thermal conductivity, stability, corrosion, and viscosity are the study areas that gained much attention by researchers in the past decade. Nanomaterials are the specially engineered materials whose size will vary in nanometers in any one dimension. Due to the superior thermophysical properties of nanoparticles, research communities have shown interest in the field of nanotechnology. Furthermore, the Stability of nanoparticles is also a significant issue to be considered while investigating the properties of nanofluids. Adding nanoscale solid particles to the HTF has proved to be a promising technique to improve its thermophysical properties. This section covers the summary of the recent advancement in the state-of-the-art HTF used in parabolic trough systems. Furthermore, heat transfer fluid with the properties suitable for use in the parabolic trough is also discussed. Figure 6 shows the classification of HTF for the PTC application.

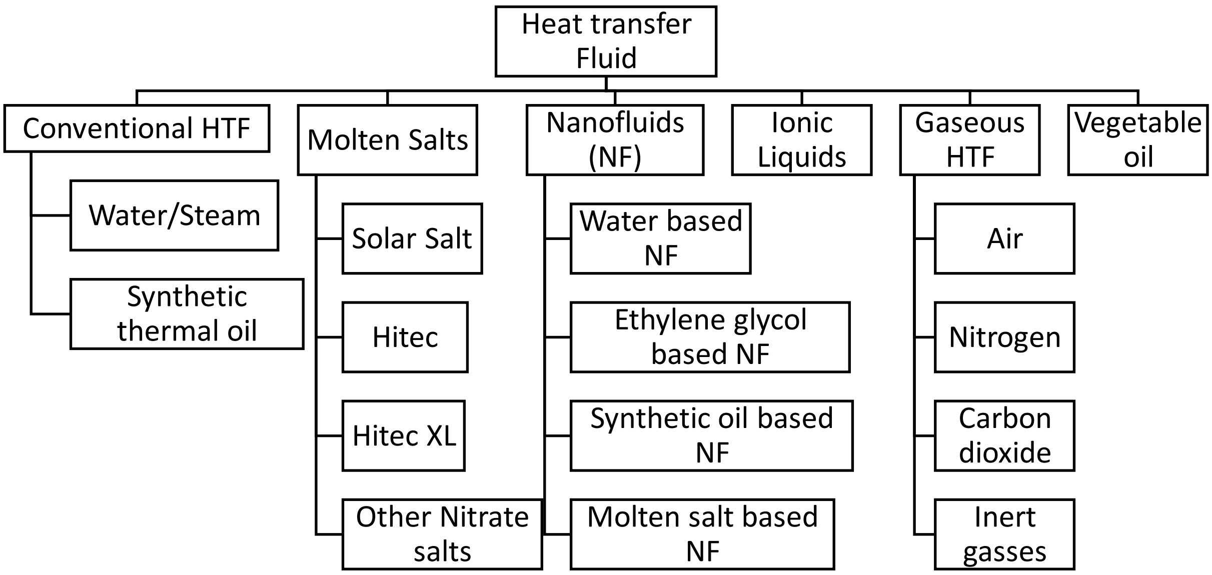

Figure 6: Classification of HTF for PTC system

Table 4: Thermophysical properties of HTF suitable for application in PTC.

Base fluid	Nanoparticles	concentration	Enthalpy (kJ/kg)	Enhancement %	Specific heat (kJ/kgK)		Enhancement %		Thermal conductivity (W/mK)		Enhancement %	Viscosity Pa·s	Decrease in Melting point (℃)	Type of Study	Ref.
					Solid	Liquid	Solid	Liquid	Solid	Liquid					
KNO_3	SiO_2	1 wt.%	102.46	12%	1.224	1.203	9.5	6.1	-	-	-	-	3	Experimental	
	Al_2O_3	1 wt.%	92.10	0.5%	1.068	1.043	-4.5	-7.8	-	-	-	-	3		[51]
	SiO_2- Al_2O_3	1 wt.%	82.90	-9.5%	1.171	1.095	4.7	-3.4	-	-	-	-	3		
$Li_2CO_3:K_2CO_3$	SiO_2	1 wt.%	-	-	-	1.365	-	10		0.677	37	-	-	Experimental	[52]
$Ca(NO_3)_2:NaNO_3:KNO_3$	-	32:24:44 wt.%	67	-	1.7	1.2	-	-	1-3		-	~0@200 ℃	-	Experimental	[53]
Thermal oil (THO)	MWCBT	0.1 – 1 wt. %	-	-	-	-	-	-	0.13-0.165 @ 60℃*		~25% @ 60℃	0.02 @90 ℃	-	Experimental	[54]
Diathermic oil	TiO_2	1 vol%	-	-	-	-	-	-	0.136 @ 50 ℃*		7 % @ 50 ℃	-	-	Experimental	[55]
Water	GNP–Pt	0.1 wt.%			-	3.849	-	-6.26	~0.74*		17.77 @ 40 ℃	0.0011	-	Experimental	[56]
Thermal oil	Al2O3-MWCNT	0.125-0.15 wt.%	-	-	-	-	-	-	0.177*		~10%	0.12@ 50 ℃	-	Experimental	[57]
Solar Salt	SiO_2	0.5-1.5 wt.%	-	-	1.342 to 1.843	1.329 to 1.661	-16.4 to 14.9	-19.3 to 0.8	-		-	-	-	Experimental	[58]
	Al_2O_3	0.5-1.5 wt.%	-	-	1.526 to 1.923	1.522 to 1.745	-4.8 to 19,9	-7.6 to 5.9	-		-	-	-		
	TiO_2	0.5-1.5 wt.%	-	-	1.372 to 1.508	1.390 to 1.544	-14.4 to -6	-15.6 to -6.3	-		-	-	-		
	SiO_2-TiO_2	0.5-1.5 wt.%	-	-	1.572 to 2.162	1.525 to 1.018	-2 to 57.7	-7.5 to 22.5	-		-	-	-		
$Li_2CO_3:K_2CO_3$	SiO_2	-	-	-	-	2.05	-	27	-		-	-	-	Experimental	[58]
	Al_2O_3	-	-	-	-	2.16	-	33	-		-	-	-		
	MgO	-	-	-	-	1.97	-	22	-		-	-	-		

* Data is not available for liquid and solid phase separately.

3.1. Water/steam as heat transfer fluid

Water is utilized as the conventional thermal fluid in the solar thermal system because of its appreciable heat capacity of 4.185 J/Kg K and due to the application of solar thermal is limited to domestic and industrial heating whose temperature ranges from 70-250 ºC. Silva et al. [59], and Coccia et al. [60], utilized demineralized water for temperature up to 85 ºC using PTC with rim angle 90º and concentration ratio 9.25. The results were compared with literature values, and the slope of the linear thermal efficiency equation related to thermal losses is found to be -0.683 indicating the quality of receiver build. Silva et al. investigated the use of PTC to generate steam for food processing applications [59]. In the study, PTC is used to produce steam for canning and thermal treatment of vegetables. The possibility of generating saturated steam with PTC for food processing industry utilizing an unfired boiler was investigated. The parameters like the outlet temperature of the solar field and temperature of generated steam are studied. Figure 7 represents the utilization of PTC in food processing applications. The results showed that by using PTC's significant demand for steam, production could be fulfilled with the small solar field, conserving land area, and reaching the annual steam demand of the food processing industry.

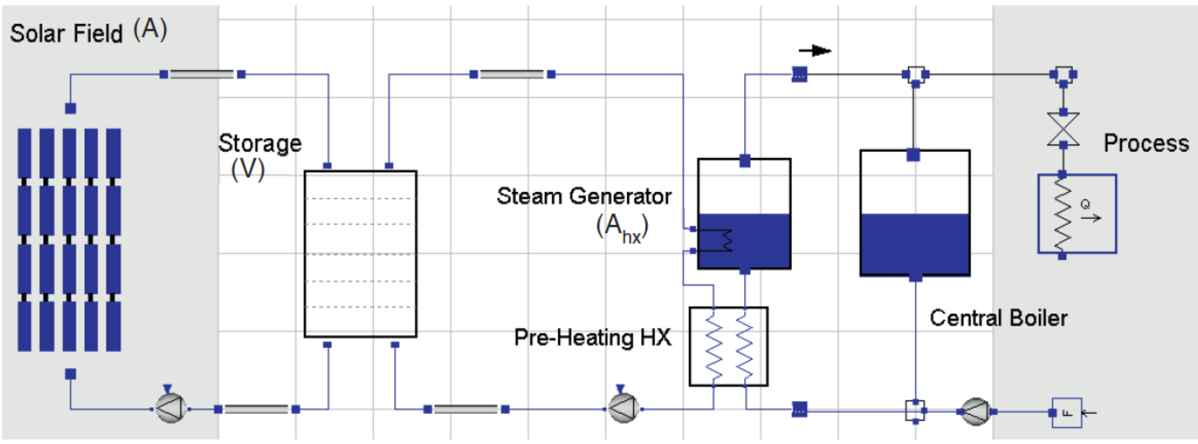

Figure 7: Application of PTC in Industrial process [59]

The Direct Steam Generation (DSG) has many advantages with few limitations. Besides higher temperatures at solar field outlets and simplified plant layout, the use of water during the change in phase permits a more significant reduction in mean temperature at which heat is transferred to the water. Required heat is absorbed during phase change at a lower temperature instead of higher temperature value, improving thermal efficiency, compared to sensible heat transfer taking place in thermal oils and molten salt. Also, water is environmentally friendly, leakage of water in the solar field does not lead to environmental hazards [61]. Also, the freezing point of water is lower than that of thermal oil and molten salts; the energy required to maintain water in the liquid state is reduced. Moreover, water is less corrosive compared to molten salts [62]. The advantage of using the direct steam generating system using water/steam heat transfer is to avoid heat exchanger and its losses. We do note; however, PTC produces high output temperature, to avoid boiling of water and the rapid increment in water pressure with an increase in temperature requires design modification of the system. Also, yet other disadvantages of water/steam heat transfer system are the scaling of the absorber tube, even with the excellent feed water treatment, which is unavoidable. The scaling phenomenon, in multiple row collector arrays, may cause a loss in flow in the affected pipes, which may lead to tube dry-out, damaging the selective receiver coating. Water/steam parabolic trough system also provides difficulties in thermal energy storage. Also, the phase transition temperature is low, and superheaters are required to increase the temperature of the steam to expand the steam in steam turbines to produce power. We argue that using water as HTF, limits the application to process heat generation and low-temperature application even though the PTC capable of producing high temperature in the range of 450 to 500 ºC. As discussed by Coccia et al. [60], collectors with a higher concentration ratio can produce higher heat flux in PTC for power generation. Therefore, HTF with a higher operating temperature range is preferable for power generating applications. Synthetic oils have the operating range up to 400 ºC, which are commonly used in power plant applications, which is discussed in the next section.

3.2. Synthetic thermal oil as heat transfer fluid

CSP power plants primarily started utilizing synthetic oil as HTF for avoiding high-pressure requirements and phase change at high temperature (>400 ºC). Synthetic oil is mostly known under the brand names of Therminol VP-1, or Dowtherm A. The stability of Therminol VP-1 is in the range of 12-400 ºC. When synthetic thermal oil is heated above the operating range, the hydrocarbon decomposes quickly, producing hydrogen gas. Degradation leads to makeup oil requirements, which reduces the lifetime of the oil. The by-products formed by overheating of the oil lead to the formation of the sludge, reducing thermal efficiency and increasing maintenance cost of the plant [63].

Selvakumar et al. estimated the performance of PTC using Therminol D-12 as HTF coupled with secondary HTF as water for quick heating [64]. The performance was analyzed for 100 cycles. The system produced 40 ºC and 68 ºC hot water at 240W/m^2 and 540W/m^2 of solar radiation, respectively. Use of Therminol D-12 along the evacuated tubes increase the efficiency by 30% in instant hot water generation using PTC.

The solidification temperature of Therminol VP-1 is 12 ºC, and it boils at 257 ºC and the thermal degradation temperature is 400 ºC. By understanding the operating temperature of Therminol VP-1, here we discuss to what extent synthetic oil can be used as HTF in PTC. The highest operating temperature attained by parabolic trough collectors is between 350 to 500 ºC. The maximum temperature attained by power plants also depends on the number of collectors used in the plant. The efficiency of the power plant depends on the maximum temperature attained by the power plant. By all these factors considered, Therminol VP-1 can be used as HTF in PTC up to 400 ºC. However, if the plant operating temperature surpasses 400 ºC oxidation of the synthetic oil takes place. The issue with the degradation of synthetic oil for the high-temperature application can be overcome by using high-temperature HTF. The suitable solution for high-temperature HTF is molten salt. The forthcoming section discusses the suitability of using molten salt in PTC applications.

3.3. Molten Salts as heat transfer fluid

In the nineteenth century, the separation of alkali metal from their fused hydroxide salt was conducted by Humphery Davy [65]. Therefore, molten salt technology dates back to a very long time in history. In the 1950s, the use of molten salts in nuclear reactors emerged. Oak Ridge National Laboratory (ONRL) pioneered the first molten salt nuclear reactor, which utilized thorium as nuclear fuel [66]. More recently, due to the arising challenges in renewable energy and environment protection, molten salts have been used for CSP plants for heat transfer and heat storage applications [67]. Figure 8 shows other applications of molten salts. Molten salts used for solar thermal applications are primarily nitrate salts, which has the potential to be used in thermal storage and heat transfer applications because of their exuberant chemical characteristics. Molten salts show several desirable properties at an elevated temperature like high density, promising specific heat, excellent stability at elavated temperature, and lower vapor pressure. Compared to synthetic oil, Molten salts are cheaper and have a low impact on the environment because they are non-polluting, non-flammable, abundantly available, and favorable for cost savings because of their ability to reduce the size of the thermal storage tank due to their high specific heat capacity. The main drawback of molten salt is its high melting point, which requires pre-heating and maintaining the liquidus temperature during the night and cloudy days. The energy required to maintain this liquidus temperature leads to high operating and maintaining costs. The composition of the Molten salt determines its characteristics.

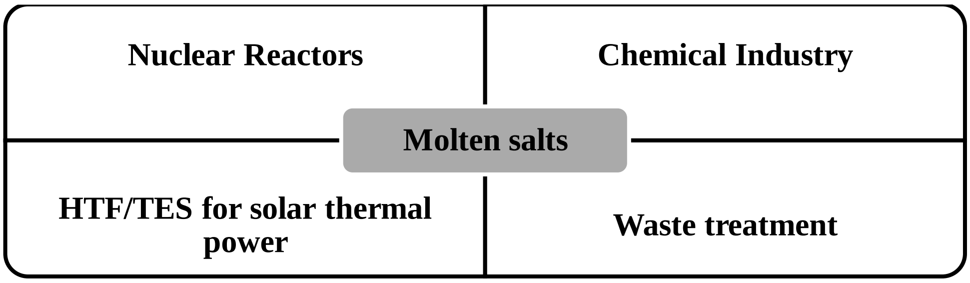

Figure 8: Applications of Molten Salts [68]

The molten salt with 60wt% of Sodium Nitrate ($NaNO_3$) and 40wt% of Potassium Nitrate (KNO_3) is called Solar salt, which is the most common salt used as HTF in CSP plants. Wang et al. conducted 3-D simulation using the FVM model, with solar salt ($NaNO_3$:KNO_3,60:40wt%) as HTF in PTC and concluded by stating that, the cross-sectional temperature increases with an increase in inlet velocity and direct normal irradiation [69]. Moreover, the thermal efficiency of oil at 573.15 is more than molten salt at 773K by 0.079 was the key finding of the research. To reduce the cost of HTF, the synthetic thermal oil is retained as HTF but replaced with molten salt as a thermal energy storage material; typically, solar salt is used for this purpose. Solar salt is made as to the standard storage medium, and many research articles take solar salts as reference material in TES and heat transfer applications [70]. The operating range of solar salt is between 222°C to 600 °C [71]. Potassium nitrate and sodium nitrate which has the melting point of 334 °C and 208 °C respectively, the mixture of both the salts reduces the melting point of the eutectic by 100 °C, compared to the pure components (Figure 9). This makes it feasible to use it in CSP plants. The properties of Solar salt estimated by correlation formulated by Bauer et al., Carling et al., Gustafsson et al., Jriri et al., and Takahashi et al. are listed in Table 5 and Figure 10 [70, 72]. The dynamic viscosity of the molten salt should be less than 0.005 Pa·s for application in PTC, because of the pumping power consumption, which goes higher with the increase in viscosity. The viscosity of molten salt synthesized by Coscia et al. [73] obtained a viscosity value of 0.06 Pa·s at 200 ºC and the viscosity reduced to 0.001 Pa·s at 550 ºC. (Chen, M. et al., [53, 74] obtained the viscosity of the molten salt close to the viscosity of water at a temperature higher than 300 °C. From the results obtained by various researchers by combining $Ca(NO3)_2$ with solar salt, the viscosity of the eutectic composite molten salt reduces significantly.

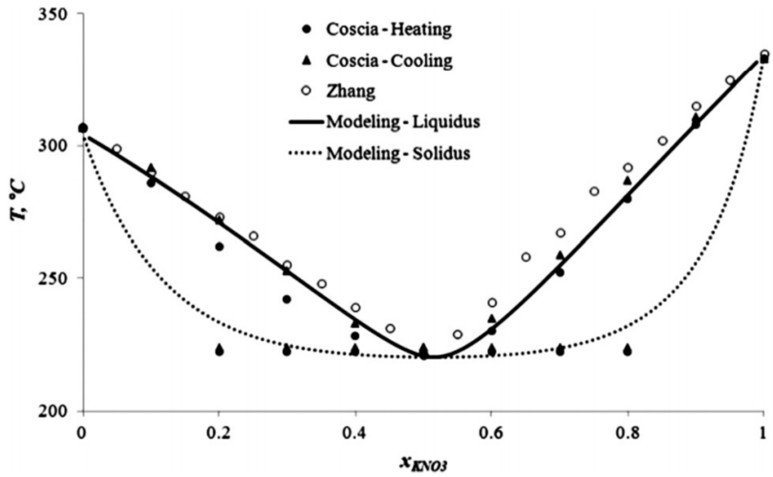

Figure 9: Phase diagram of KNO_3: $NaNO_3$[73]

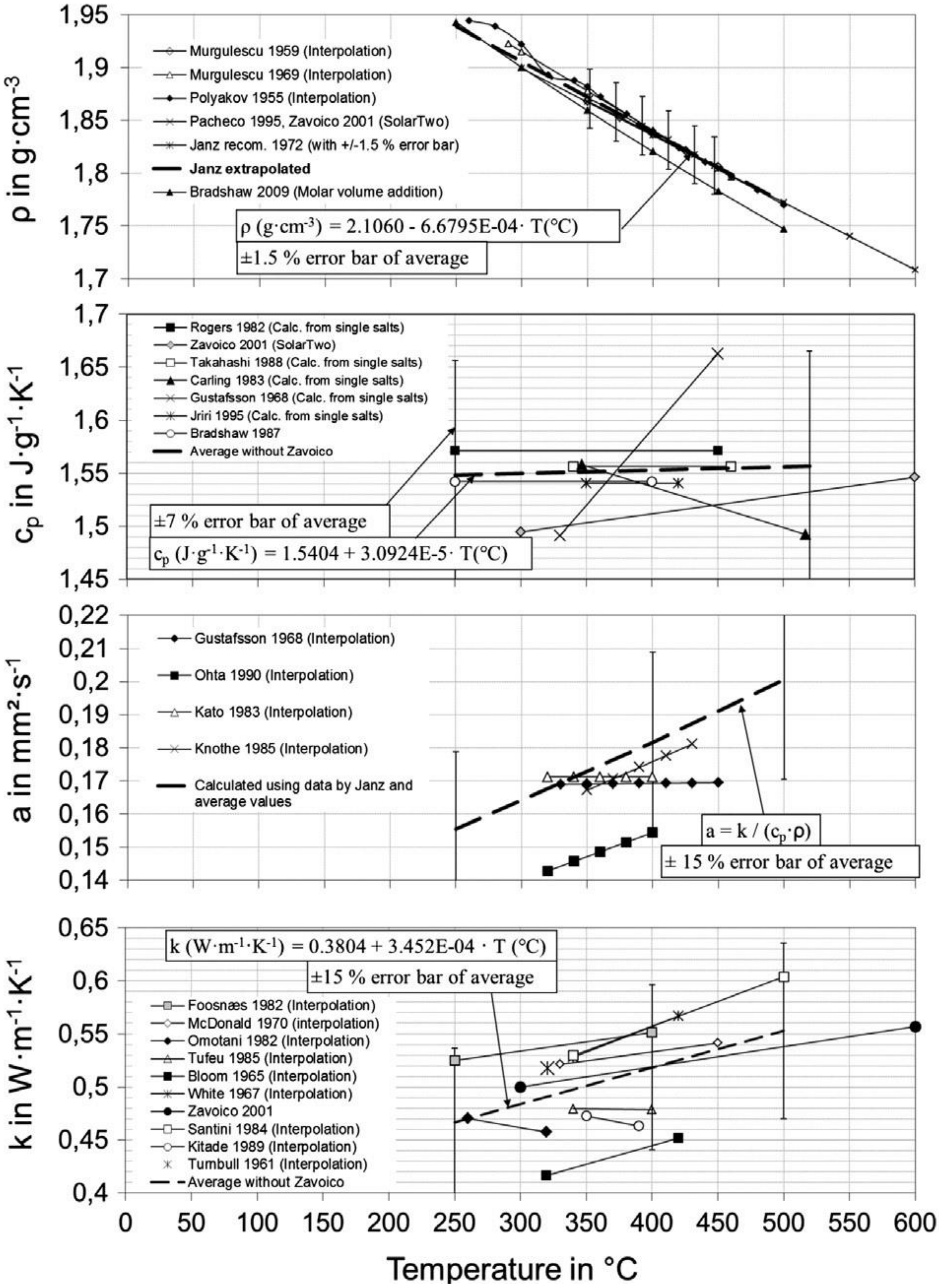

Figure 10: Thermophysical properties of solar salt-dependent on temperature [70]. Reprinted with permission from Elsevier Books, Molten Salts Chemistry, Thomas Bauer, Lic.No. 4676481124638.

Hitec molten salt is a ternary eutectic mixture of KNO_3:$NaNO_2$: $NaNO_3$ with mass fraction 53%,40%, and 7% respectively. The stability of Hitec is in the temperature range of 142-535°C. The properties of Hitec can be calculated using the correlation presented in Table 5. Extensive research has been carried out on fluid flow properties and heat transfer characteristics of HITEC molten salt flow. Xiao et al., investigated on heat transfer and flow parameters using HITEC (53% KNO_3 – 40% $NaNO_2$ – 7% $NaNO_3$, mol.%) in the helical heat exchanger, where HITEC is used as the hot side HTF and DI water at the cold side [75]. Their findings demonstrated that frictional pressure drop in laminar and turbulent flow regimes agreed within 15% with that of past literature. Figure 11 shows the thermophysical properties of HITEC salt. By the analysis of the graph, HITEC salt is highly viscous at low-temperature range (150ºC -300ºC), which results in a higher Prandtl number (Pr>7). Higher Prandtl number results in a velocity boundary layer being much more significant than the thermal boundary layer, enhancing the heat transfer process in the absorber tube. As the temperature increase (300ºC -500ºC), the viscosity reduces drastically. Therefore, HITEC can be considered a suitable HTF for PTC, which has a similar working temperature range of PTC.

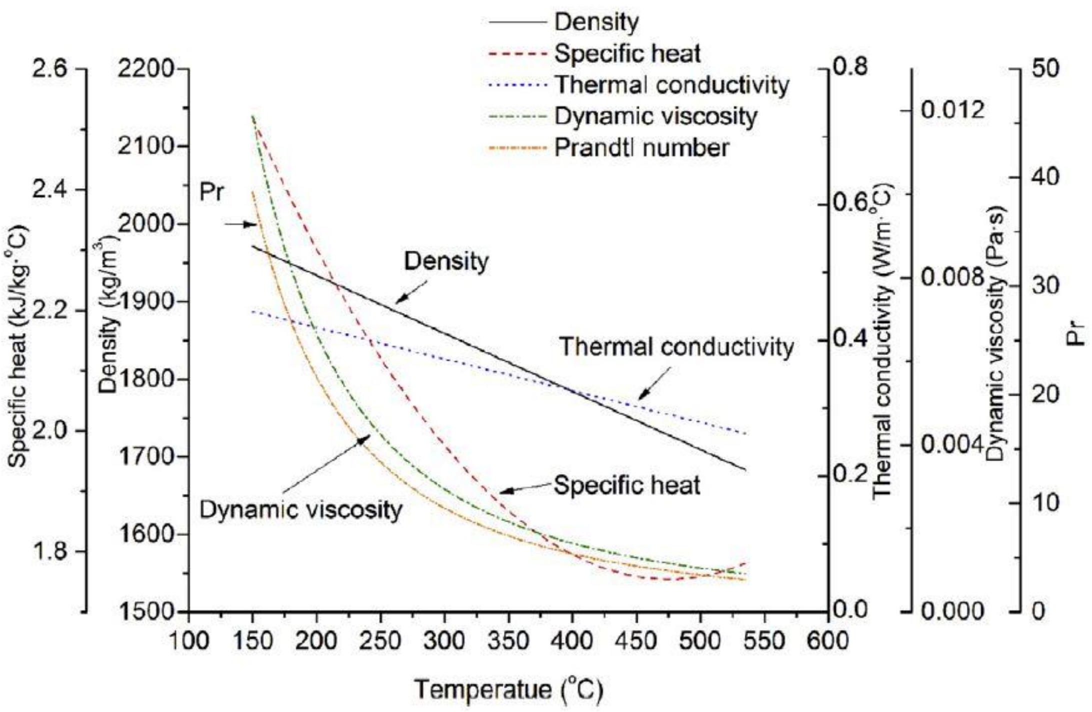

Figure 11: Thermophysical properties of Hitec Molten salt (KNO_3:$NaNO_3$: $NaNO_2$, 53:7:40 mol.%) [75]. Reprinted with permission from Elsevier, Applied Thermal Engineering, Investigations on heat transfer characteristic of molten salt flow in the helical annular duct, Peng Xiao, Lic.No. 460589142713.

Hitec XL is a ternary eutectic mixture of $Ca(NO_3)_2$, KNO_3, $NaNO_3$ with a mass fraction of 42 %, 43%, and 15% respectively. It is clear from the components of the eutectic mixture that by the addition of $Ca(NO_3)_2$ to solar salt forms Hitec XL molten salt. Fernandez et al. studied the thermal and physical properties by adding $Ca(NO_3)_2$ and LiNO3 to solar salt and observed that by adding calcium nitrate to solar salt, the mixture reduced the freezing temperature and economic cost of the power plant [76]. These mixtures were designed to replace synthetic oil as HTF in the PTC system by reducing economic cost and by improving thermal storage capacity. Chen et al., experimentally verified and predicted 3D stable molten temperature diagram for 42% KNO_3-17% $NaNO_3$-41% $Ca(NO_3)_2$ [74]. The predicted melting temperature of 129.1 °C and decomposition temperature of 597.9 °C were in an excellent match with the prediction. Chen and Zhao investigated a unique composition of Hitec XL ($Ca(NO_3)_2$-$NaNO_3$-KNO_3, 32:24:44 wt%) and found that the composition had the best performance by reduced melting point to 80 °C having 1.7J/g °C and 1.2 J/g °C of specific heat for solid and liquid phase respectively [53]. Figure 12a shows the rise in heat capacity in the range of 50-68 °C and the curve becomes stable irrespective of temperature rise and Figure 12b. The specific heat capacity of liquid salt increases with the rise in temperature, indicating its sensitivity to variation in temperature. The viscosity is found to be near to zero at 200 °C, and the thermal conductivity of the composition is about 1-3 W/mK. The thermophysical properties of Hitec XL are calculated using the correlation presented in Table 4. Therefore, Hitec XL can be used as both HTF and TES material for line focusing collectors due to its high stability, significant heat of fusion, and economic price.

Olivares et al. [76] and Fernandez et al. [76] investigated the thermal stability of the ternary nitrate mixture. In this composite $LiNO_3$ salt is combined with solar salt composite to enhance the thermal stability of the eutectic composite. From the analysis, the working temperature range is obtained in the range of 130-600 °C by the addition of $LiNO_3$. The viscosity of this eutectic mixture is found to be 0.03 Pa·s at 300 °C making it a candidate salt for PTC application. The only disadvantage of this composite is the high cost of $LiNO_3$ ($4.32/kg) [7].

Zhao and Wu investigated 50-80 wt.% of KNO_3, 0-25 wt.% of $LiNO_3$ and 10-45 wt.% of $Ca(NO_3)_2$ to obtain a eutectic mixture which will serve both as HTF and TES material [77]. The experimental results showed better thermophysical properties like melting point (<100 °C), viscosity (< 0.003 Pa·s at 190 °C), and high-temperature stability (>500 °C) is obtained in this range of a mass fraction of KNO_3, $LiNO_3$, and $Ca(NO_3)_2$. Due to their low melting point, which is less than the melting point of Hitec XL (120 ºC), and high-temperature stability, which is higher than the conventional organic HTF [78], KNO_3:$LiNO_3$:$Ca(NO_3)_2$ will lead to higher Rankine Cycle efficiency. Therefore, these special eutectic salts make them more suitable for HTF and TES replacing synthetic oils in PTC plants.

Wang et al. investigated quaternary eutectic salts of alkali-nitrites and nitrates to explore their possibility of usage as thermal fluids in the CSP system [79]. They found that the freezing point of the composite eutectic combination was estimated to be <100 ºC by differential scanning calorimeter measurements, as shown in Figure 13. The stability of the molten salt is found to be 430 ºC, which is lower than Hitec XL, Hitec, and solar salt. However, it is observed that the specific heat capacity of the salt is greater than the specific heat capacity of Hitec and solar salt. The economic evaluation of the salt-containing $LiNO_3$, as available HTF and TES material for solar power plants, limits its usage in commercial power plants.

Bradshaw and Brosseau developed a unique molten salt at the Sandia National Laboratory known by the name "Sandia Mix." This eutectic mixture is a quaternary molten salt with mass ratio $NaNO_3$ (9–18%)–KNO_3 (40–52%)–$LiNO_3$ (13–21%)–$Ca(NO_3)_2$(20–27%) [80]. In the study, three different mass ratios (QA, QB, QC) have been studied, and each ratio had a melting point below 100 ºC and thermal stability greater than 500 ºC. The viscosity of the composite mixture is found to be 0.003 Pa·s, which is suitable for PTC applications. The main drawback of Sandia Mix for a commercial application is due to the economic limitations of $LiNO_3$. However, by large scale production of the $LiNO_3$ salt by the conversion of $LiCO_3$ using HNO_3, the cost of production can be minimized [80, 81].

Justin et al. developed a eutectic salt with KNO_3 (23% wt.%)–$LiNO_3$ (8% wt.%) – $CsNO_3$ (44% wt.%)– $NaNO_3$ (6% wt.%)–$Ca(NO_3)_2$(19% wt.%) at Halotechnics Inc., and hence the name Halotechnics SS-500 [82]. Testing of this salt is done under nitrogen and air atmosphere, the result showed that the melting point and stability of this molten eutectic salt is 65 ºC and up to 500 ºC respectively. The addition of $CsNO_3$ (caesium-nitrate) to the molten salt mixture brings down the melting point but, $CsNO_3$ is uneconomical compared to other molten salts for application in PTC power plants. Currently, Halotechnics is optimizing the weight ratio of $CsNO_3$ to lessen the cost while maintaining the freezing point very low.

Molten alkali eutectic salts have been used successfully as HTF and TES. Lower melting point, high-temperature stability, low viscosity, a balance between specific heat capacity and thermal conductivity are the key features to develop molten salt for PTC application. The focus of the current scenario is to develop HTF, which can serve both as HTF and TES by various researchers. The comparison of the melting point of various alkali slats and their relevant eutectic composite is compared in Figure 14.

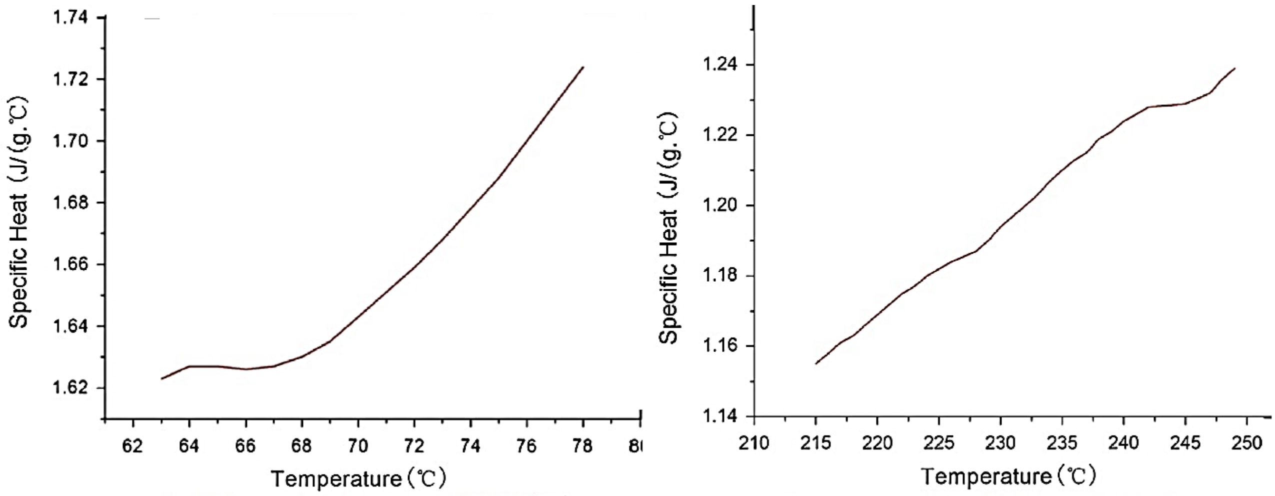

(a) Curve of solid phase (50-80℃)　　(b) Curve of liquid phase (200-250℃)

Figure 12: Specific heat curves for Hitec XL [53]. Reprinted with permission from Elsevier, Solar Energy, Thermophysical properties of Ca(NO3)2-NaNO3-KNO3 mixtures for heat transfer and thermal storage, Y.Y. Chen, Lic.No. 4605900521014.

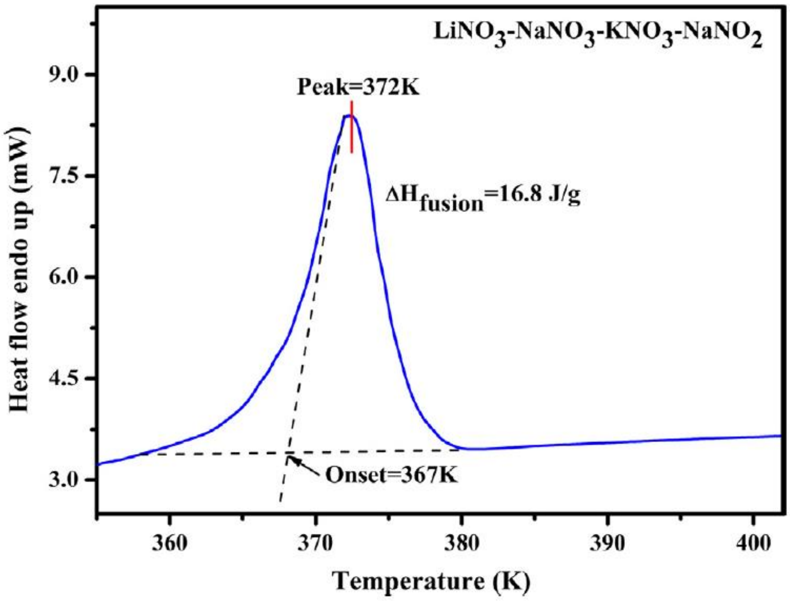

Figure 13: Melting point of $LiNO_3$–NaNO3–KNO3-$NaNO_2$ [83]. Reprinted with permission from Springer Nature, Oxidation of Metals, Molten Salt Corrosion of Stainless Steels and Low-Cr Steel in CSP Plants, A. G. Fernández, Lic.No.4611460040655.

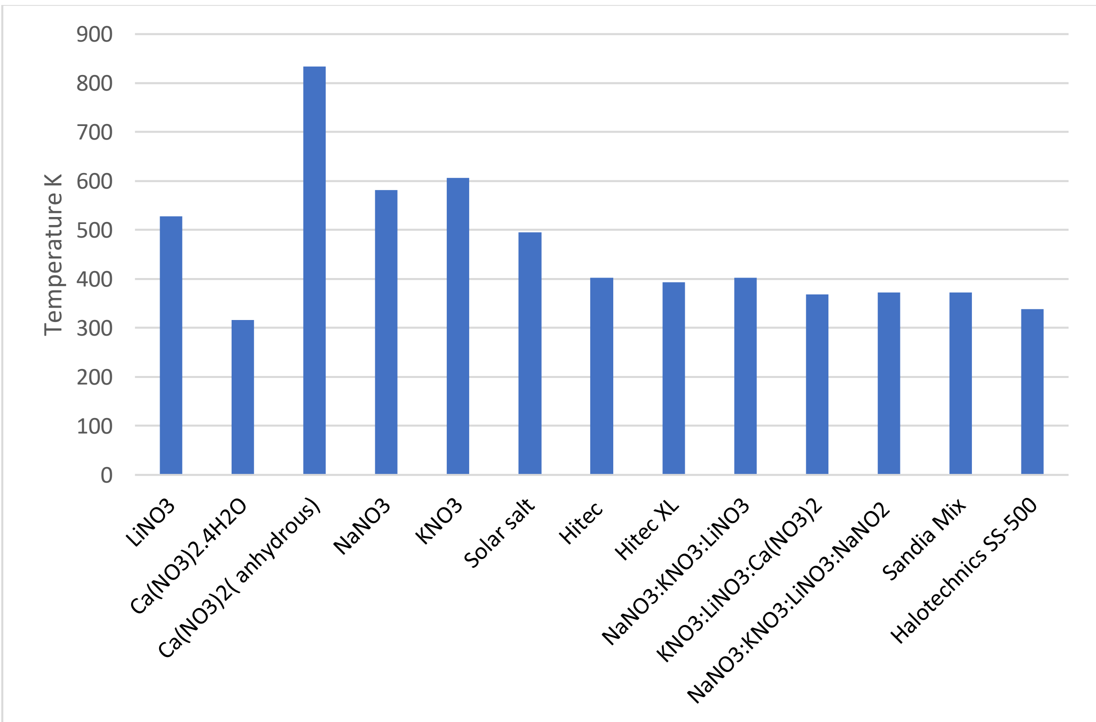

Figure 14. Melting point of Alkali salts and their relevant eutectic salt.

According to the literature, adding $LiNO_3$ and $Ca(NO_3)_2$ to $NaNO_3$ and KNO_3 (Solar Salt) to obtain the eutectic mixture was studied by various researchers, the primary motivation behind adding $LiNO_3$ and $Ca(NO_3)_2$ is to reduce the melting point of the eutectic mixture. Coscia et al. [73], Fernandez et al. [76], and Zhao et al. [77] obtained a eutectic mixture of $Ca(NO_3)_2$ KNO_3 and $LiNO_3$. From the results, it can be concluded that by the addition of $LiNO_3$, the freezing point reduced considerably in comparison with individual molten salt. The results obtained by Chen et al., [74] by adding $Ca(NO_3)_2$ to solar salt had reduced the melting point to 80 ºC which is the highest drop in temperature and not following the melting point reduction pattern followed by other researchers which is between 100 and 120 ºC. The reduction in melting point may be due to the preparation methods followed by the researchers. The preparation methods of adding, $LiNO_3$ and $Ca(NO_3)_2$ to solar salt is very critical because of the hygroscopic nature of the compound. Various precautionary measures need to be taken to reduce the moisture of the compounds especially $Ca(NO_3)_2 \cdot 4H_2O$ to make them anhydrous.

By the addition of $LiNO_3$ and $Ca(NO_3)_2$ to solar salt shows enhancement in the specific heat of the eutectic mixture. According to Fernandez et al. [76], enhancement in specific heat is higher by adding $LiNO_3$ to solar salt. Zhao et al., [77] and Chen et al.[74] has obtained comparatively similar specific heat capacity by adding $Ca(NO_3)_2$ to solar salt.

The dynamic viscosity value of the molten salt should be less than 0.005 Pa·s for application in PTC, because of the pumping power consumption, which goes higher with the increase in viscosity. From the molten salt synthesized by Coscia et al. [73] viscosity value of 0.06 Pa·s is obtained at 200 ºC and the viscosity reduced to 0.001 Pa·s is obtained at 550 ºC. Chen et al. obtained the viscosity of the molten salt close to the viscosity of water [74]. From the results obtained by various researchers combining $LiNO_3$ and $Ca(NO_3)_2$ to solar salt reduces the viscosity of the eutectic composite molten salt significantly.

Table 5: HTF thermophysical properties correlations as a function of Temperature [63]

	Property	**Equation**	**Validity temperature range**
Therminol VP-1	Specific heat(J/KgK)	c_p=2.82T +716	285 K < T < 673K
	Thermal Conductivity (W/mK)	$\lambda = 1.73\times10^{-7}\ T^2+7.62\times\ 10^{-6}T+0.14$	285 K <T < 673K
	Density (kg/m^3)	$\rho = -7.61\times10^{-4}T^2-2.24\times10^{-1}T+1191$	285 K< T < 673K

	Dynamic viscosity (Pa.s)	$\mu = (-23\times10^{-5}T^{3}+5.61\times10^{-3}\,T^{2}-19.89T+1822)^{-1}$	285 K < T < 673K
Solar Salt	Specific heat(J/KgK)	$c_p = 1443+0.172\,(T-273.15)$	533 K < T < 873K
	Thermal Conductivity (W/mK)	$\lambda = 0.443+1.9\times10^{-4}\,(T-273.15)$	533 K < T < 873K
	Density (kg/m^3)	$\rho = 2090-0.636\,(T-273.15)$	533 K < T < 873K
	Dynamic viscosity [Pa.s]	$\mu = 2.2714\times10^{-2}-1.2\times10^{-4}(T-273.15)^{2}+2.281\times10^{-7}(T-273.15)^{2}-1.147\times10^{-10}\,(T-273.15)^{3}$	533 K < T < 873K
Hitec	Specific heat(J/KgK)	$c_p = 1.56\times 10-3$	415K < T < 808K
	Thermal Conductivity (W/mK)	$\lambda = 0.411+4.36\times10^{-4}(T-273.15)-1.54\times10^{-6}(T-273.15)^{2}$	415K < T < 808K
	Density (kg/m^3)	$\rho = -0.74\times(T-273.15)+208$	415K < T < 808K
	Dynamic viscosity (Pa.s)	$\mu = 10^{2.7374}\times(T-273.15)^{-2.104}$	415K < T < 808K
Hitec XL	Specific heat(J/KgK)	$c_p = -0.33T+1634$	403K < T < 823K
	Thermal Conductivity (W/mK)	$\lambda = 0.519$	403K < T < 823K
	Density (kg/m^3)	$\rho = 2240-0.827\times(T-273.15)$	403K < T < 823K
	Dynamic viscosity ([Pa.s)	$\mu = 10^{6.1374}\times(T-273.15)^{-3.36406}$	403K < T < 823K

Table 6: HTF Thermophysical Properties at various temperature [84]

Tin (K)	Property	Pressurized Water	Liquid Sodium	Air	CO2	He
300	**Thermal Conductivity** k(W/mK)	0.628	-	0.036	0.031	0.16
	Density ρ(kg/m^3)	994	-	0.769	1.098	0.146
	Specific Heat Capacity c_p (J/kgK)	4164	-	1021	1004	5193
	Dynamic Viscosity	5.9×10^{-4}	-	2.5×10^{-5}	2.3×10^{-5}	2.1×10^{-5}

	μ(Pa.s)					
400	**Thermal Conductivity** k(W/mK)	0.674	86.9	0.043	0.037	0.191
	Density ρ(kg/m3)	926	918	0.632	0.939	0.112
	Specific Heat Capacity c_p (J/kgK)	4277	1370	1040	1057	5193
	Dynamic Viscosity μ(Pa.s)	1.9×10^{-4}	5.9×10^{-4}	2.9×10^{-5}	2.6×10^{-5}	2.5×10^{-5}
500	**Thermal Conductivity** k(W/mK)	0.622	79.8	0.049	0.044	0.221
	Density ρ(kg/m3)	813	896	0.537	0.813	0.091
	Specific Heat Capacity c_p (J/kgK)	4741	1332	1062	1104	5193
	Dynamic Viscosity μ(Pa.s)	1.1×10^{-4}	4.1×10^{-4}	3.2×10^{-5}	3.0×10^{-5}	2.9×10^{-5}
600	**Thermal Conductivity** k(W/mK)	-	73.4	0.054	0.051	0.251
	Density ρ(kg/m3)	-	873	0.467	0.713	0.076
	Specific Heat Capacity c_p (J/kgK)	-	1300	1086	1145	5193
	Dynamic Viscosity μ(Pa.s)	-	3.2×10^{-4}	3.5×10^{-5}	3.3×10^{-5}	3.3×10^{-5}
700	**Thermal Conductivity** k(W/mK)	-	67.8	0.059	0.057	0.281
	Density ρ(kg/m3)	-	851	0.413	0.633	0.066
	Specific Heat Capacity c_p (J/kgK)	-	1276	1108	1180	5193
	Dynamic Viscosity μ(Pa.s)	-	2.6×10^{-4}	3.8×10^{-5}	3.6×10^{-5}	3.7×10^{-5}
800	**Thermal Conductivity** k(W/mK)	-	62.7	0.064	0.064	0.31
	Density ρ(kg/m3)	-	827	0.371	0.568	0.058

	Specific Heat Capacity c_p (J/kgK)	-	1260	1129	1211	5193
	Dynamic Viscosity μ(Pa.s)	-	2.3×10^{-4}	4.0×10^{-5}	3.9×10^{-5}	4.0×10^{-5}
900	**Thermal Conductivity** k(W/mK)	-	58.1	0.069	0.07	0.338
	Density ρ(kg/m3)	-	804	0.336	0.515	0.052
	Specific Heat Capacity c_p (J/kgK)	-	1252	1148	1238	5193
	Dynamic Viscosity μ(Pa.s)	-	2.0×10^{-4}	4.3×10^{-5}	4.2×10^{-5}	4.4×10^{-5}
1000	**Thermal Conductivity** k(W/mK)	-	54.1	0.073	0.076	0.366
	Density ρ(kg/m3)	-	780	0.307	0.471	0.047
	Specific Heat Capacity c_p (J/kgK)	-	1252	1164	1262	5193
	Dynamic Viscosity μ(Pa.s)	-	1.8×10^{-4}	4.5×10^{-5}	4.5×10^{-5}	4.7×10^{-5}
1100	**Thermal Conductivity** k(W/mK)	-	50.4	0.077	0.082	0.394
	Density ρ(kg/m3)	-	755	0.283	0.433	0.043
	Specific Heat Capacity c_p (J/kgK)	-	1262	1179	1282	5193
	Dynamic Viscosity μ(Pa.s)	-	1.7×10^{-4}	4.7×10^{-5}	4.8×10^{-5}	5.1×10^{-5}
1200	**Thermal Conductivity** k(W/mK)	-	-	0.081	0.087	0.421
	Density ρ(kg/m3)	-	-	0.262	0.401	0.039
	Specific Heat Capacity c_p (J/kgK)	-	-	1192	1300	5193
	Dynamic Viscosity μ(Pa.s)	-	-	5.0×10^{-5}	5.0×10^{-5}	5.4×10^{-5}
1300	**Thermal Conductivity**	-	-	0.085	0.092	0.448

k(W/mK)					
Density ρ(kg/m3)	-	-	0.244	0.373	0.036
Specific Heat Capacity c_p (J/kgK)	-	-	1203	1316	5193
Dynamic Viscosity μ(Pa.s)	-	-	5.2×10^{-5}	5.3×10^{-5}	5.7×10^{-5}

Montes et al. [85] conducted a comparative analysis using a typical PTC loop of 20 MW_e power output for three different HTF, water/steam, Therminol VP-1, and solar salt, which is presented in Table 7. It can be observed that the Energy efficiency decreases with an increase in length due to the increase in heat loss along the length of the receiver. However, with the outlet temperature rise, Exergy efficiency increases and follows the opposite trend. However, for lengthier collector loops, exergy efficiency drops down due to the increase in pressure drop. It is interesting to note that for a similar length of the receiver, molten salt has higher exergy efficiency and water/steam has higher energy efficiency compared to the other two HTFs.

Table 7: Thermodynamic performance of PTC with different loop lengths using Therminol VP-1, Molten salt, and water as HTF [85].

HTF	Total collector loop length (m)	Heat Loss (kW)	Pressure drop (bar)	Outlet Temperature (ºC)	Energy Efficiency	Exergy Efficiency
Therminol VP-1	539.9	129.7	4.53	353	69.7	33.6
	662.6	172.4	5.63	374.2	69.3	34
	711.7	189.8	6.09	382.5	69.2	34.2
	736.2	199.3	6.32	386.6	69.1	34.3
	760.7	209	6.55	390.6	69	34.3
	785.3	219	6.78	394.6	68.9	34.4
Solar Salt	294.5	109	0.53	438.6	69.4	37
	429.5	198.5	0.77	556.3	67.6	37.3
	589	349.8	1.04	565.9	66.9	38.3
	613.5	378.1	1.08	575.2	66.5	38.2
	638	407.7	1.13	584.4	66	38.1
	662.6	438.8	1.17	593.3	65.5	37.9
Water Steam	736.2	195.2	5.35	353.8	70.6	34
	957.1	340.4	8.63	541.3	68.8	34.4
	981.6	367.8	9.08	580.9	68.4	34.4
	1006.1	398.2	9.56	561.5	68	34.4

1030.7	431.7	10.04	599.5	67.5	34.3
1227	818.6	14.42	711.6	62.6	32.6

3.4. Nanofluids as heat transfer fluid

In order to enhance the optical and thermal performance of the PTC, researchers around the world are researching on enhancing the design of collectors and thermophysical properties of the HTF. Doping nanoparticles to the base fluid is one such attempt to enhance the optical and thermal properties of HTF. Nanofluids are broadly classified into two categories, Metallic solids nanoparticles, and Nonmetallic solids nanoparticles. Metallic nanoparticles often used in the preparation of nanofluids, as stated in the research articles are Cu, Fe, Al, Ag, and Au. Moreover, Nonmetallic solids are Al_2O_3, CuO, Si, SiC, Carbon nanotubes (CNTs), Boron Nitrate Nanotubes (BNNTs, and Nanodroplets. Table 8 summarises the recent works on heat transfer enhancement using various nanoparticles in PTC. These nanofluids are dispersed into a dispersion medium called base fluids, commonly used base fluids are water, Synthetic oil or Engine oil, and Ethylene Glycol (EG). Nanofluids enhances the thermophysical properties of the base fluid, enhancing the efficiency of the heat transfer system [86]. Sarafraz et al. investigated the effect of zirconia acetone nanofluid on thermal resistance, heat transfer coefficient, and thermal performance of a thermosyphon evaporator and the results showed that there was reduction in thermal resistance of the evaporator, enhancement in boiling heat transfer mechanism at the highest heat flux (~200 suns) on the evaporator when doped with zirconia nanoparticles [87]. However, the addition of nanoparticles may enhance the certain thermophysical property of the base fluid while some other properties may degrade by doping nanoparticles. Sarafraz et al. conducted experiments on methanol doped with graphene nanoplatelets in evacuated tube solar collectors and found that the thermal conductivity of the heat transfer fluid enhanced by 19% by the addition of 0.1 wt.% of graphene nanoplatelets. Meanwhile, the heat capacity of the HTF was decreased by 4% at 0.1 wt.% of the nanoparticles [88]. In yet another research on doping carbon nanoparticles in acetone, they found an enhancement in thermophysical properties like thermal conductivity and specific heat capacity but the viscosity of the fluid increases by increasing the mass fraction of nanoparticles [89-91].

Both Metallic solids and non-metallic solids can be further categorized into mono and hybrid nanofluids. Mono nanofluid is an HTF where a single nanomaterial is doped into the base fluid, whereas hybrid nanofluid is an HTF where two or more nanoparticles are doped to the base fluid [92]. Mono nanofluids are discussed in the first part of this section while a separate subsection is dedicated to hybrid nanofluid at the end of this section.

Also, some researchers predict the behavior of nanofluids in the solar thermal application using two approaches using numerical studies. The first one is the single-phase approach and the second is the two-phase approach. In the first approach, the base fluid and nanoparticles have the same velocity field and temperature, making the HTF behave as classical newtonian fluid whereas, the latter approach assumes that base fluid and the nanoparticle has separate velocity vector field. Therefore, within the control volume, there is a volume fraction of base fluid and volume fraction of nanoparticles. The second approach gives successful prediction even when the nanoparticles are in lower concentration [93].

Table 8: Recent works on Heat Transfer enhancement using Nanoparticles in PTC.

Nanofluids		**Methods**	**% Enhancement**		**References**
Base fluids	**Nanoparticles**		**η_{th}**	**h**	
Water	Al_2O_3	Experimental	7	32	[94]
Water	Al_2O_3, Fe_2O_3, SiO_2, TiO_2,ZnO	Experimental	<1	-	[95]
Water	Al_2O_3, CuO	CFD	-	28, 35	[96]
Water	Al_2O_3	CFD	-	22	[97]
Water	Al_2O_3, Fe_2O_3	Experimental	13, 11	-	[98]
Water	Al_2O_3	Experimental	8.54	-	[99]
Water	TiO_2	Experimental	8.66	23	[100]
Ethylene glycol	Fe_2O_3	Experimental	-	13.3	[101]
Ethylene glycol	Carbon black	Experimental	27.9	-	[102]
Thermal oil	Al_2O_3	CFD	4.25	11	[103]
Synthetic oil	Al_2O_3, CuO, TiO_2	Mathematical model	1.17,1.06, 1.14	-	[104]
Synthetic oil	Al_2O_3	Mathematical model	0.1	60	[105]
Synthetic oil	Al_2O_3	CFD	7	-	[106]
Synthetic oil	Al_2O_3	CFD	-	15	[107]
Synthetic oil	Al_2O_3	CFD	-	40	[108]
Syltherm 800	Ag, Al_2O_3, Cu, CuO	Mathematical model	-	36, 18, 33, 27	[109]
Syltherm 800	Al_2O_3, CuO	Mathematical model	1.13, 1.26	35, 41	[110]
Syltherm 800	Al_2O_3 and TiO_2	Mathematical model	1.31	117	[111]
Syltherm 800	CuO	CFD	0.76	35	[112]
Syltherm 800	Al_2O_3	CFD	8	-	[113]
Syltherm 800	Al_2O_3	CFD	7.6	7.6	[93]
Syltherm 800	CuO	CFD	15	38	[114]
Syltherm 800	Al_2O_3	CFD	-	40	[115]

Dowtherm A	Al_2O_3, C, Cu, SiC	CFD	-	68	[116]
Therminol-VP1	Cu	CFD	12.5	32	[117]
Therminol-VP1	Ag, Al_2O_3, Cu	CFD	13.9, 7.2, 12.5	7.9, 3.9, 6.4	[118]
Therminol-VP1	SWCNT	CFD	4.4	234	[119]
Therminol 66	Al_2O_3	Mathematical model	0.1	60	[120]
Molten salt	CuO	CFD	0.26	12	[112]
Mineral oil	MWCNT	Experimental	11	-	[121]

3.4.1. Properties and preparation

The methods used in the preparation of nanofluids are the main factors that can contribute significantly to the stability of nanofluid [122]. A good number of review papers have discussed the preparation methods of nanofluids [123, 124]. Two kinds of methods, which are a single-step method, and two-step have been used in producing nanofluids. In the single-step method, nanoparticle manufacturing and nanofluid preparation are done concurrently. One of the examples of equipment to prepare nanofluid by using single-step method is to use Plasma Nano Colloid Maker, this method uses the Electrical Explosion of Wire (EEW) technique to convert the primary wire into nanoparticles by using pulse explosive process, and this explosion dispersed the metallic nano colloids in the base fluid at the same time. Researchers that have applied this technique in nanofluid preparations include Bahremand et al., Khoshvaght-Aliabadi et al. Mirfendereski et al. and Rakhsha et al. Bahremand, Abbassi and Saffar-Avval [125], Mirfendereski, Abbassi and Saffar-avval [126], Khoshvaght-Aliabadi, Tavasoli and Hormozi [127] Rakhsha, Akbaridoust, Abbassi and Majid [128]. The disadvantage of the single-step method is that the leftover residuals of the reaction are difficult to remove from the nanofluid.

The two-step method is a technique more commonly applied by researchers. This method is more attractive because it is a more straightforward method compared to the single-step method. Dry nanoparticles will be produced first in large quantities. Then, a small number of nanoparticles will be dispersed in a base liquid according to the intended weight or volume fraction. However, making a stable solution is more challenging for the two-step method as ultrafine particles have a higher surface energy that will immediately lead to aggregation, clustering, and sedimentation [122]. Therefore, researchers have applied different methods of making a stable nanofluid in the two-step method, including stirring or shaking, ultrasonication, surface functionalization, or adding on dispersant or surfactant in the solution.

Stirring or shaking is the simplest and cheapest method to make a solution. For example, Mahbubul et al. Mahbubul, Saidur and Amalina [129] had prepared Al_2O_3/R141b nano-refrigerant with an orbital incubator shaker continuously shaken at 240 rpm for about one hour while maintaining a constant temperature of 15ºC to avoid evaporation of refrigerant. Ultrasonication or ultrasonic homogenizer is the most common method applied by researchers to prepare a nanofluid. The ultrasonication process can break down agglomeration or clustering of nanoparticles that cannot be achieved by stirring or shaking. Ultrasonication mainly depends on the frequency, nominal power of sonication and sonication time [130]. For the engineering applications, the stability of nanofluid is the major challenge [131], natural sedimentation of nanoparticles is observed over time. This sedimentation may clog the pipes carrying HTF in the solar field creating pressure loss. Theoretically, particles will have both attractive and repulsive forces, which result in the agglomeration and dispersion of particles in the base fluid [132]. The attractive forces are due to vanderwaals force of attraction, and the electrostatic repulsive force causes the particles to repel each other. Nanoparticle will not agglomerate if the repulsive force is higher than the vanderwaals force of attraction, making the particle disperse evenly in the base fluid. Electrostatic repulsion can be increased by adding surfactants into the nanofluids. Sodium dodecyl sulfate, sodium dodecylbenzene sulfonate, or Triton X-100 are the surfactants which had been tested and proven to stabilize nanofluid [133]. However, when the Brownian motion of the particles is dominating, and when the nanofluids are heated, the effect might be weakened.

Yang and Liu [134] proposed a suitable way to stabilize the nanoparticles in the base fluid is by grafting polymers on to the surface of nanoparticles. This method is also known as surface functionalization. Silanes were attached to silica nanoparticles making "Si-O-Si" covalent bonding and resulting in a steric stabilization effect even when heated. Functionalized SiO_2 nanoparticles have been reported to keep dispersing well after six months, and no sedimentation was observed [134, 135].

Various methods can test the stability of nanofluid. Some methods that were commonly applied by researchers include zeta potential measurement, dynamic light scattering, electron microscopy, optical spectrum analysis, and observation of the natural sedimentation method.

Zeta potential measurement is a method to measure the level of the repulsion force between particles with the same charge. Zeta potential value can indicate how stable the dispersion is for nanofluid. The higher is the zeta potential value, the more the nanoparticles will resist aggregation due to higher repulsive force and therefore, resulting in a more extended period of stability [136]. The relationship between zeta potential value and stability of nanofluid is shown more precisely in Table 9. The zeta potential values of various nanofluids obtained in the literature are presented in Table 10. The surface functionalization of nanoparticles is another method to enhance the zeta potential of the nanofluid. Hadi Karami et al. used carboxyl functionalization of graphene nanoparticles and obtained a stable nanofluid, and the results also proved that the zeta potential decreased with an increase in the mass concentration of nanoparticles.

Table 9: Relationship between zeta potential value and stability of nanofluid

Zeta potential value	**Stability**	**References**
0 mV and ±5mV	Strongly tends to precipitate	
±10mV to ±30mV	Tends to precipitate	
±30mV to ±40mV	Moderate stability	Dukhin et al. [137]
±40mV to ±60mV	good stability	
higher than ±61mV	excellent stability	

A dynamic light scattering (DLS) method can be used to determine the nanoparticle size distribution in a nanofluid. However, the particle size distribution measurement can be affected by the concentration of the suspension, composition of solvents, dust, and other additives and therefore may lead to incorrect results to evaluate the stability of nanofluids [138]. Electron microscopy equipment such as Transmission Electron Microscopy (TEM) and Scanning Electron Microscope (SEM) are very useful tools to measure the shape and particle size distribution (PSD) of nanoparticles [139]. However, electron microscopy cannot accurately present the real situation of nanofluids because, in order to use the electron microscopy, the nanofluid sample needs to be dried first. An example of SEM image of SiO_2 nanoparticles, ultrasonically dispersed in deionized water, after drying is shown in Figure 15.

Table 10: Zeta-potential values obtained by different nanofluids in literature

Base Fluid	Nanoparticle	composition	Method	Zeta potential	Remarks	References
Ethylene glycol	RGO-TiO_2	0.015 wt.% & 0.025 wt.%	without using surfactant	-21.5 mV	Hydrodynamic radius was in the range of 100 nm and 450 nm	[140]
Water	Al_2O_3-SiO_2	0.2 wt.%, 0.4 wt.% and 0.6 wt.%	Two step method of preparation	-60.7 mV	0.2 wt.% has leas stability and 0.6 wt. % has comparatively high stability more than a month.	[141]
Deionized water	GNP-COOH	0.1 wt.%	Covalent functionalization of carbon nanoparticles	-20.9 mV	Zeta potential decreased with increase in mass concentration of nanoparticles.	[142]
	GNP-COOH	0.2 wt.%		-19 mV		
	MWCNT-COOH	0.1 wt.%		-20.9 mV		
	MWCNT-COOH	0.2 wt.%		-20.7 mV		
Water	CuO	0.02 wt. %	Cetyl trimethyl ammonium bromide (CTAB) is used as the surfactant	42 mV	With the increase in loading of nanoparticles, the zeta potential value decreased resulting in low stability	[143]
		0.05 wt. %		42.1 mV		
		0.1 wt. %		38.9 mV		
		0.2 wt. %		34.3 mV		
		0.5 wt. %		15.5 mV		
Diathermic oil	TiO_2	Up to 1 vol%	Two-step method of preparation	52 mV	The mean diameter of nanoparticles increased from 22.2 nm to 48.5 nm after 10 days showing some cluster formation. However, the fluid was said to be stable.	[55]
Thermal oil	Al2O3-MWCNT	0.125% wt. to 1.5 wt.%	Two-step method of preparation	55mV $<\zeta<$ 64 mV	Stability of the nanofluid was observed until seven days, and the zeta potential value was above 55 mV	[57]
Transformer oil	Ag- WO3	1 wt.%	Prepared by the electric explosion of wire (one-step method)	47 mV@ 313K 52mV @ 373K	Zetasizer Nano ZS manufactured by Malvern, Britain was used to finding the zeta potential at two	[144]
		2 wt.%		51mV@ 313K		

				54mV @373K	different temperatures	
		4 wt.%		50mV@313K 51mV@373K		
Diphenyl oxide and biphenyl eutectic mixture	TiO_2	2.5 wt.%	Two-step method of preparation, ODT (1-octadecanethiol) is used as the surfactant	>50 mV	UV-vis spectrometry was used to verify the coagulation process in the nanofluid. 2.5% of ODT and 2.5 wt.% of TiO_2 revealed the best stability	[145]
Thermal oil	MWCNT-ZnO	0.125 wt.%, 0.25 wt.%, 0.5 wt.%, 0.75 wt.%, and 1 wt.%	MWCNT-ZnO in 15% and 85% ratio and two step method is used for preparation	$52\ mV < \zeta < 56\ mV$	The samples are observed for agglomeration for 7 days	[146]
Dowtherm A	Boron nitride nanotubes	0.001 wt.% 0.003 wt.% 0.005 wt.%	Triton X-100 is used as a surfactant and two-step method is used for nanoparticle preparation	$-10mV < \zeta < -55\ mV$	The measurements were taken for several times in a day for 30 days	[147]

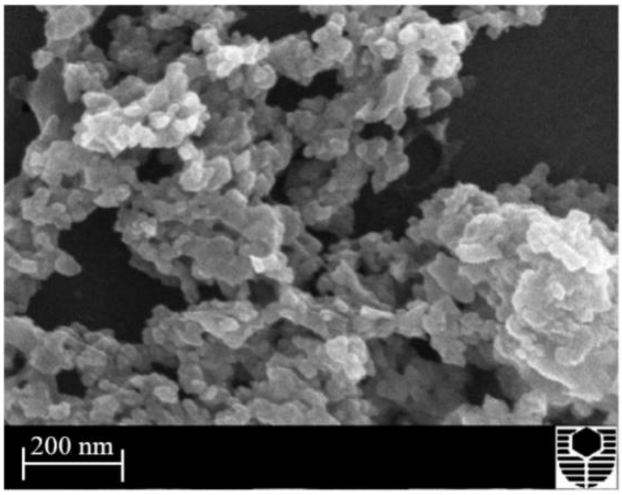

Figure 15: SEM image of SiO_2 nanoparticles [148]. Reprinted with permission from Elsevier, Journal of Colloid and Interface Science, Stabilising nanofluids in saline environments, Sarmad Al-Anssari, Lic.No. 4676391395847.

Spectral analysis by using Ultra Violet-Visible spectrophotometer (UV-Vis) measurement is a method to evaluate the optical absorption spectrum and nanofluids peak absorption by using different wavelengths (nm) of light passing through the nanofluid [149]. An example of optical spectrum measurement results is shown in Figure 16. To measure the stability of nanofluids, the transmittance can be measured against time. It can be understood that as the transmittance increases, stability decreases [124]. However, take note that this method is not suitable for high concentration or darker colored nanofluid.

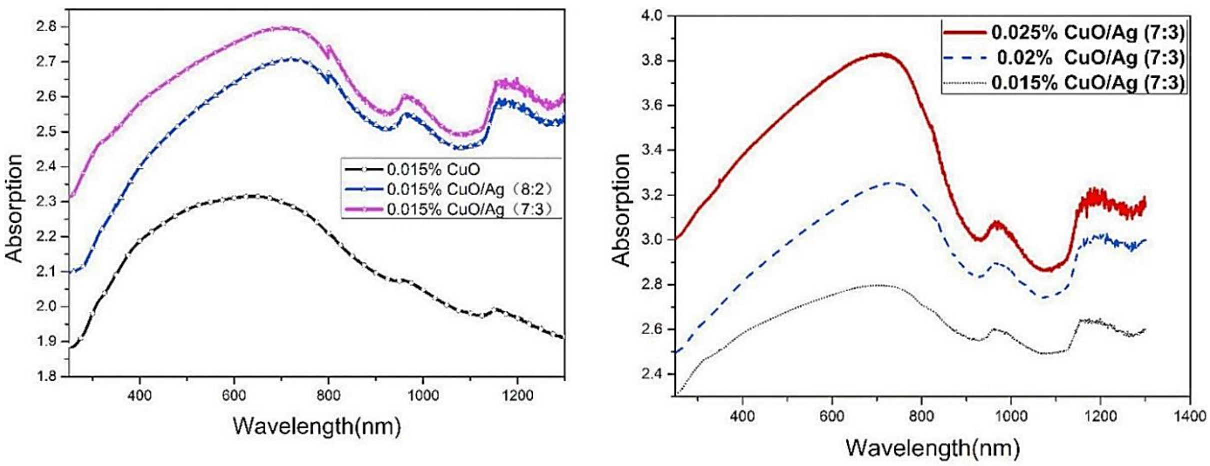

(a) (b)

Figure 16: UV–vis spectra (a) CuO, CuO/Ag (8:2) and CuO/Ag (7:3) in the same volume fraction; (b) CuO/Ag (7:3) as the function of volume fraction [149]. Reprinted with permission from Elsevier, Solar Energy, Investigation on thermo-optical properties of CuO/Ag plasmonic Nanofluids, Xiao Yu, Lic.No. 4676390986826.

Observing the natural sedimentation is the simplest and yet the most effective method to evaluate the stability of nanofluid. Photos of prepared nanofluids with various concentration or preparation methods will be taken after some time to show whether there is any visible sedimentation occurred. An example of photo capturing can be seen in Figure 17. The research communities agree that agglomeration plays a vital role in the thermal transport of nanofluid. Agglomeration is a complex process that relies on the properties of the base fluid and the surface energy of the nanoparticles. The electric charges present in the solution play a dynamic role in the agglomeration and resulting dispersion of particles can be categorized into different regimes of dispersion such as well dispersed, weakly dispersed, chain-like aggregation, partial aggregation, and complete agglomeration. These dispersion mechanisms may weaken the possible mechanism behind the enhancement in thermal conductivity. Most of the studies report that an optimum agglomeration may result in maximum thermal conductivity enhancement due to the nanoclustering effect and the excessive flocculation is unfavorable for enhancement of thermal conductivity [150].

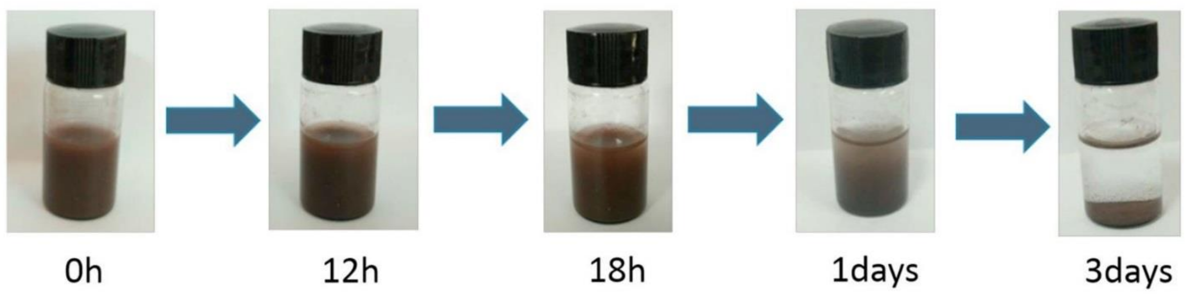

Figure 17: Natural sedimentation image of CuO/Ag nanofluid [149]. Reprinted with permission from Elsevier, Solar Energy, Investigation on thermo-optical properties of CuO/Ag plasmonic Nanofluids, Xiaoxiao Yu, Lic.No. 4676390986826.

3.4.2. Progress in obtaining stable nanofluid.

The interest in nanofluid research has been increasing rapidly due to its unique properties such as optical properties [151], electrical properties [152] and thermal properties [153]. The types that are commonly applied and studied by researchers include metallic, metal oxide, ceramic, and carbon-based nanoparticles [154]. Some of the metallic nanoparticles that had been tested by researchers include Copper (Cu), Aluminum (Al), Iron (Fe), Gold (Au) and Silver (Ag) [155-159]. Oxides of materials are significant in the area of chemistry, physics and material sciences that can display semiconductor characteristics in their electronic and magnetic properties. Alumina (Al_2O_3), Copper (II) oxide (CuO), Iron (II, III) oxide (Fe_3O_4), Titanium dioxide (TiO_2) and Silicon dioxide (SiO2) are some example of metal oxide nanoparticles commonly utilized by researchers [160-164]. Carbon nanofibers and nanotubes (CNTs) are desirable candidates for a wide range of applications due to their unique physical, chemical, optical and electrical properties [165, 166]. The most interesting of all are carbon nanotubes. The properties of carbon nanotubes are very close to theoretical limits. Three exceptional qualities in the properties of carbon nanotubes include the electrical conductivity, which is as conductive as copper, the mechanical strength, which is stronger but lighter than steel and the thermal conductivity, which is more than five times than thermal conductivity of copper. Iijima [167] was the pioneer observers of multi-walled carbon nanotubes (MWCNT) produced using an arc-discharge evaporation method. Later in 1993, his group also managed to synthesis Single-walled carbon nanotubes (SWCNT) in their lab [168]. Nevertheless, when nanoparticles are used as a dopant in base HTF, there will be a chance of fouling in heat exchangers, mainly when wick type thermosyphon absorbers are used. Arya et al. investigated the fouling phenomenon in a thermosyphon heat pipe absorber with varying heat flux by using CNT nanofluid as a heat transfer medium. They found that with the increase of heat flux, the thermal performance of the evaporator increased. It was also observed that CNT enhanced the thermal performance and capillarity of the mesh by producing a fouling layer by changing the contact angle of liquid with the mesh surface [169]. Sarafraz et al. investigated the thermal performance of a thermosyphon evaporator equipped with mesh screen wick using TiO_2 doped water as HTF. They found that the increase in loading of nanoparticles fouling on wick and walls of the evaporator increases reducing the thermal performance of the system which eventually causes system failure [170]. Both the research by Arya et al., and Sarafraz et al. presented the same background with different results; this shows that nanoparticles disadvantages can be utilized as an advantage and some times vice-versa [171] [172].

The right method of preparing the nanofluids is required in order to have stable and well-dispersed nanofluids [173]. The viscosity of the base fluid strongly influences the dynamic properties of nanoparticles dispersed in a fluid. The higher the viscosity of the base fluid, the higher the drag force experienced by the nanoparticles resulting to lower Brownian velocity and lower thermal conductivity of nanofluid [174]. Commonly, nanoparticles are dispersed in water, ethylene glycol (automotive antifreeze) or oil as the base fluids, and thus the nanofluids can be classified as either water-based or oil-based fluids [175]. Over the past ten years, the number of research studies on nanoparticles and nanofluids has been increasing dramatically. There is substantial data available including theoretical and experimental evidence of enhanced thermal and physical properties of working fluids after dispersing a small number of nanoparticles inside the working fluids for various applications [176-187]. However, if the nanoparticles present in the base fluid failed to continue remaining stable after some time, all the intended enhanced properties of nanofluid will not be possible, and some adverse effects like clogging and reduction in performance can occur in the system. The stability of nanofluids is an essential parameter towards long-term practical use in any industrial application. In the nanometer scale, the high surface area of the particles causes a significant increase in interactive forces on the surfaces of the nanomaterials. These forces attract other particles to agglomerate. Stability being the most critical aspect of nanofluid, was covered in almost every study in this area. Unfortunately, the information on the stability of nanofluid is still unorganized. Therefore, this section aims to organize all the recent information regarding the stability of nanofluid and present it in a tabular form.

The summary of recent progress on the stability of nanofluid is shown in Table 11 Long-term stability of nanofluid is an essential element for any practical applications. Without the long-term stability, the use of nanofluid as working fluid will not be practical and may cause an adverse effect on the system. Studies from Hordy et al., Wang et al., and Ilyas et al. has shown the evidence of long-term stability from natural sedimentation after two years, 20 months and three months respectively [54, 188]. All these proven long-term stable nanofluids were carbon-based nanoparticles, including graphene and multi-walled carbon nanotubes (MWCNT). However, the preparation method from Wang et al. [188] was not clearly described in their research, and the findings are somewhat doubtful. In reference Hordy et al.[189], the MWCNT nanoparticles have been surface treated as functionalized nanofluid and had shown excellent stability even after 20 months. Another MWCNT nanofluid in the research of Ilyas et al., [54] used thermal oil as a working fluid. It was stated that the nanofluid understudy remains stable after three months. However, there is still uncertainty about whether the nanofluid can stay stable for a more extended period or not. The same case with Sarafraz et al. [190] as well, that uses Ag nanofluids. It was shown in their paper that the nanofluid remains stable after 14 days. However, the study also supplemented by Zeta potential study showing the potential of 30 mV (moderate stability). All other findings also showed moderate stability in terms of Zeta potential except from [191] which is also MWCNT nanofluid, showing Zeta potential of more than 40 mV; meaning excellent stability.

Table 11: Summary of recent reports on the stability of Nanofluid

Reference	Nanoparticle	Base fluid	Concentration	Preparation method	Stability
[188]	Graphene nanoparticles (GNP)	Distilled water	1 wt%	N/A	Stable after 2 years
[189]	Mwcnts	Denatured alcohol (85% ethanol, 14% Methanol)	5 to 53mg/L. 0.00050 to 0.00530 % (weight/volume %)	Plasma surface-functionalized. Ultrasonication	Stable after 20 months
[54]	MWCNT	Thermal oil	1 wt%	Ultrasonication in cooling water bath (45 minutes, maintained at 20°C)	Stable for more than 3 months
[190]	Ag (silver)	Deionized water	0.1 wt%	Ultrasonication (20 minutes)	Stable after 45 days Zeta potential 30 mv
[192]	Al_2O_3	Paraffinic-thermal oil	0 to 3 wt%	Functionalized with oleic acid Ultrasonication (25 minutes)	Stable after 30 days
[193]	Au (gold) Plasmonic	Doubly deionized water (DDI water)	178 ppm	Centrifuged at 10,000 rpm for 1 h	Stable after 14 days
[194]	Binary MWCNT-sio_2/Ag		0.1 vol%	Surfactant (hexadecyl trimethyl ammonium bromide (CTAB)) Ultrasonication (1 hour)	Stable after 7 days Zeta potential 30mv
[195]	Nio	Eutectic mixture of biphenyl (C12H10, 26.5%) and diphenyl oxide (C12H10O, 73.5%)	0.01 wt.%	Surfactant (A mixture of benzalkonium chloride (BAC) and 1-Octadecanethiol (ODT). Ultrasonication (20 minutes)	Stable after 7 days Zeta potential less than -30 mv
[196]	Al_2O_3 Tio_2	Water	0.1 wt%	Stirred (30 mins) Ultrasonication (40 mins)	Stable after 3 days
[197]	Al_2O_3	Water	0.15 wt%	Ultrasonication (30 minutes)	Stable after 3 days

				Surfactant (Triton X-100)	
[149]	CuO/Ag plasmonic composite	Deionized water	0.025 vol%	Ultrasonication (30 minutes)	Stable after 12 hours Sediment after 3 days
[198]	Chinese ink nanopowder	Water	0.05 wt%	Stirring	Stable after 24 hours
	Cu, CuO, and carbon black nanopowders	Water	0.05 wt%	Ultrasonication (30 minutes)	Sediment after 24 hours
[199]	Sio_2	A mixture of ethylene glycol and water	0.3 wt%	Magnetic stirring (6 hours) Ultrasonication (2 hours)	Stable after 5 hours
[191]	Magnetic mounts	Saline water (1000 ppm salt concentration)	0.04 wt%	PVP-K30 as dispersant Mechanical stirrer (30 minutes) Ultrasonication (2 hours)	Zeta potential more than 40 mv
[200]	Cuo	Liquid paraffin	6 wt%	Ultrasonication (1 hour)	Zeta potentials less than 40 mv
[201]	Nio	Eutectic mixture of biphenyl (C12H10, 26.5%) and diphenyl oxide (C12H10O, 73.5%)	0.01 wt%	1) Ultrasonication (20 minutes) 2) Surfactant (Benzalkonium chloride (BAC))	Zeta potential more than 30 mv
				Surfactant 1-Octadecanethiol (ODT)	Zeta potential lower than 30 mv
[202]	Al_2O_3	Distilled water	0.1 wt%	Ultrasonication (1 hour) Surfactant (polyethylene glycol)	Zeta potential more than 30 mv
	Tio_2			Surfactant (cetyltrimethylammonium bromide)	
[203]	Chromium (Cr_2O_3)	Distilled water	0.01 vol%	Ph was modified to 10 by putting an adequate amount of NaOH solution Ultrasonication (10 minutes)	Zeta potential less than -30 mv

3.4.3. Water-based Nanofluids

As the development in concentrated solar thermal technology increased, the need for improving the heat capacity of thermal fluid used in solar thermal increased. Hence initially studies were conducted to test nanoparticles in water as base fluid initiated and lead to further developments (Table 12). The preparation of nanofluids was initiated by using water as base fluid, and it is observed that the thermal properties of the nanofluid had increased compared to the base fluid [204]. Khanjari et al. tested Ag/water and Al_2O_3/water nanofluids., and CFD simulation was conducted on the system and concluded that Ag/water showed an increase in heat transfer coefficient than Al_2O_3 compared with pure water [205]. Al_2O_3/water showed a 43% increase in heat transfer coefficient, while Al_2O_3 leads to a 12% increase when compared to pure water. This proves that Al_2O_3 nanoparticles have a moderately low contribution to the enhancement of thermophysical properties of water, which is in line with the outcome of Sardarabadi et al. [206]. Subramani et al. investigated the performance of PTC using DI (Deionised water) H_2O and TiO_2 nanoparticles at various flow rated in the turbulent region ($2950 \leq Re \leq 8142$) [100]. With the use of TiO_2 nanoparticle, there was a 22.76% improvement in convective heat transfer coefficients compared to DI-H_2O. With 0.2% vol.% of TiO_2 and mass flow rate of 0.0667 kg/s provided maximum efficiency, 8.66% higher than a water-based collector.

Ghasemi and team performed CFD simulation using FLUENT on PTC designed using GAMBIT. CuO/water and Al_2O_3/water HTFs are used in the simulation, and the results showed that with the addition of nanoparticles, the Nusselt number enhanced considerably compared to the base fluid [96]. The study also found that CuO/water increased the thermal performance of PTC and at the same Reynolds number and volume fraction Al_2O_3/water lowered the friction factor compared to the base fluid.

Coccia and team investigated the effect of six types of water-based nanofluid composed of Fe_2O_3, SiO_2, TiO_2, ZnO, Al_2O_3, and Au nanoparticle in low entropy PTC and found that viscosity increase with the increase in the concentration of nanoparticles resulted in the decrease in efficiency of HTF [95]. The convective heat transfer coefficient of the HTF with nanoparticles in the receiver was measured using a gauged apparatus in the experimental setup installed on the rooftop. The investigation conducted by Coccia et al., and Nicola et al., are summarised in Table 13. From the investigation, lower concentration of Au, ZnO, TiO_2, and Al_2O_3 nanoparticles show minimal thermal efficiency enhancements, while increasing their concentration had minimal improvements in heat transfer efficiency [95, 207].

Table 12: Recent study on water-based Nanofluid

References	**Research methods**	**Nanofluid used**	**Research outcomes**
			% increase in thermal efficiency
[208]	Experimental	Water/Al_2O_3	15.63-28.3
[209]	Experimental	Water/CuO	0.4-6.3
[210]	Experimental	Water/TiO_2	48-60
[211]	Experimental	Water/MgO	4-9.34
[212]	Experimental	Water/Al_2O_3	27.51-52.79

Since water is rarely used for very high-temperature applications (where direct heat transfer takes place), attempts are made to understand the results of adding nanoparticles in water. The results from various researchers show that there is heat transfer enhancement in the nanofluid compared to the base fluid. Different nanoparticles acted differently in the enhancement of heat transfer coefficients. Al-Waeli et al.,[213] Sardarabadi et al.[206], Khanjari et al.[205], and Ghasemi et al. [96] revealed in their results that Al_2O_3 nanoparticle exhibited moderately lower thermal property enhancement compared to TiO_2, ZnO, SiC, and Ag nanoparticles.

Table 13: Maximum outlet temperature of HTF with water as base fluid and corresponding thermal efficiency for 40, 50 60, and 70 °C temperature [214].

HTF	**40°C**		**50°C**		**60°C**		**70°C**	
	T_{max} (°C)	**$\eta(T_{max})$ %**	**T_{max} (°C)**	**$\eta(T_{max})$ %**	**T_{max} (°C)**	**$\eta(T_{max})$ %**	**T_{max} (°C)**	**$\eta(T_{max})$ %**
H_2O	47.79	63.14	57.73	62.73	67.67	62.30	77.61	61.85
TiO_2 1 wt.%	47.85	63.14	57.80	62.74	67.74	62.30	77.67	61.85
TiO_2 10 wt.%	48.49	63.12	58.43	62.71	68.36	62.28	78.29	61.83
TiO_2 20 wt.%	49.33	63.07	59.26	62.67	69.19	62.24	79.11	61.79
TiO_2 35 wt.%	50.94	62.96	60.87	62.55	70.78	62.13	80.69	61.68
SiO_2 1 wt.%	47.85	63.14	57.79	62.73	67.73	62.29	77.66	61.84

SiO_2 5 wt.%	48.09	63.13	58.04	62.72	67.97	62.29	77.90	61.83
SiO_2 25 wt.%	49.60	63.03	59.53	62.61	69.45	62.18	79.37	61.73
Fe_2O_3 5 wt.%	48.13	63.12	58.07	62.71	68.01	62.28	77.94	61.83
$Fe_2O_3$10wt.%	48.50	63.09	58.44	62.68	68.38	62.25	78.30	61.80
$Fe_2O_3$20wt.%	49.36	63.02	59.30	62.62	69.22	62.19	79.14	61.74
ZnO 1 wt.%	47.86	63.14	57.80	62.73	67.74	62.30	77.67	61.85
ZnO 5 wt.%	48.14	63.13	58.8	62.73	68.02	62.29	77.95	61.84
ZnO 10 wt.%	48.53	63.12	58.47	62.71	68.40	62.28	78.33	61.83
$Al_2O_3$0.1wt%	47.79	63.14	57.74	62.73	67.68	62.30	77.61	61.85
Al_2O_3 1 wt.%	47.85	63.14	57.79	62.73	67.73	62.30	77.67	61.85
Al_2O_3 2 wt.%	47.91	63.13	57.85	62.73	67.79	62.30	77.73	61.85
Au 0.1 wt.%	47.79	63.15	57.73	62.74	67.67	62.31	77.61	61.86

3.4.4. Ethylene glycol-based Nanofluids

One of the challenges faced while using water-based nanofluids is the nature of water to freeze in sub-zero condition; the best solution to reduce this condition is by using anti freeing agents like ethylene glycol. This anti-freezing property of ethylene glycol (EG) is used in solar thermal systems to reduce freezing in cold weather, and by adding nanoparticles, the thermal properties can be increased. Rashin et al. conducted a thermal and ultrasonic investigation on CuO-EG at a different temperature ranging from 308K and 328K and found that CuO/EG interactions predominate over CuO-CuO interactions at all temperatures[215]. Also, due to the weakening of the attractive intermolecular forces at high-temperature, the velocity was reduced. The reduction in velocity indicates that there is a threshold temperature beyond which the viscosity of CuO/EG molecule will increase beyond which the nanofluid cannot be used as HTF, also in conclusion this nanofluid can be used for low and medium temperature solar thermal applications.

Rose et al. investigated the application of GO/EG nanofluids in direct absorbing solar collectors for 0.004 - 0.016 vol.% and found that 0.012vol% of GO has better absorption and minimum reflectance over the visible spectral range [216]. Also, at an optimal weight of 0.045%, there was a significant improvement in absorbing solar radiation up to 99.6% found in the investigation done by Lavasani et al. [217].

The effect of specific heat, thermal conductivity and viscosity were studied by Suleiman Akilu et al. [218], using ceramic copper oxide/carbon nanoparticles in 80:20 wt.% which is dispersed in a fluid mixture of Ethylene glycol and glycerol (G) using 2 step process. The temperature range of 303.15 to 353.15 is taken for examination of the performance of the nanofluid. It is found that with the use of SiO_2-G/EG the specific heat capacity decreased by 5.7% and thermal conductivity by 6.9% and viscosity increased by 1.33 times compared to G/EG at a maximum concentration of 2% at 353.15K. However, 80% SiO_2 with 20% CuO in G/EG mixture resulted in a reduction in specific heat by 21.1%, an increase in thermal conductivity by 26.9% and viscosity enhanced by 1.15 times compared to G/EG base fluid. A study on Parabolic trough collector is made by Kasaeian et al. [219] using EG/MWCNT nanofluid with the volume fraction up to 0.3%, which revealed that the optical efficiency of the collector reached up to 71.4% with 0.3% volume fraction. It should also be noted that in this case, compared to pure base fluid, the solar collector has thermal efficiency up to 17%, which also added to the overall efficiency of the system.

By doping nanoparticles, EG has shown increment in thermal conductivity, but there was a decrement in specific heat capacity reported by Suleiman Akilu et al. [218]. Improvement in thermal conductivity is presented by Rashin et al. [215] and is in good agreement with Suleiman Akilu et al.[218] and Kasaeian et al.[219]. From the analysis of data, it can be concluded that EG can be used as heat transfer fluid but, the chance of using it as a storage material is infrequent. Therefore, ethylene glycol-based nanofluids can be used for those PTC power plants which do not have the requirement for thermal energy storage. Furthermore, works can be done in the enhancement of thermal conductivity by using a special kind of nanomaterials like Graphene and MXenes [78].

3.4.5. Synthetic Oil-based Nanofluids

Bellos et al. investigated the performance of Thermal oil, Thermal oil doped with Al_2O_3, and pressurized water in PTC designed and simulated using Solidworks for numerous operating conditions [103]. Al_2O_3 increased the mean efficiency of Thermal oil by 4.25% and pressurized water by 6.34%. Due to the turbulence created by rough inner surface (which acted like converging-diverging pattern) improved the mean efficiency by 4.55%. Collector pressure loss due to the rough inner surface is the main drawback of the design.

Somayeh Toghyani et al. investigated the performance of PTC and TES, using four different nanofluids (CuO, SiO_2, TiO_2, and Al_2O_3) operating under integrated Rankine power cycle using the concept of finite-time thermodynamic simulations[220]. CuO/Therminol-55 produces higher energy and exergy efficiency in comparisons with other HTF. The overall exergy efficiency of SiO_2, Al_2O_3, TiO_2, and CuO during TES charging are 24.2%, 29.4%, 32.8%, and 32.1%, respectively.

Kaloudis et al. investigated the performance of PTC using syltherm/Al_2O_3 nanofluid as HTF using CFD simulations [93]. In order to address the nanofluid modeling challenges, the two-phase model of HTF is preferred for simulation. The presence of nanoparticle enhanced heat transfer and absorber efficiency and found that a 10% boost in the efficiency can be obtained with Al_2O_3 concentration of 4%.

Wang et al. investigated the performance of PTC using synthetic oil (Dawtherm A)/Al_2O_3 nanofluid as HTF [115]. In the CFD simulation, it is found that as the concentration of Al_2O_3 increased the maximum temperature and temperature gradient of the collector decreased, increasing the performance of the collector. The results were compared with the conventional PTC system and found that using Nanofluids, the efficiency of the collector can be increased due to the reduction in a temperature gradient.

The absorber performance improved by 8%, 18% and 32% with the increase in the volume fraction of CuO in Terminol VP-1 from 0%, 2%, 4%, and 6% respectively. The thermal efficiency increased by 12.5% with CuO volume fraction of 6%. Also, the entropy generation reduced between 20% and 30% as the CuO volume fraction increases between 0% and 6% are the key findings of the simulation of performance investigation of PTC with CuO/Therminol-VP-1as HTF [117].

Since most of the PTC power plants in operation round the clock uses synthetic oil as HTF, it would be easier to enhance the thermal efficiency of the PTC by doping with nanoparticles. By comparing the studies of Somayeh Toghyani et al. [220] and Mwesigye et al.[117]. CuO nanoparticles have positive effects on the thermophysical properties of synthetic oil compared to SiO_2, TiO_2, Al_2O_3. Bellos et al. [103] accomplish the reduction of the temperature gradient, increase in thermal efficiency by 0.76%, and Nusselt number by 40% by doping CuO nanoparticles which are in line with the thermophysical enhancement obtained by SomayehToghyani [220] and Mwesigye et al.[117] using CuO nanoparticle.

3.4.6. Molten salt-based Nanofluids

The investigations on MSBNF is an interesting area of research, which is still in its early stages. Recently, significant efforts have been imposed on developing empirical results. A brief review of the existing works on MSBNF is reported in this section.

Ho and Pan investigated the performance of pure Hitec salt by measuring the mean Nusselt number by adding 0.25 wt.% Al_2O_3 Nanoparticles, found that there is an 11.6% increase in the Nusselt number, but the result was lasting approximately for 30 min [221]. In conclusion, the study proved that Hitec Molten salt doped with Al_2O_3 Nanoparticle, enhanced specific heat capacity by less than 0.25%. The major drawback of molten salts is its high melting point. By doping of nanoparticles, it is possible to reduce the melting point of eutectic salts [222]. Different combination of inorganic salts doped with different Nanoparticles is presented in Table 14.

Table 14: Summary of experimental work on MSBNF with base fluid, melting point, and Nanoparticles used.

Base fluid	Composition	Nanoparticles used	Melting point ^0C	Reference
Solar Salt	$NaNO_3$-KNO_3 (50:50mol)	Al_2O_3	222	[58, 223]
		SiO_2		[58]
		TiO_2		[58]
Potassium nitrate	KNO_3	Al_2O_3	334	[51, 223]
	$BaCl_2$-NaCl-$CaCl_2$-LiCl (15.9:34.5:29.1:20.5mol)	SiO_2	378	[224]
	KCl-$CaCl_2$-LiCl (44.2:50.5:5.3 mol)	SiO_2	340	[225]
	Li_2CO_3 (62:38mol)	Al_2O_3	488	[226, 227]
	KNO_3-$LiNO_3$ (58.8:41.2mol)	SiO_2	130	[228]
	$LiNO_3$-$NaNO_3$ (45:55mol)	SiO_2	192	[228]
	LiCl-$LiNO_3$	SiO_2	224	[228]
	Li_2Co_3-K_2CO_3 (62:38 mol)	Al_2O_3	488	[227, 229]
HitecXL	$Ca(NO_3)2$:KNO_3-$NaNO_3$ (49:30:21 mol)	SiO_2	120	[41]
	$LiNO_3$-$NaNO_3$-KNO_3	SiO_2	<100	[230]

	(38:15:47 mol)			
	$LiNO_3$-KNO_3-$NaNO_3$-KNO_2 (9:33.6:42.3:15.1 wt.)	Al_2O_3	<100	[231]
	$NaNO_3$	Al_2O_3	308	[232]
	NaCl-KCl(50:50 wt.)	Al_2O_3	658	[232]
	$Li2CO_3$-$K2CO_3$ (62:38mol)	SiO_2	488	[233]
Hitec	KNO_3-$NaNO_3$-$NaNO_2$ (53:40:7 mol)	SiO_2	141	[233]
	$LiNO_3$	Al_2O_3	254	[233]

Stability of Molten Salt-Based Nanofluids at high temperature

The stability of MSBNFs is the critical property that needs to be ensured before its application in the PTC system. Depending upon the working temperature range of the PTC, the thermal degradation temperature of MSBNF should be determined by thermogravimetric analysis. Gomez et al. used the T3 method to determine the thermal stability of Hitec XL molten salt, where maximum stability temperature is determined when the salt has lost 3% of its anhydrous weight [234]. The test depicted that the salt has stability up to 500ºC and can be utilized for PTC systems.

Investigation on Kinetics of thermal decomposition of Hitec salt by adding Na_2CO_3 was investigated by Gimenez and Fereres [235], interestingly the result showed that the stability of the salt increased meanwhile, Na_2CO_3 had a negative effect on the thermal stability of solar salt. Figure 18 shows the thermal stability curve for pure Hitec and Hitec with 5% Na_2CO_3 at different heating rates.

Zhou and Eames examined the thermal stability of $LiNO_3$–NaCl eutectic mixtures by heating and cooling the salt from 50ºC to 250ºC in 50 cycles [236]. From the study, it was found that the weight loss is within 0.02% for every cycle. For high-temperature stability, the salt is tested for TGA, and the results showed that the decomposition temperature of the salt is between 400ºC and 450ºC.

Chen and Zhao investigated on the thermophysical properties of Hitec XL molten salt using STA (Simultaneous Thermal Analysis) and XRD analysis [53]. The STA and XRD result showed that cyclic thermal stability is higher in the temperature range 50-250ºC, and the decomposition temperature of the salt is 600ºC, respectively. Figure 19 shows the decomposition curve for Hitec XL molten salt with the composition 32wt.%$Ca(NO_3)_2$-24 wt.% $NaNO_3$ and 44wt.%KNO_3.

Xiong et al. investigated the thermophysical properties of solar salt doped with nano-silica by TGA(Thermo Gravimetric Analysis) the decomposition temperature of the solar salt, $NaNO_3$, KNO_3 is 601ºC, 603.3ºC, 610.4ºC respectively [237]. By the addition of nano-silica, the decomposition temperature of the eutectic mixture increased to 619ºC, 631.5ºC and 630.2ºC for the solar salt, KNO3, and NaNO3 salts respectively and there was a noticeable increase in thermal stability and working temperature range when compared with solar salt. Figure 20 shows the thermogravimetric analysis of solar salt, $NaNO_3$, and KNO_3.

Chen, M. et al.[74], and Zhao and Wu [77] studied the decomposition temperature of solar salt by adding $LiNO_3$ and $Ca(NO_3)_2$ and reported that the decomposition temperature lies between 500 to 600 ºC. However, Olivares and Edwards [238] reported that the decomposition of solar salt depends on the working atmosphere of the molten salt. It was found that NO gas release by the Nitrate salts occurs at 325 ºC, 425 ºC, 475 ºC, 540 ºC in the presence of argon, nitrogen, air, and oxygen respectively. The results obtained by Coscia et al. [73] Fernández et al.[76], Chen, M. et al. [74], and Zhao and Wu [77] justifies the decomposition value obtained by Olivares and Edwards [238]. From the literature, it can be concluded that PTC need not be maintained in any particular atmospheric condition to preserve the chemical structure of the molten salt from decomposition.

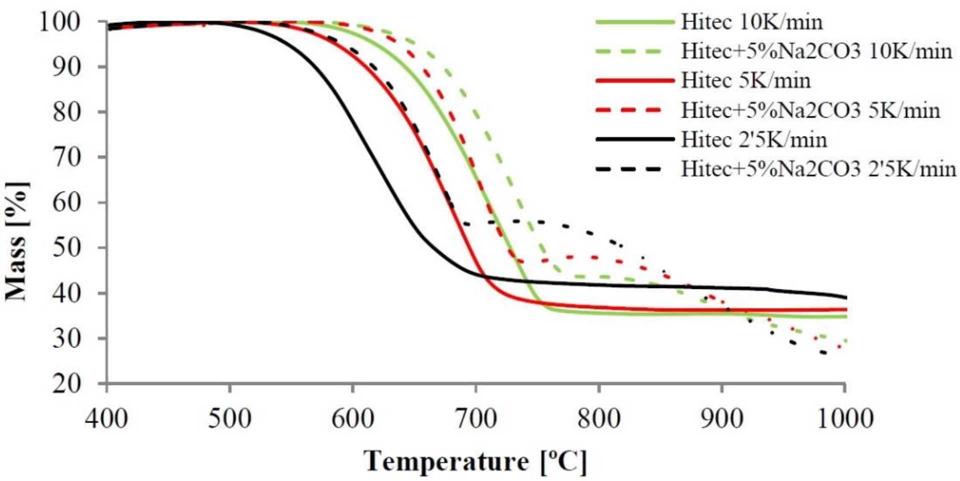

Figure 18: Thermal stability of pure Hitec and Hitec with 5% Na_2CO_3 at different heating rates [235]. Reprinted with permission from Elsevier, Energy Procedia "Effect of Heating Rates and Composition on the Thermal Decomposition of Nitrate Based Molten Salts" P. Gimenez, Lic.No. 4676390056874.

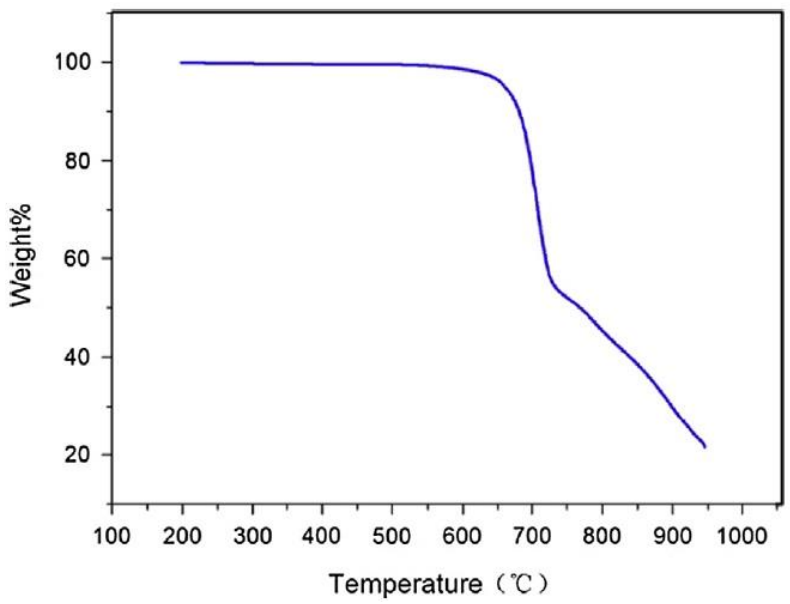

Figure 19: Decomposition of Hitec XL ($Ca(NO_3)_2$:KNO_3: $NaNO_3$ 32:24:44) [53], Reprinted with permission from the Elsevier, Solar Energy "Thermophysical properties of $Ca(NO_3)_2$-$NaNO_3$-KNO_3 mixtures for heat transfer and thermal storage" (p.177) Lic.No. 4676380886632.

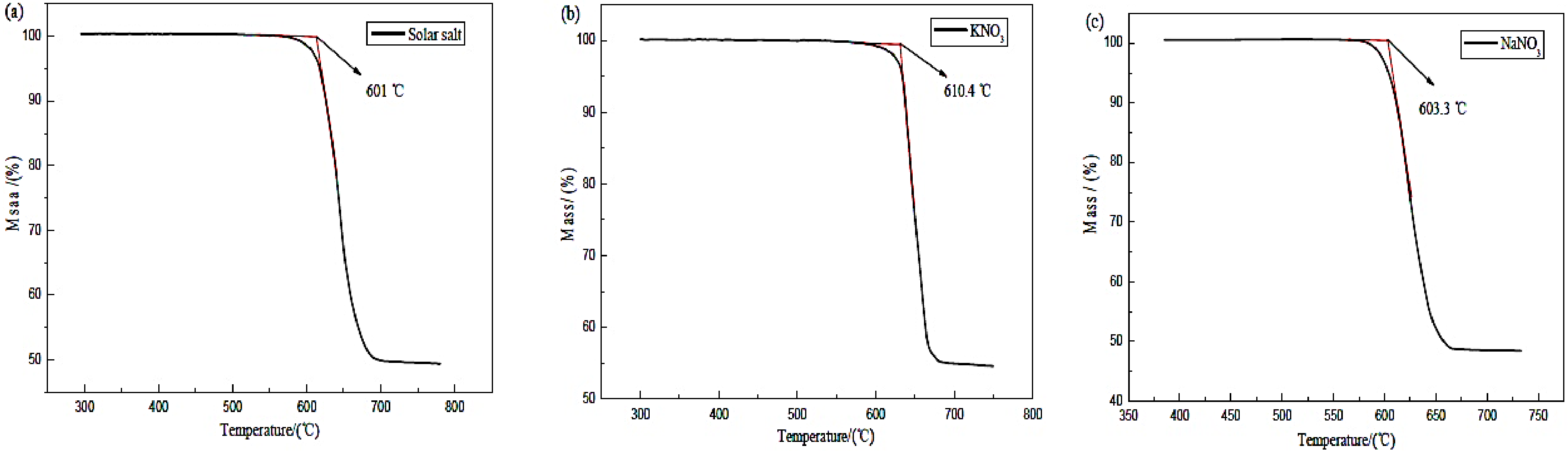

Figure 20: TGA Analysis of Solar salt KNO_3 and $NaNO_3$[237], Reprinted with permission from the Elsevier, Energy Procedia "Experimental investigation into the thermos physical properties by dispersing nanoparticles to the nitrates, Yaxuan Xiong, (p. 5554) Lic.No. 4676351284616.

3.4.7. Hybrid nanofluids

Doping of nanofluids into the HTFs acquired importance as a result of challenges in achieving superior thermal and optical characteristics of conventional HTFs like water, synthetic oil, and Ethylene glycol. Therefore, a state-of-the-art heat transfer fluid can be introduced by doping two or more kinds of nanoscale solid particles into the base HTF for enhancing its thermal and optical properties to absorb maximum solar radiation. Exceptional enhanced thermophysical properties can be obtained by these HTFs when compared with conventional HTFs [239]. Recently, by the experimental investigation, researchers focused on a different combination of these HTFs in solar thermal applications. Tullis et al. investigated the effect of radiation on the synthesized hybrid nanofluid [240]. Additionally, CuO and Al_2O_3 nanoparticles are doped in the base of water, ethylene glycol and combination of both to examine the consequence of direct average radiation on the hybrid nanofluid. Based on the outcome, water-based hybrid nanofluid improved the extinction coefficient value compared to ethylene glycol-based and the mixture of water and ethylene glycol-based hybrid nanofluid. Chen et al. investigated the solar energy absorbing capacity of copper oxide/antimony doped tin oxide (CuO/ATO) and found an increment of 10.1% and 9.8% in SWAF (solar weighted absorption fraction) contributed to CuO and ATO nanofluid respectively [241]. In the research performed by Fang and Xuan on CuO-ZnO/water hybrid nanofluid, three different nanofluids comprising of CuO/water, CuO-ZnO/water with 0.5:0.5 concentration and CuO-ZnO/water with 0.7:0.3 concentration of nanoparticles is investigated. The volume fraction from 0.001 % to 0.01 % is considered for the study; they found the optimum performance is achieved with a volume fraction of 0.01%. According to the investigation performed Cu-ZnO/water hybrid nanofluid with 30% zinc oxide gave the photothermal conversion efficiency of 97.35% which is highest among the studied samples. The effect of temperature on photothermal efficiency is presented in Figure 21 [242].

Due to the high thermal conductivity of hybrid nanofluids, they are suitable for solar thermal systems [218]. Akilu et al. conducted a comparative study between SiO_2/EG and SiO_2-CuO/EG nanofluids by investigating their performance in solar thermal systems. They studied and compared the specific heat capacity, thermal conductivity, and viscosity of both the nanofluids whose results are presented in Figure 22. In the research conducted by Bellos et al., hybrid and conventional nanofluids are compared by testing their performance in PTC. They tested 3% Al_2O_3/oil, 3% TiO_2/oil, and 1.5%Al_2O_3-1.5% TiO_2/oil in PTC and found a 1.8% enhancement in the efficiency mainly due to enhancement in Nusselt number when hybrid nanofluid is used as HTF [111]. The enhancement of thermal properties by the hybrid nanofluids, when compared with mono nanofluids, is presented in Figure 23.

From the above discussions, it can be summarised that hybrid nanofluids have the ability to enhance the performance of the PTC system significantly. In addition to enhancement in the thermodynamic properties, hybrid nanofluid also enhance the optical efficiency of the system which results in further increment in the overall efficiency.

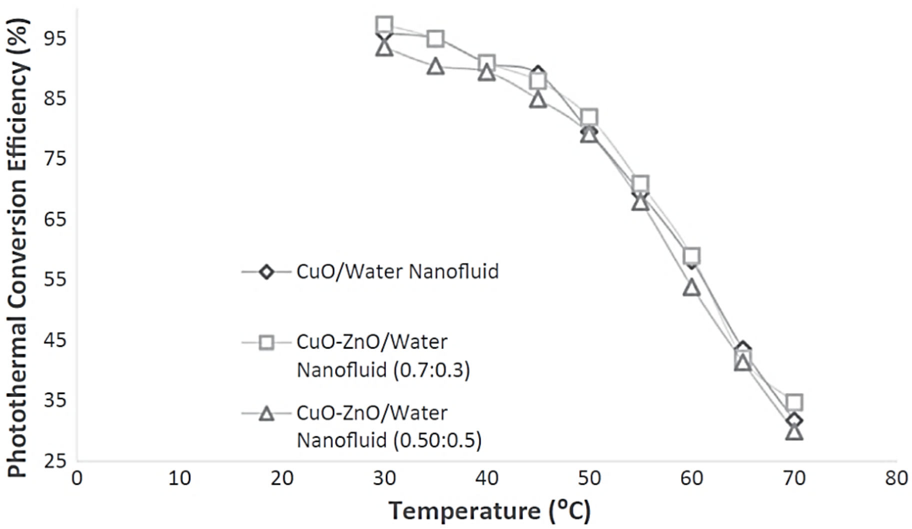

Figure 21: Effect on Photothermal conversion efficiency as a function of temperature for mono and hybrid nanofluid, a comparison [242].

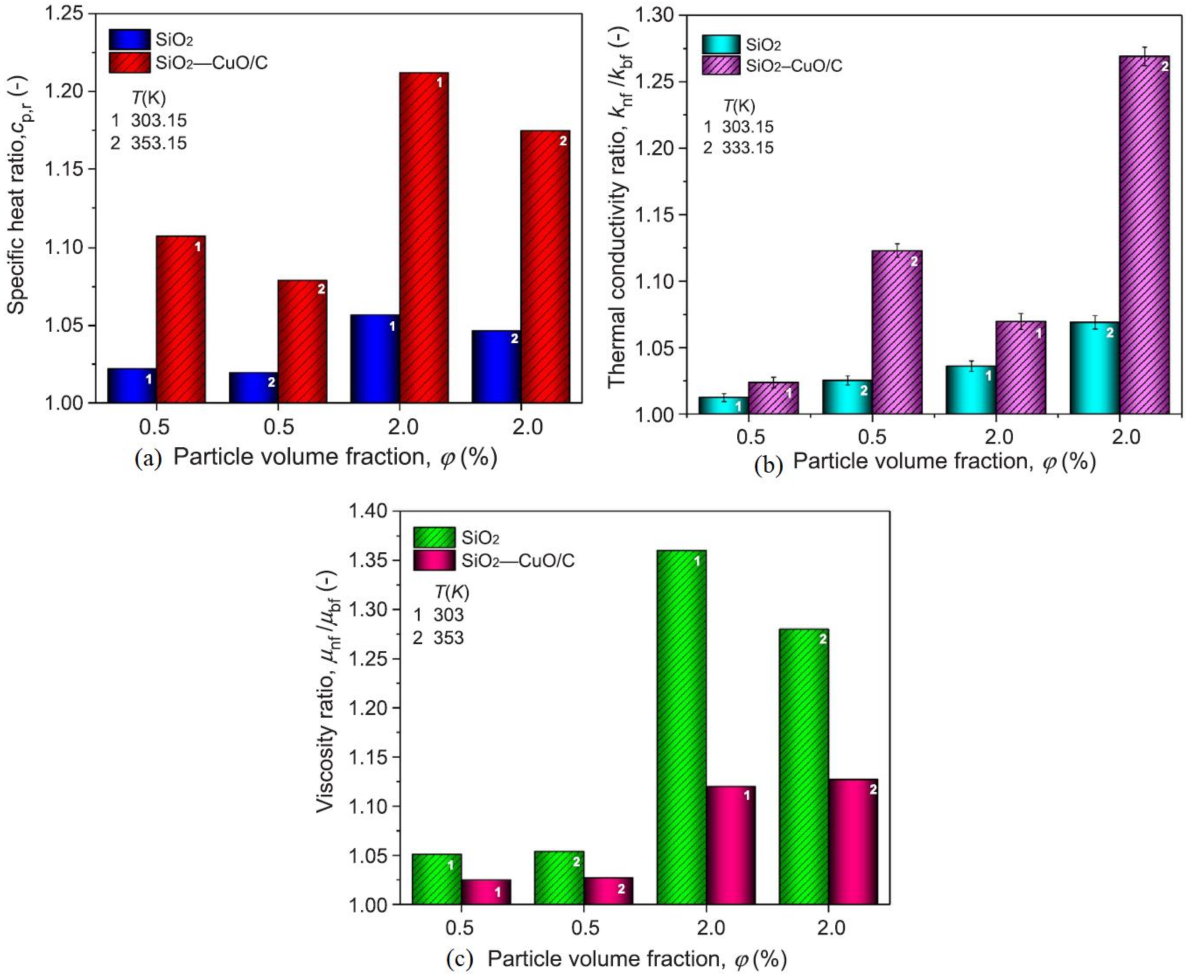

Figure 22: Thermophysical properties comparison between SiO_2 and SiO_2-CuO nanofluids. (a) Specific heat capacity, (b) Thermal conductivity, (c) Viscosity [218].

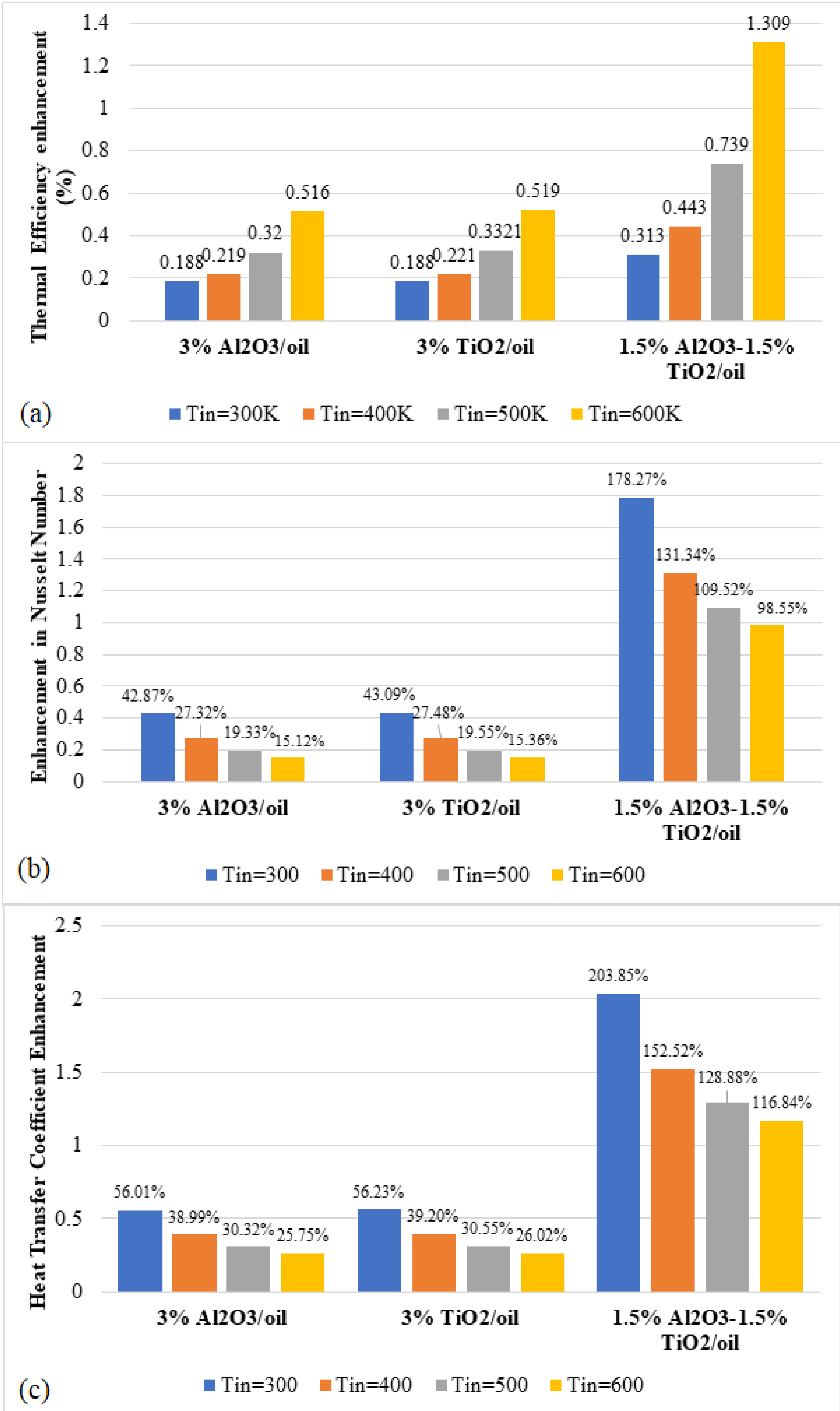

Figure 23: Comparison of (a) thermal efficiency enhancement, (b) Enhancement in Nusselt number, (c) heat transfer coefficient enhancement of Al_2O_3/oil, TiO_2/oil, and Al_2O_3-TiO_2/oil nanofluids [111].

3.5. Gaseous Heat transfer fluids

The utilization of gaseous working fluid in PTC is yet another method to fulfill the necessity of operating at higher temperature levels. Using water/steam, synthetic oil, or molten salt as HTF in PTC has some limitations [243]. They are

- Maintaining high pressure of water to keep it in a liquid state in water operated PTC.
- Low thermal stability at high temperatures in synthetic oil.
- High freezing point in molten salt.
- High corrosion of absorber tube by synthetic oil and molten salt.
- Poor environmental friendliness and cost-effectiveness.

To overcome these disadvantages, gaseous heat transfer fluids are utilized as HTF in PTC. For instance, gasses like air, carbon dioxide, nitrogen, helium, and neon are non-toxic, and they are abundantly available making it cost-effective. The use of gasses in PTC makes it possible to operate the plant at high-temperature levels, hence enhancing thermodynamic cycle efficiency[39].

Due to limitations like thermal stability, operating temperature corrosiveness and eco-friendliness of the HTF, the air is used as HTF for the first time in a peak pilot-scale solar power plant at Ait Baha, Morocco. The plant has a maximum operating temperature of 650 ºC and thermal power output of 3.9 MW_{th} [243]. The design parameters of collectors and receivers of the PTC are unique and different from other trough collectors. Bi-axially oriented polyester films whose top membrane is silvered are used as collectors. Interestingly, the receiver and the absorber tube is protected from dust, wind, and external impact by an inflated membrane of ethylene tetrafluoroethylene (ETFE) at the top, which is shown the Figure 24 and Figure 25. Moreover, the design of absorber follows a cross-flow design where temperature gain is attained in each absorber cavity, the inlet and outlet of the absorber are placed on the same side for this reason as shown in Figure 26.

PTC using air as HTF is effectively used in the desalination plant humidification and dehumidification (HDH) system. Fahad et al. [244] conducted a comprehensive thermodynamic analysis of an HDH system by the integration of PTC using air as HTF. Two types of systems are investigated, in the first system, PTC is placed before the humidifier and in the later system, PTC is placed between humidifier and dehumidifier. The study demonstrated that the gained output ratio (GOR) is higher in the other system and emerged as the best configuration for the desalination plant.

Figure 24: Parabolic trough collector using air as HTF at Ait Baha, Morocco [245].

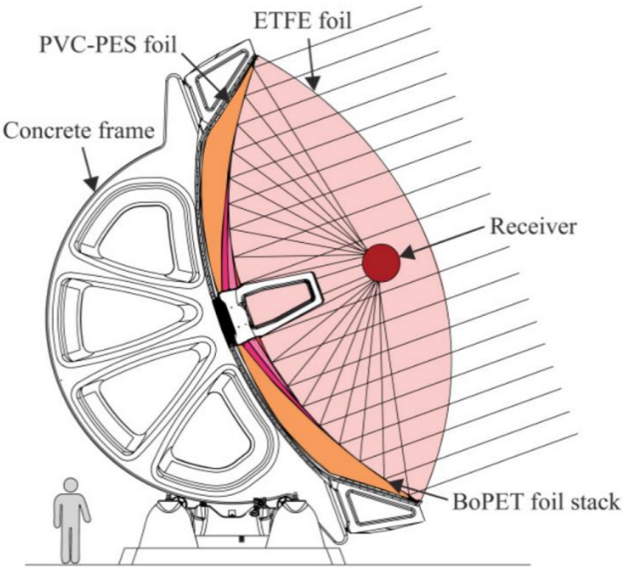

Figure 25: Schematic representation of Ait Baha, solar Morocco power plant [243].

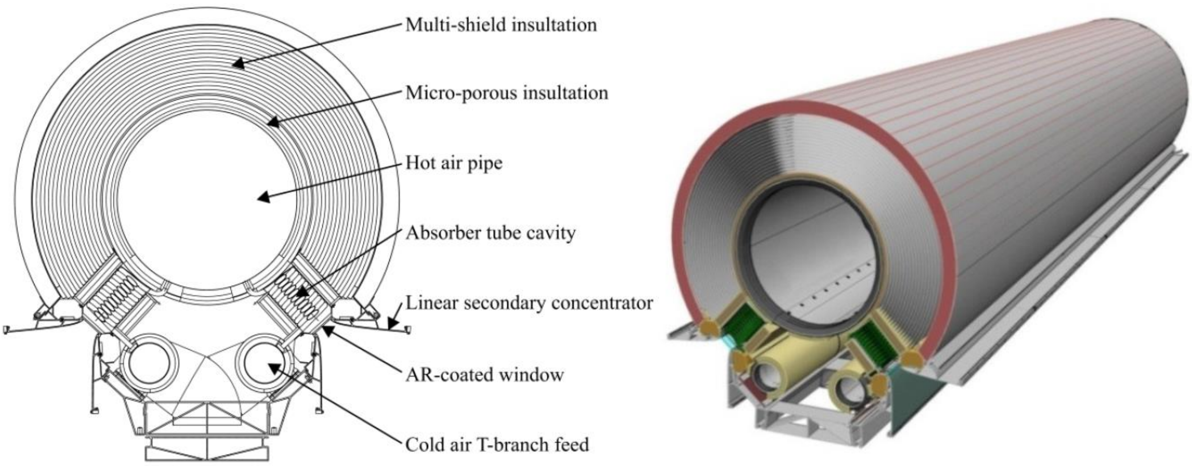

Figure 26: Schematic representation (Left) and CAD model (Right) of the receiver at Ait Baha Morocco [243].

Carbon dioxide was demonstrated to perform better at high temperature compared to air. Moreover, carbon dioxide behaves as a supercritical fluid above 30.98 ^{o}C temperature and 73.77 bar pressure. At this point, the density and thermal conductivity of carbon dioxide is higher compared to its gaseous state. This property of supercritical carbon dioxide makes it better HTF for the PTC application. In supercritical state carbon dioxide gives better thermal and hydronic performance compared to gaseous state hence enhancing the exergy efficiency of the system [246]. Islam et al. investigated the influence of thermodynamic and flow parameters like heat removal factor, collector aperture area, collector efficiency, and mass flow rate. Carbon dioxide, nitrogen, and ammonia are used as HTF for the analysis. It is concluded that the collector aperture area, mass flow rate, and concentration ratio of the collector significantly affect the heat removal factor and collector efficiency [247].

Bellos et al. investigated the energetic and exergetic performance of nitrogen, carbon dioxide, helium, argon, and neon. They found that nitrogen has a similar performance to air with the exergetic efficiency of 0.4169 for inlet temperature of 893 ^{o}C and a flow rate of 0.15 Kg/s. The exergetic efficiency of CO_2 is found to be 0.431 for inlet temperature of 922 ^{o}C and a mass flow rate of 0.2 Kg/s. Among all the gases considered, helium is considered as the best HTF which showed the best exergetic efficiency of 0.4338, while neon showed 0.4047 and 0.3857 by argon. Helium gave the best output because of its higher heat transfer coefficient and lower pressure drop in the absorber. The optimum flow rate of 0.0365 Kg/s is maintained for helium gas which is lowest compared to other gases in 913 ^{o}C for maximum exergy efficiency. The maximum flow rate and inlet temperature of 0.125 kg/s at 853 ^{o}C and 0.225 kg/s at 833 ^{o}C are maintained for Neon and argon respectively for optimum exergetic efficiency. Table 16 presents the energetic and exergetic efficiency of various gases obtained by Bellos et al. and Table 6 compares the thermophysical properties of gaseous and other high-temperature HTF [39].

Ravindra et al. conducted a detailed comparative study of HTF for concentrated solar power applications. They concluded that for similar collector conditions, gaseous fluids required larger absorber tube diameters compared to Hitec XL molten salt and liquid fluids working between 673-1150 ^{o}C temperature. Helium proved to be more compact in terms of absorber tube diameter compared to CO_2 in the temperature range of 773- 1150 ^{o}C. However, CO_2 is more feasible because of its ease of availability in nature. When compared to molten salt and helium, the performance of both is best in terms of heat transfer area and length of the absorber tube. Compared to all gaseous and liquidus HTF, CO_2 performs better for the entire working temperature range in terms of energy and exergy efficiencies. Table 15 presents the comparison of the physical properties of gaseous HTF with liquidus HTF [248].

Table 15: Comparison of physical properties of liquid and gaseous HTF [248].

Working fluid	Toxicity	Flammability	Corrosivity	Temperature limit for stable performance
Therminol VP1	Toxic	Flashpoint(383K)	Copper corrosive	Up to 400°C
Dowtherm Q	Toxic	Flashpoint(393K)	Noncorrosive	Upto400°C
Hitec XL	Non-toxic	Non-flammable	Low Corrosivity	Upto550 °C
He	Nontoxic	Non flammable	Noncorrosive	>550 °C
CO2	Nontoxic	Non flammable	Noncorrosive	>550 °C

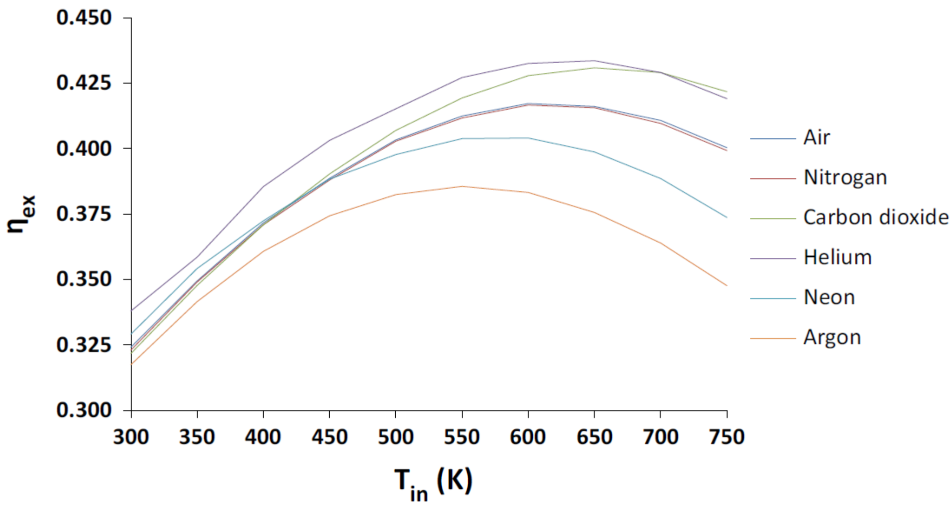

Figure 27: Maximum possible exergetic efficiency of various gaseous HTF as a function of inlet temperature

Table 16: Exergy and Energy efficiency of various gases used as HTF in PTC [39].

Working Fluid	**$T_{in, Optimum}$ (K)**	**$m_{optimum}$ (Kg/s)**	**η_{ex}**	**η_{th}**	**ΔP (kPa)**	**h (W/m^{2}K)**
Air	620	0.15	0.4174	0.6459	6.728	139.8
Nitrogen	620	0.15	0.4169	0.6475	6.886	139.5
Carbon dioxide	660	0.2	0.431	0.6771	7.012	172.6
Helium	640	0.035	0.4338	0.6631	3.839	216.1
Neon	580	0.125	0.4047	0.643	7.598	130.2
Argon	560	0.225	0.3857	0.6274	10.22	100.6

3.6. Liquid Metals as the heat transfer fluid

The application of liquid metals for heat transfer applications has been used in thermo-nuclear industries. Lately, liquid metals are being investigated for their use in solar thermal applications. However, until now the utilization of liquid metals in commercial parabolic trough power plant has not been done, but their promising properties like broad working temperature range (98 ºC – 883 ºC) [249] efficient heat transfer properties, low viscosity has drawn the attention of researchers towards the application of liquid metals in solar thermal engineering [7]. Some of the key properties of liquid metals are discussed in Table 17. From the Table 17 we can say that liquid metals are relatively costlier when compared to air (0 $/kg) water (~0 $/Kg), oil (0.3-5 $/kg), molten salt HTFs (0.93-1.3 $/Kg). Also, the specific heat capacities of the liquid metals are lower and hence they are poor sections for TES systems. The following section discusses state-of-the-art liquid metals that are under research which can be used as HTF in parabolic trough collectors.

Almeria solar test plant in Spain first used liquid sodium as HTF for the operation of 500 KWe plant. Even though the performance of the sodium was appreciable, the test plant was decommissioned because of sodium fire occurred in 1986 [250]. The fundamental thermophysical properties of sodium are discussed in Table 17. The main disadvantages of sodium metal are its combustibility when exposed to moisture or water, costlier compared to state-of-the-art HTFs. Sodium is less corrosive compared to other liquid metals with steel. However, extensive research needs to be conducted on the corrosivity of liquid metals. Therefore, silicon carbide and stainless steels are the compatible piping material suitable for liquid metals.

Pb-Bi liquid metal eutectic mixture is another HTF under investigation in research communities. It is a eutectic mixture of 44.5 wt.% of Lead and 55.5 wt.% of Bismuth. The mixture is also called as LBE. The eutectic mixture melts at ~125 ºC, which is similar to the melting point of Hitec XL molten salt. The boiling point of the mixture is ~1533 ºC, the specific heat capacity, thermal conductivity, and viscosity of LBE is 0.15 KJ/kgK, 12.8 W/mK and 0.00108 Pa.s respectively at 600 ºC [250].

However, another liquid metal under research is the eutectic mixture of Na-K. It is a eutectic mixture of 22.2 wt.% of sodium and 77.8 wt. % of potassium. The specialty of these metal mixtures is that it is in the liquid phase even at 25 ºC. The melting point of Na-K is -12 ºC and stable up to 785 ºC which is an added advantage [7]. The mixture has a specific heat capacity of 0.87 KJ/kgK, the thermal conductivity of 26.2 W/mK, and viscosity of 0.00018 Pa·s at 600 ºC. The cost of the mixture is four times the cost of solar salt. Investigation on the corrosion of Na-K needs to be conducted since the data is not available in the literature.

Interestingly, there are very few investigations on liquid metals, in which the liquid metals are enriched by doping them with nanoparticles. Sarafraz et al. investigated the performance of nano-enhanced gallium metal by enriching it by doping with 5wt.%, 10 wt.%, and 15 wt.% of Al_2O_3 nanoparticles. The prepared gallium nanosuspensions were tested in microchannel blocks at 200 ºC. The results showed that the thermal performance of gallium nanosuspensions was maximum in laminar and turbulent regime at the mass fraction of 10 wt.%. However, with the increase in the mass concentration of Al_2O_3 reduced the thermo-hydraulic performance of the HTF [251]. A similar investigation was conducted on liquid Indium by doping copper oxide nanoparticles under lower heat flux conditions. The experiment was conducted to determine the effect on pressure drop, heat transfer coefficient, and friction factor in a microchannel when indium doped with copper oxide is used as HTF. The results showed that for a lower concentration of copper oxide, there was no significant enhancement in the heat transfer properties. However, the maximum heat transfer properties were obtained at a mass concentration of 8 wt.% and the heat transfer coefficient decreased for the mass concentration greater than 8 wt.% [252].

When compared to state of the art heat transfer fluids for parabolic trough collectors like synthetic oil and molten salts, extensive research needs to be conducted to enhance the properties of liquid metals [7]. The properties like specific heat capacity, enthalpy, and corrosion-resistant properties of liquid metals are possible to be enhanced by doping it with an optimum quantity of nanoparticles [252].

Table 17: Properties of liquid metals that are under investigation for application in PTC [7].

Name	**Composition (wt.%)**	**Melting point (ºC)**	**Specific heat capacity @ 600 ºC (KJ/KgK)**	**Thermal Conductivity @ 600 ºC (W/mK)**	**Viscosity @ 600 ºC (Pa.s)**	**Stability limit (ºC)**	**Cost ($/kg)**
Na	-	98	1.25	46.0	0.00021	883	2
Pb-Bi	Pb:Bi:44.5:55.5	125	0.15	12.8	0.00108	1533	13
Na-K	Na:K:22.2:	-12	0.87	26.2	0.00018	785	2

	77.8

3.7. Ionic Liquids

High thermal energy storage capacity and high thermal stability are considered as significant requirements for the next generation of solar thermal collectors in terms of cost-effectiveness [253]. Ionic liquids (ILs) have promising potential as working fluids, especially for the next generation solar thermal collectors due to the superior thermo-physical properties. The unique combination of properties of ILs such as negligible volatility, electrochemical stability, thermal stability, and ionic conductivity highlights the use of these materials as a supreme replacement for volatile organic solvents [254]. Due to the presence of the enormous number of anions and cations, there is a large number of possibilities for the proposed ILs with varying properties. Organic cations (imidazolium, pyrazolium, triazolium, thiazolium, oxazdium, pyridinium, pyridazinium, pyrimidinium, and pyrazinium) and organic or inorganic anions (halogen, fluorinated) are a major part of the ILs. However, relatively few applications have considered these materials (ILs) due to the physical properties (notable viscosity) which limits the applicability of ILs. This drawback can be addressed by using molecular solvents, although lower thermal stability might be considered as another issue of using molecular solvent for reducing viscosity. A mixture of a variety of ILs (IL-ILs mixture) seems a possible method to maintain the desirable properties of these materials. There are several applications with IL-ILs mixture that indicates promising consequential outputs comprised of dye-sensitized solar cells [255], solvent reaction media [256], gas solubilities [257] and a gas chromatography stationary phase [258]. According to the literature, there have been some limitations of physical measurements for IL-ILs mixtures including melting performance [259], nanostructures [260], molecular interrelation [261], dielectric measurements [262], transport and volumetric properties [263], responses to solvatochromic probes [264] and optical heterodyne-detected Raman-induced Kerr effect spectroscopy (OHD-RIKES) [265]. ILs are a specific class of molten salt with a low melting point of less than 100 °C as heat transfer fluids (HTFs) with maximum operating temperature of 459 °C [266]. A recent study has revealed that ILs have less thermal stability in the range of 200-250 °C [267]. The operation of the collector field with Therminol VP-1 is similar to the collector which is operated with IL. Despite that ILs are expected to operate as high-temperature HTF for parabolic trough power plants, but there is scarce available data on corrosiveness, hydrogen formation or freezing of these materials during operation. In terms of safety aspects, ILs are eco-friendly materials with low environmental effects and considered as not toxic, not flammable and not hazardous [268]. Eck et al. reported that the expected price for IL is meager, but due to the low operation temperature, the efficiency of the power block will be lower too. Due to this deficiency (low operation temperature), there is a necessity of increasing the collector field size which will outweigh the cost-effectiveness of the HTF (IL). Paul TC et al. [269] evaluated the effectiveness of the IL induced with nanoparticles in parabolic trough collectors. They used Al2O3 nanoparticles with a concentration ratio of 0.9 wt% and reported thermal conductivity enhancement by 11% and heat capacity increment by 49%. Bridges et al. [270] mentioned that Nanoparticle Enhanced Ionic Liquids (NEILs) based HTF are fulfilling the required characteristics for concentrated sola power (CSP) systems. According to Nieto de Castro et al. [271] IoNanofluids, a combination of several imidazolium and pyrrolidinium based ILs/MWCNTs represents higher heat capacity and thermal conductivity in compare with the base ILs. Bridges et al. [270] mixed 1-Butyl-2,3-dimethylimidazolium bis(trifluoromethylsulfonyl)imide ([C4mmim][NTf2]) with Al2O3 nanoparticles (40 nm) and achieved enhancement by 40 % at volumetric heat capacity. In the conducted experiments by Wittmar et al.[272] they used hydrophobic and hydrophilic imidazolium-based ionic liquids with surface-functionalized SiO2 with achievement of higher colloidal stability and promising rheological performance. The effect of particle size, surface state and volume fraction of gold nanoparticles on thermal conductivity of a stable ionic liquid based nanofluid proved significant improvement in thermal conductivity value [273]. Perissi et al. [274] evaluated the corrosiveness of four different ILs in contact with AISI 304 and AISI 1080 steels (frequently used in solar collector plants). They conducted the experiments at 220 °C within ten days. According to their experiments, the resistance of the corrosion-resistance of the steel substances in contact with different ILs is still not satisfactory in the working operating temperature of parabolic trough collectors (220 °C) in open-air condition and more studies are necessary to be conducted comprehensively. Wu et al.[266] synthesized many types of ILs such as [C4min][PF6], [C8min][PF6], [C4min][bistrifluromethane sulflonimide], [C4min][BF4], [C8min][BF4] and [C4min][bistrifluromethane sulflonimide] and conducted comprehensive study in term of thermos-physical properties such as degradation temperature, melting point, viscosity, heat capacity and thermal conductivity. They found highly promising thermal storage and heat transfer properties for the studied ILs which proved the excellent performance of these materials for solar thermal power plants. Jian Liu et al. [275] studied experimentally and numerically ionic liquid/graphene nanofluids as a special heat transfer fluid with high stability and very low vapor pressure (highly desirable characters) for both concentrated solar collector and high temperature direct solar collectors. They reported that with concentration of 0.0005 wt% of graphene in 5 cm receiver under 20 kW m-2 the receiver efficiency could be maintained 0.7 at 600 K. Zhang et al. [276] showed that addition of small amount of carbon-coated Ni (Ni/C) to [HMIM][MTF2] can noticeably enhance optical properties of the ILs.

3.8. Vegetable oil

Vegetable oil is used in food processing industries, electrical industries, cutting oil for machining, biodiesels for the internal combustion engine and HTF for heating and cooling applications. However, due to depletion in fossil fuel reserves, vegetable oil is an alternative for high-temperature applications, especially solar thermal plants. Moreover, vegetable oil has thermophysical properties like thermal oil used for solar power applications. Very less work has been done in the thermophysical and rheological study of vegetable oil as HTF.

Pikra et al.[277] investigated the development of a small-scale concentrated power plant of 10 kW_{el} utilizing parabolic trough as a solar collector and used palm oil as the HTF and TES. They picked palm oil rather than mineral oil due to accessibility, ease, and comparable physical properties with synthetic oil and mineral oil. The TES capacity limit of the small-scale plant is 107 kW for 6 h run time with palm oil temperatures of 150 °C and 200 °C, for the low and high working temperature respectively.

Hoffmann et al. investigated density, specific heat and thermal conductivity of soybean, palm, rapeseed, sunflower, copra, and jatropha oils at the temperature range of ambient and 250ºC. They found that rapeseed oil offered better thermophysical properties at 210ºC; results showed that thermal conductivity, dynamic viscosity, specific heat, and density was 0.14 W/mK, 3.2 mPas, 2.49 kJ/ kgK, and 788 kg/m^3 respectively. It was found that all seven vegetable oils had similar heat transfer properties. Vegetable oils are widely used in solar CSP due to their low cost, availability, biodegradability, and lower greenhouse gas emissions. However, the main disadvantage of vegetable oils is their tendency to oxidate. Therefore, substantial research is required to enhance their oxidation stability, to provide adequate feedback on their application [278].

4. Prospects of parabolic trough collector

The parabolic trough collector is considered as the future of clean energy generation technology. The cost of PTC has radically reduced, and the performance has drastically enhanced due to the extensive research conducted on PTC by research institutes like International Energy Agency (IEA) on solar projects like SolarPACES [279]. Due to the enhancement in the performance of pilot plants, R&D in large scale testing of PTC plants, and increased mass production of these power plants, made PTCs to produce lowest cost green energy in the world and promises competitiveness in cost with fossil fuel utilizing power plants [280]. Due to the design parameters of PTC and its thermal characteristics, the PTC can be hybridized in many ways to improve the availability of power by the system. The PTC power plant can be hybridized with fossil fuel or natural gas power plants to produce power round the clock which in turn will cut the cost of power production. PTC along with a photovoltaic and thermoelectric generator, will be an innovative way to enhance the performance of the photovoltaic systems and augment the overall thermal efficiency of the PTC [281].

Various methods have been adopted to reduce the losses and improve the thermal efficiency of the PTC. By optimizing the design of the collectors and refining the operation and maintenance procedures, Karmer junction PTC power plant achieved a 30% reduction in their operation and maintenance cost [282]. The critical investigation of using water as HTF instead of synthetic oil in order to reduce the cost must be conducted. Using nanofluids must not get restricted for experimentation in laboratories but also need to be applied in pilot plants to observe the broader effect of nanofluids on the thermal performance of the PTC power plant. For instance, doping nanoparticles in molten salt will enhance the specific heat capacity of the HTF which in turn boosts the thermal energy storage capacity of the plant [283].

5. Conclusion

Parabolic Trough collectors are the most developed among concentrated solar power technologies, having medium and high temperature working range. The objective of this review is to present and discuss various heat transfer fluid applicable for PTC systems. While discussing the HTFs, it is also essential to present the literature on its preparation and thermophysical properties, which will help in designing the PTC systems. Various state of the art HTFs are reviewed in this article focusing on the enhancement of the overall thermal efficiency of PTC systems. The most important conclusion of this survey is summarised below:

- The thermophysical properties which govern the selection of HTF are low melting point, stability at high temperature >400 ^{o}C, low pressure (<1atm), high specific heat or heat storage capacity, high thermal conductivity, low corrosion rate, low dynamic viscosity, low cost, low toxicity flammability, and explosivity and Industrial availability.
- Enhancement in thermal properties like specific heat, melting point, thermal conductivity, stability at a high temperature of HTF is more promising option to improve the thermal efficiency of PTC systems because thermal modifications of the physical system can enhance efficiency up to 2% only, due to low thermal losses in the physical system.
- One of the most suitable ways to enhance thermal efficiency is by using HTF having superior thermophysical properties. Instead of using water as HTF, HTFs with higher latent heat capacity than water can be used in the system. This will also help in TES, increasing the power output of the system.
- Adding Nanoparticles to HTFs to modify the thermal properties like specific heat and melting point will make the HTFs, more suitable for PTC applications. The addition of Nanoparticles like CuO, Ag, SiO_2, MWCNT, CNT, and hybrid mixtures will enhance the thermal conductivity of HTFs. However, the stability of nanoparticles in the base fluid is an important issue that needs to be addressed to make the PTC system entirely depend on HTFs doped with nanoparticles. Also, there is a need for investigating the optical and thermal performances of nanofluids at high temperatures.
- To overcome the stability of nanoparticles in the base fluid MSBNFs are introduced to PTC systems. State of the art Molten salts used in the PTC systems are discussed in the article.
- The stability of both Nanofluids and MSBNFs is surveyed, and recent works in the area are presented. In which the addition of NPs in Molten salt has reduced the melting temperature when compared to base molten salt, making it suitable for PTC applications.

This article can be used as a guideway for the development of alternative HTFs for PTC systems for better performance. There is a need for experimentation and comparative study on a large scale in solar fields rather than laboratory-scale experiments to gain more promising and practical results.

Acknowledgment

This work was supported by Taylor's University through its TAYLOR'S RESEARCH SCHOLARSHIP Programme. The authors would like to thank Mohd Najib, Universiti Tun Hussein Onn Malaysia (UTHM) Johor for proof reading this review article.

References

[1] I.E.A. (IEA), Global energy and CO2 status report, IEA, 2018.

[2] S. Sripadmanabhan Indira, C. Aravind Vaithilingam, K.S.P. Oruganti, F. Mohd, S. Rahman, Nanogenerators as a Sustainable Power Source: State of Art, Applications, and Challenges, Nanomaterials, 9(5) (2019) 773.

[3] N.S. Lewis, D.G. Nocera, Powering the planet: Chemical challenges in solar energy utilization, Proceedings of the National Academy of Sciences, 103(43) (2006) 15729-15735.

[4] N.S. Lewis, Research opportunities to advance solar energy utilization, Science, 351(6271) (2016) aad1920.

[5] Y. Wang, X. Gao, P. Chen, Z. Huang, T. Xu, Y. Fang, Z. Zhang, Preparation and thermal performance of paraffin/Nano-SiO2 nanocomposite for passive thermal protection of electronic devices, Applied Thermal Engineering, 96 (2016) 699-707.

[6] S. Dubey, J.N. Sarvaiya, B. Seshadri, Temperature Dependent Photovoltaic (PV) Efficiency and Its Effect on PV Production in the World – A Review, Energy Procedia, 33 (2013) 311-321.

[7] K. Vignarooban, Xinhai Xu, A. Arvay, K. Hsu, A.M. Kannan, Heat transfer fluids for concentrating solar power systems – A review, Applied Energy, 146 (2015) 383-396.

[8] S. Akbarzadeh, M.S. Valipour, Heat transfer enhancement in parabolic trough collectors: A comprehensive review, Renewable and Sustainable Energy Reviews, 92 (2018) 198-218.

[9] A. Bonk, S. Sau, N. Uranga, M. Hernaiz, T. Bauer, Advanced heat transfer fluids for direct molten salt line-focusing CSP plants, Progress in energy and combustion science, 67 (2018) 69-87.

[10] K. Farhana, K. Kadirgama, M.M. Rahman, D. Ramasamy, M.M. Noor, G. Najafi, M. Samykano, A.S.F. Mahamude, Improvement in the performance of solar collectors with nanofluids — A state-of-the-art review, Nano-Structures & Nano-Objects, 18 (2019) 100276.

[11] AsianBiomassOffice, Progress Seen in the Development of Concentrating Solar Power in India, in, 2018.

[12] E. World Bank Group, Solargis, Solar Resource Map Direct Solar Irradiation, in, 2016.

[13] E. Yin, Q. Li, Y. Xuan, Optimal design method for concentrating photovoltaic-thermoelectric hybrid system, Applied Energy, 226 (2018) 320-329.

[14] M.T. Islam, N. Huda, A.B. Abdullah, R. Saidur, A comprehensive review of state-of-the-art concentrating solar power (CSP) technologies: Current status and research trends, Renewable and Sustainable Energy Reviews, 91 (2018) 987-1018.

[15] Ali Jaber Abdulhamed, Nor Mariah Adam, Mohd Zainal Abidin Ab-Kadir, A.A. Hairuddin, Review of solar parabolic-trough collector geometrical and thermal analyses, performance, and applications, Renewable and Sustainable Energy Reviews, 91 (2018) 822-831.

[16] C. Bachelier, W. Jäger, Thermal and hydraulic evaluation of a linear Fresnel solar collector loop operated with molten salt and liquid metal, Applied Energy, 248 (2019) 207-216.

[17] M Abid, TAH Ratlamwala, U.Atikol, Performance assessment of parabolic dish and parabolic trough solar thermal power plant using nanofluids and molten salts, International journal of energy research, 40(4) (2016).

[18] M. Atif, F. Al-Sulaiman, Supercritical Carbon Dioxide Brayton Cycles Driven by Solar Thermal Power Tower System, Advanced Materials Research, 1116 (2015) 94-129.

[19] A.A. Mills, R. Clift, Reflections of the'Burning mirrors of Archimedes'. With a consideration of the geometry and intensity of sunlight reflected from plane mirrors, European journal of physics, 13(6) (1992) 268.

[20] A.B. Mouchot, (La) Chaleur solaire et ses applications industrielles, Gauthier-Villars, 1869.

[21] C. Silvi, The use of solar energy in human activities throughout the centuries. *Steam and Electricity Generated From Solar Heat with Flat Mirrors: An Italian Story*, GSES – Solar Energy History Group, Italy, 2010.

[22] I.L. García, J.L. Álvarez, D. Blanco, Performance model for parabolic trough solar thermal power plants with thermal storage: Comparison to operating plant data, Solar Energy, 85(10) (2011) 2443-2460.

[23] R.H. Goddard, A new Inventions to harness the sun, in: Popular scienece Magazine, USA, 1929, pp. 2.

[24] K. Butti, J. Perlin, A golden thread: 2500 years of solar architecture and technology, Cheshire books, 1980.

[25] W.B.S.a. R.W.Harrigan, Power From The Sun, in: Power From The Sun, John Wiley and Sons, Inc. 1986, 2011.

[26] T.W. Africa, Archimedes through the looking-glass, The Classical World, 68(5) (1975) 305-308.

[27] D. Mills, P. Le Lievre, G. Morrison, First results from compact linear Fresnel reflector installation, Proceedings of ANZSES Solar2004, (2004).

[28] A. Giostri, M. Binotti, M. Astolfi, P. Silva, E. Macchi, G. Manzolini, Comparison of different solar plants based on parabolic trough technology, Solar Energy, 86(5) (2012) 1208-1221.

[29] T.M. Pavlović, I.S. Radonjić, D.D. Milosavljević, L.S. Pantić, A review of concentrating solar power plants in the world and their potential use in Serbia, Renewable and Sustainable Energy Reviews, 16(6) (2012) 3891-3902.

[30] J.I. Burgaleta, S. Arias, D. Ramirez, Gemasolar, the first tower thermosolar commercial plant with molten salt storage, SolarPACES, Granada, Spain, (2011) 20-23.

[31] Y. Tian, C.-Y. Zhao, A review of solar collectors and thermal energy storage in solar thermal applications, Applied Energy, 104 (2013) 538-553.

[32] S.-W. World Solar Thermal Electricity Association, STE/CSP TECHNOLOGIES > LINEAR FRESNEL REFLECTOR, in.

[33] R. De Groot, V. Van der Veen, A. Sebitosi, Comparing solar PV (photovoltaic) with coal-fired electricity production in the centralized network of South Africa, Energy, 55 (2013) 823-837.

[34] C. Tzivanidis, E. Bellos, D. Korres, K.A. Antonopoulos, G. Mitsopoulos, Thermal and optical efficiency investigation of a parabolic trough collector, Case Studies in Thermal Engineering, 6 (2015) 226-237.

[35] E. Bellos, D. Korres, C. Tzivanidis, K.A. Antonopoulos, Design, simulation and optimization of a compound parabolic collector, Sustainable Energy Technologies and Assessments, 16 (2016) 53-63.

[36] Arslan F Mertkan, G. Hüseyin, Investigation of energetic and exergetic performances of parabolic trough collector with using different heat transfer fluids., in: CLIMA 2019, Les Ulis, 2019.

[37] X. Ju, C. Xu, G. Wei, X. Du, Y. Yang, A novel hybrid storage system integrating a packed-bed thermocline tank and a two-tank storage system for concentrating solar power (CSP) plants, Applied Thermal Engineering, 92 (2016) 24-31.

[38] N. Enteria, A. Akbarzadeh, Solar energy sciences and engineering applications, CRC Press, 2013.

[39] E. Bellos, C. Tzivanidis, K.A. Antonopoulos, I. Daniil, The use of gas working fluids in parabolic trough collectors – An energetic and exergetic analysis, Applied Thermal Engineering, 109 (2016) 1-14.

[40] H. Riazi, T. Murphy, G.B. Webber, R. Atkin, S.S.M. Tehrani, R.A. Taylor, Specific heat control of nanofluids: A critical review, International Journal of Thermal Sciences, 107 (2016) 25-38.

[41] R. Devaradjane, Utilization of molten nitrate salt nanomaterials for heat capacity enhancement in solar power applications, rc.library.uta.edu, 2013.

[42] S. Gschwander, T. Haussmann, G. Hagelstein, A. Sole, G. Diarce, W. Hohenauer, D. Lager, C. Rathgeber, P. Hennemann, A. Lazaro, Standard to determine the heat storage capacity of PCM using hf-DSC with constant heating/cooling rate (dynamic mode) DSC 4229 PCM Standard, A technical report of subtask, 2015.

[43] A. Solé, L. Miró, C. Barreneche, I. Martorell, L.F. Cabeza, Review of the T-history method to determine thermophysical properties of phase change materials (PCM), Renewable and Sustainable Energy Reviews, 26 (2013) 425-436.

[44] J.W. Raade, D. Padowitz, Development of Molten Salt Heat Transfer Fluid With Low Melting Point and High Thermal Stability, Journal of Solar Energy Engineering, 133(3) (2011).

[45] T. Bauer, N. Pfleger, N. Breidenbach, M. Eck, D. Laing, S. Kaesche, Material aspects of Solar Salt for sensible heat storage, Applied Energy, 111 (2013) 1114-1119.

[46] M.V. Smirnov, V.A. Khokhlov, E.S. Filatov, Thermal conductivity of molten alkali halides and their mixtures, Electrochimica Acta, 32(7) (1987) 1019-1026.

[47] Q. Peng, J. Ding, X. Wei, J. Yang, X. Yang, The preparation and properties of multi-component molten salts, Applied Energy, 87(9) (2010) 2812-2817.

[48] R.H. Perry, D.W.G. (Eds.), Perry's Chemical Engineers' Handbook, seventh ed., McGraw-Hill, 1997.

[49] Y. Rong, C.M. Gregson, A. Parker, Thermogravimetric measurements of liquid vapor pressure, The Journal of Chemical Thermodynamics, 51 (2012) 25-30.

[50] R.B. Cundall, T. Frank Palmer, C.E.C. Wood, Vapour pressure measurements on some organic high explosives, Journal of the Chemical Society, Faraday Transactions 1: Physical Chemistry in Condensed Phases, 74(0) (1978) 1339-1345.

[51] M. Chieruzzi, A. Miliozzi, T. Crescenzi, L. Torre, J.M. Kenny, A new phase change material based on potassium nitrate with silica and alumina nanoparticles for thermal energy storage, Nanoscale research letters, 10(1) (2015) 273.

[52] D. Shin, D. Banerjee, Enhanced thermal properties of SiO2 nanocomposite for solar thermal energy storage applications, International Journal of Heat and Mass Transfer, 84 (2015) 898-902.

[53] Y.Y. Chen, C.Y. Zhao, Thermophysical properties of Ca(NO3)2-NaNO3-KNO3 mixtures for heat transfer and thermal storage, Solar Energy, 146 (2017) 172-179.

[54] S.U. Ilyas, R. Pendyala, M. Narahari, Stability and thermal analysis of MWCNT-thermal oil-based nanofluids, Colloids and Surfaces A: Physicochemical and Engineering Aspects, 527 (2017) 11-22.

[55] B. Wei, C. Zou, X. Li, Experimental investigation on stability and thermal conductivity of diathermic oil based TiO2 nanofluids, International Journal of Heat and Mass Transfer, 104 (2017) 537-543.

[56] H. Yarmand, S. Gharehkhani, S.F.S. Shirazi, M. Goodarzi, A. Amiri, W.S. Sarsam, M.S. Alehashem, M. Dahari, S.N. Kazi, Study of synthesis, stability and thermo-physical properties of graphene nanoplatelet/platinum hybrid nanofluid, International Communications in Heat and Mass Transfer, 77 (2016) 15-21.

[57] A. Asadi, M. Asadi, A. Rezaniakolaei, L.A. Rosendahl, M. Afrand, S. Wongwises, Heat transfer efficiency of Al2O3-MWCNT/thermal oil hybrid nanofluid as a cooling fluid in thermal and energy management applications: An experimental and theoretical investigation, International Journal of Heat and Mass Transfer, 117 (2018) 474-486.

[58] M. Chieruzzi, G.F. Cerritelli, A. Miliozzi, J.M. Kenny, Effect of nanoparticles on heat capacity of nanofluids based on molten salts as PCM for thermal energy storage, Nanoscale research letters, 8(1) (2013) 448.

[59] R. Silva, F.J. Cabrera, M. Pérez-García, Process Heat Generation with Parabolic Trough Collectors for a Vegetables Preservation Industry in Southern Spain, Energy Procedia, 48 (2014) 1210-1216.

[60] G. Coccia, G. Di Nicola, M. Sotte, Design, manufacture, and test of a prototype for a parabolic trough collector for industrial process heat, Renewable Energy, 74 (2015) 727-736.

[61] A. Fernández-García, E. Zarza, L. Valenzuela, M. Pérez, Parabolic-trough solar collectors and their applications, Renewable and Sustainable Energy Reviews, 14(7) (2010) 1695-1721.

[62] Andrea Giglio, Andrea Lanzini, Pierluigi Leone, Margarita M.Rodríguez García, Eduardo Zarza Moyab, Direct steam generation in parabolic-trough collectors: a review about the technology and a thermo-economic analysis of a hybrid system, Renewable and Sustainable Energy Reviews, 74 (2017) 453-473.

[63] H.Benoit, L.Spreafico, D.Gauthier, G.Flaman, Review of heat transfer fluids in tube-receivers used in concentrating solar thermal systems: Properties and heat transfer coefficients, Renewable and Sustainable Energy Reviews, 55 (2016) 298-315.

[64] P. Selvakumar, P. Somasundaram, P. Thangavel, Performance study on evacuated tube solar collector using therminol D-12 as heat transfer fluid coupled with parabolic trough, Energy Conversion and Management, 85 (2014) 505-510.

[65] D.G. Lovering, Molten salt technology, Springer Science + Bussiness Media, 2014.

[66] A.M. Weinberg, A review of molten salt reactor technology. Preface. Molten-salt reactors, in, 1970.

[67] H. Zhang, J. Baeyens, J. Degrève, G. Cacères, Concentrated solar power plants: Review and design methodology, Renewable and Sustainable Energy Reviews, 22 (2013) 466-481.

[68] V.M.B. Nunes, C.S. Queirós, M.J.V. Lourenço, F.J.V. Santos, C.A. Nieto de Castro, Molten salts as engineering fluids – A review: Part I. Molten alkali nitrates, Applied Energy, 183 (2016) 603-611.

[69] Y. Wang, Q. Liu, J. Lei, H. Jin, A three-dimensional simulation of a parabolic trough solar collector system using molten salt as heat transfer fluid, Applied Thermal Engineering, 70(1) (2014) 462-476.

[70] T. Bauer, N. Pfleger, D. Laing, W.-D. Steinmann, M. Eck, S. Kaesche, 20 - High-Temperature Molten Salts for Solar Power Application, in: F. Lantelme, H. Groult (Eds.) Molten Salts Chemistry, Elsevier, Oxford, 2013, pp. 415-438.

[71] M. Chieruzzi, Nanofluids with Enhanced Heat Transfer Properties for Thermal Energy Storage, Rome, Italy, 2016.

[72] T. Jriri, J. Rogez, C. Bergman, J. Mathieu, Thermodynamic study of the condensed phases of NaNO3, KNO3 and CsNO3 and their transitions, Thermochimica Acta, 266 (1995) 147-161.

[73] K. Coscia, T. Elliott, S. Mohapatra, A. Oztekin, S. Neti, Binary and Ternary Nitrate Solar Heat Transfer Fluids, Journal of Solar Energy Engineering, 135(2) (2013) 021011-021011-021016.

[74] M. Chen, Y. Shen, S. Zhu, P. Li, Digital phase diagram and thermophysical properties of KNO3-NaNO3-Ca(NO3)2 ternary system for solar energy storage, Vacuum, 145 (2017) 225-233.

[75] P. Xiao, L. Guo, X. Zhang, Investigations on heat transfer characteristic of molten salt flow in helical annular duct, Applied Thermal Engineering, 88 (2015) 22-32.

[76] A. Fernández, S. Ushak, H. Galleguillos, F. Pérez, Development of new molten salts with LiNO3 and Ca (NO3) 2 for energy storage in CSP plants, Elsevier, 2014.

[77] C. Zhao, Z. Wu, Thermal property characterization of a low melting-temperature ternary nitrate salt mixture for thermal energy storage systems, Solar Energy Materials and Solar Cells, 95(12) (2011) 3341-3346.

[78] Yathin Krishna, R Saidur, Navid Aslfattahi, Mohd Faizal Fauzan, K. Ng, Enhancing the Thermal properties of Organic Phase Change Material (palmitic acid) by doping MXene Nanoflakes, in: 13th International Engineering Research Conference (13th EURECA 2019), AIP Conference Proceedings, Malaysia, 2019.

[79] T. Wang, D. Mantha, R.G. Reddy, Novel low melting point quaternary eutectic system for solar thermal energy storage, Applied Energy, 102 (2013) 1422-1429.

[80] R.W. Bradshaw, D.A. Brosseau, Low-melting point inorganic nitrate salt heat transfer fluid, in, Google Patents, 2009.

[81] Q. Peng, X. Yang, J. Ding, X. Wei, J. Yang, Design of new molten salt thermal energy storage material for solar thermal power plant, Applied Energy, 112 (2013) 682-689.

[82] Justin W. Raade, David Padowitz, Development of molten salt heat transfer fluid with low melting point and high thermal stability, Journal of solar energy engineering, 3(133) (August 2011).

[83] A.G. Fernández, M.I. Lasanta, F.J. Pérez, Molten Salt Corrosion of Stainless Steels and Low-Cr Steel in CSP Plants, Oxidation of Metals, 78(5) (2012) 329-348.

[84] E. Bellos, C. Tzivanidis, K.A. Antonopoulos, A detailed working fluid investigation for solar parabolic trough collectors, Applied Thermal Engineering, 114 (2017) 374-386.

[85] M.J. Montes, A. Abánades, J.M. Martínez-Val, Thermofluidynamic Model and Comparative Analysis of Parabolic Trough Collectors Using Oil, Water/Steam, or Molten Salt as Heat Transfer Fluids, Journal of Solar Energy Engineering, 132(2) (2010).

[86] Yathin Krishna, Abdul Razak R. K, A. Afzal, The CFD analysis of flat plate collector-nanofluid as working medium, AIP Conference Proceedings, 2039(1) (2018) 020062.

[87] M.M. Sarafraz, O. Pourmehran, B. Yang, M. Arjomandi, Assessment of the thermal performance of a thermosyphon heat pipe using zirconia-acetone nanofluids, Renewable Energy, 136 (2019) 884-895.

[88] M.M. Sarafraz, M.R. Safaei, Diurnal thermal evaluation of an evacuated tube solar collector (ETSC) charged with graphene nanoplatelets-methanol nano-suspension, Renewable Energy, 142 (2019) 364-372.

[89] Sarafraz M.M, Tlili I, Abdul Baseer M, S. M.R, Potential of Solar Collectors for Clean Thermal Energy Production in Smart Cities using Nanofluids: Experimental Assessment and Efficiency Improvement., Applied sciences, MDPI, 9(9) (2019) 1877.

[90] M.M. Sarafraz, F. Hormozi, Convective boiling and particulate fouling of stabilized CuO-ethylene glycol nanofluids inside the annular heat exchanger, International Communications in Heat and Mass Transfer, 53 (2014) 116-123.

[91] E. Salari, S.M. Peyghambarzadeh, M.M. Sarafraz, F. Hormozi, V. Nikkhah, Thermal behavior of aqueous iron oxide nano-fluid as a coolant on a flat disc heater under the pool boiling condition, Heat and Mass Transfer, 53(1) (2017) 265-275.

[92] M.H. Ahmadi, M. Ghazvini, M. Sadeghzadeh, M. Alhuyi Nazari, M. Ghalandari, Utilization of hybrid nanofluids in solar energy applications: A review, Nano-Structures & Nano-Objects, 20 (2019) 100386.

[93] E. Kaloudis, E. Papanicolaou, V. Belessiotis, Numerical simulations of a parabolic trough solar collector with nanofluid using a two-phase model, Renewable Energy, 97 (2016) 218-229.

[94] P.V.W. K. S. Chaudhari, U. S. Wankhede, R. S. Shelke, An Experimental Investigation of a Nanofluid (Al2O3+H2O) Based Parabolic Trough Solar Collectors, British Journal of Applied Science & Technology, 9(6) (2015) 7.

[95] G. Coccia, G. Di Nicola, L. Colla, L. Fedele, M. Scattolini, Adoption of nanofluids in low-enthalpy parabolic trough solar collectors: Numerical simulation of the yearly yield, Energy Conversion and Management, 118 (2016) 306-319.

[96] S.E. Ghasemi, A.A. Ranjbar, Thermal performance analysis of solar parabolic trough collector using nanofluid as working fluid: A CFD modelling study, Journal of Molecular Liquids, 222 (2016) 159-166.

[97] A. Mwesigye, Z. Huan, Thermodynamic analysis and optimization of fully developed turbulent forced convection in a circular tube with water–Al2O3 nanofluid, International Journal of Heat and Mass Transfer, 89 (2015) 694-706.

[98] M.A. Rehan, M. Ali, N.A. Sheikh, M.S. Khalil, G.Q. Chaudhary, T.u. Rashid, M. Shehryar, Experimental performance analysis of low concentration ratio solar parabolic trough collectors with nanofluids in winter conditions, Renewable Energy, 118 (2018) 742-751.

[99] J. Subramani, P.K. Nagarajan, S. Wongwises, S.A. El-Agouz, R. Sathyamurthy, Experimental study on the thermal performance and heat transfer characteristics of solar parabolic trough collector using Al2O3 nanofluids, Environmental Progress & Sustainable Energy, 37(3) (2018) 1149-1159.

[100] J. Subramani, P.K. Nagarajan, O. Mahian, R. Sathyamurthy, Efficiency and heat transfer improvements in a parabolic trough solar collector using TiO2 nanofluids under turbulent flow regime, Renewable Energy, 119 (2018) 19-31.

[101] N. Kumar, S.S. Sonawane, Experimental study of Fe2O3/water and Fe2O3/ethylene glycol nanofluid heat transfer enhancement in a shell and tube heat exchanger, International Communications in Heat and Mass Transfer, 78 (2016) 277-284.

[102] S.K. Hazra, S. Ghosh, T.K. Nandi, Photo-thermal conversion characteristics of carbon black-ethylene glycol nanofluids for applications in direct absorption solar collectors, Applied Thermal Engineering, 163 (2019) 114402.

[103] E. Bellos, C. Tzivanidis, K.A. Antonopoulos, G. Gkinis, Thermal enhancement of solar parabolic trough collectors by using nanofluids and converging-diverging absorber tube, Renewable Energy, 94 (2016) 213-222.

[104] A. Allouhi, M. Benzakour Amine, R. Saidur, T. Kousksou, A. Jamil, Energy and exergy analyses of a parabolic trough collector operated with nanofluids for medium and high temperature applications, Energy Conversion and Management, 155 (2018) 201-217.

[105] V. Ferraro, J. Settino, M.A. Cucumo, D. Kaliakatsos, Parabolic Trough System Operating with Nanofluids: Comparison with the Conventional Working Fluids and Influence on the System Performance, Energy Procedia, 101 (2016) 782-789.

[106] H. Khakrah, A. Shamloo, S. Kazemzadeh Hannani, Determination of Parabolic Trough Solar Collector Efficiency Using Nanofluid: A Comprehensive Numerical Study, Journal of Solar Energy Engineering, 139(5) (2017).

[107] T. Sokhansefat, A.B. Kasaeian, F. Kowsary, Heat transfer enhancement in parabolic trough collector tube using Al2O3/synthetic oil nanofluid, Renewable and Sustainable Energy Reviews, 33 (2014) 636-644.

[108] P. Mohammad Zadeh, T. Sokhansefat, A.B. Kasaeian, F. Kowsary, A. Akbarzadeh, Hybrid optimization algorithm for thermal analysis in a solar parabolic trough collector based on nanofluid, Energy, 82 (2015) 857-864.

[109] N. Basbous, M. Taqi, M.A. Janan, Thermal performances analysis of a parabolic trough solar collector using different nanofluids, in: 2016 International Renewable and Sustainable Energy Conference (IRSEC), 2016, pp. 322-326.

[110] E. Bellos, C. Tzivanidis, Parametric investigation of nanofluids utilization in parabolic trough collectors, Thermal Science and Engineering Progress, 2 (2017) 71-79.

[111] E. Bellos, C. Tzivanidis, Thermal analysis of parabolic trough collector operating with mono and hybrid nanofluids, Sustainable Energy Technologies and Assessments, 26 (2018) 105-115.

[112] E. Bellos, C. Tzivanidis, D. Tsimpoukis, Thermal, hydraulic and exergetic evaluation of a parabolic trough collector operating with thermal oil and molten salt based nanofluids, Energy Conversion and Management, 156 (2018) 388-402.

[113] A. Mwesigye, Z. Huan, J.P. Meyer, Thermodynamic optimisation of the performance of a parabolic trough receiver using synthetic oil–Al2O3 nanofluid, Applied Energy, 156 (2015) 398-412.

[114] A. Mwesigye, Z. Huan, J.P. Meyer, Thermal Performance of a Receiver Tube for a High Concentration Ratio Parabolic Trough System and Potential for Improved Performance With Syltherm800-CuO Nanofluid, in: ASME 2015 International Mechanical Engineering Congress and Exposition, 2015.

[115] Yanjuan Wang, Jinliang Xu, Qibin Liu, Yuanyuan Chen, Huan Liu, Performance analysis of a parabolic trough solar collector using Al_2O_3/synthetic oil nanofluid, Applied Thermal Engineering, 107 (2016) 469-478.

[116] B. Amina, A. Miloud, L. Samir, B. Abdelylah, J.P. Solano, Heat transfer enhancement in a parabolic trough solar receiver using longitudinal fins and nanofluids, Journal of Thermal Science, 25(5) (2016) 410-417.

[117] A. Mwesigye, Z. Huan, J.P. Meyer, Thermal performance and entropy generation analysis of a high concentration ratio parabolic trough solar collector with Cu-Therminol®VP-1 nanofluid, Energy Conversion and Management, 120 (2016) 449-465.

[118] A. Mwesigye, J.P. Meyer, Optimal thermal and thermodynamic performance of a solar parabolic trough receiver with different nanofluids and at different concentration ratios, Applied Energy, 193 (2017) 393-413.

[119] A. Mwesigye, J. Meyer, Heat Transfer Performance of a Parabolic Trough Receiver Using SWCNTs-Therminol® VP-1 Nanofluids, in: ASME International Mechanical Engineering Congress and Exposition, Proceedings of the ASME 2017, Tampa, Florida, USA, 2017, pp. 13.

[120] S.E. Ghasemi, A.A. Ranjbar, Effect of using nanofluids on efficiency of parabolic trough collectors in solar thermal electric power plants, International Journal of Hydrogen Energy, 42(34) (2017) 21626-21634.

[121] A. Kasaeian, S. Daviran, R.D. Azarian, A. Rashidi, Performance evaluation and nanofluid using capability study of a solar parabolic trough collector, Energy Conversion and Management, 89 (2015) 368-375.

[122] A. Ghadimi, R. Saidur, H.S.C. Metselaar, A review of nanofluid stability properties and characterization in stationary conditions, International Journal of Heat and Mass Transfer, 54(17) (2011) 4051-4068.

[123] Z. Haddad, C. Abid, H.F. Oztop, A. Mataoui, A review on how the researchers prepare their nanofluids, International Journal of Thermal Sciences, 76 (2014) 168-189.

[124] V. Fuskele, R.M. Sarviya, Recent developments in Nanoparticles Synthesis, Preparation and Stability of Nanofluids, Materials Today: Proceedings, 4(2, Part A) (2017) 4049-4060.

[125] H. Bahremand, A. Abbassi, M. Saffar-Avval, Experimental and numerical investigation of turbulent nanofluid flow in helically coiled tubes under constant wall heat flux using Eulerian–Lagrangian approach, Powder Technology, 269 (2015) 93-100.

[126] S. Mirfendereski, A. Abbassi, M. Saffar-avval, Experimental and numerical investigation of nanofluid heat transfer in helically coiled tubes at constant wall heat flux, Advanced Powder Technology, 26(5) (2015) 1483-1494.

[127] M. Khoshvaght-Aliabadi, M. Tavasoli, F. Hormozi, Comparative analysis on thermal–hydraulic performance of curved tubes: Different geometrical parameters and working fluids, Energy, 91 (2015) 588-600.

[128] M. Rakhsha, F. Akbaridoust, A. Abbassi, S.-A. Majid, Experimental and numerical investigations of turbulent forced convection flow of nano-fluid in helical coiled tubes at constant surface temperature, Powder Technology, 283 (2015) 178-189.

[129] I.M. Mahbubul, R. Saidur, M.A. Amalina, Thermal Conductivity, Viscosity and Density of R141b Refrigerant based Nanofluid, Procedia Engineering, 56 (2013) 310-315.

[130] M. Kamalgharibi, F. Hormozi, S.A.H. Zamzamian, M.M. Sarafraz, Experimental studies on the stability of CuO nanoparticles dispersed in different base fluids: influence of stirring, sonication and surface active agents, Heat and Mass Transfer, 52(1) (2016) 55-62.

[131] Z.-h. Liu, L. Liao, Sorption and agglutination phenomenon of nanofluids on a plain heating surface during pool boiling, International Journal of Heat and Mass Transfer, 51(9-10) (2008) 2593-2602.

[132] N. Ise, I. Sogami, Structure Formation in Solution: Ionic Polymers and Colloidal Particles, in, Springer, Berlin, 2005.

[133] H. Wang, Dispersing carbon nanotubes using surfactants, Current Opinion in Colloid & Interface Science, 14(5) (2009) 364-371.

[134] X. Yang, Z.-h. Liu, A kind of nanofluid consisting of surface-functionalized nanoparticles, Nanoscale research letters, 5(8) (2010) 1324.

[135] M. Faizal, R. Saidur, S. Mekhilef, A. Hepbasli, I.M. Mahbubul, Energy, economic, and environmental analysis of a flat-plate solar collector operated with SiO2 nanofluid, Clean Technologies and Environmental Policy, 17(6) (2014) 1457–1473.

[136] N.S. Souza, A.D. Rodrigues, C.A. Cardoso, H. Pardo, R. Faccio, A.W. Mombru, J.C. Galzerani, O.F. de Lima, S. Sergeenkov, F.M. Araujo-Moreira, Physical properties of nanofluid suspension of ferromagnetic graphite with high Zeta potential, Physics Letters A, 376(4) (2012) 544-546.

[137] Dukhin, Andrei S, Ultrasound for Characterizing Colloids Particle Sizing, Zeta Potential, Rheology, San Diego, CA: Elsevier, 2002.

[138] S.-C. Yang, S.-Y.-R. Paik, J. Ryu, K.-O. Choi, T.S. Kang, J.K. Lee, C.W. Song, S. Ko, Dynamic light scattering-based method to determine primary particle size of iron oxide nanoparticles in simulated gastrointestinal fluid, Food Chemistry, 161 (2014) 185-191.

[139] C. Wang, X. Zhang, M. Su, Synthesis and thermal stability of Field's alloy nanoparticles and nanofluid, Materials Letters, 205 (2017) 6-9.

[140] M.M. Bhunia, S. Das, K.K. Chattopadhyay, P. Chattopadhyay, Enhanced heat transfer properties of RGO-TiO2 based Ethylene Glycol Nanofluids, Materials Today: Proceedings, 18 (2019) 1096-1107.

[141] P.C. Mukesh Kumar, K. Palanisamy, V. Vijayan, Stability analysis of heat transfer hybrid/water nanofluids, Materials Today: Proceedings, (2019).

[142] H. Karami, S. Papari-Zare, M. Shanbedi, H. Eshghi, A. Dashtbozorg, A. Akbari, E. Mohammadian, M. Heidari, A.Z. Sahin, C.B. Teng, The thermophysical properties and the stability of nanofluids containing carboxyl-functionalized graphene nano-platelets and multi-walled carbon nanotubes, International Communications in Heat and Mass Transfer, 108 (2019) 104302.

[143] V. Singh, M. Gupta, Characterisation and Zeta Potential Measurements of CuO–Water Nanofluids, in: M. Kumar, R.K. Pandey, V. Kumar (Eds.) Advances in Interdisciplinary Engineering, Springer Singapore, Singapore, 2019, pp. 741-747.

[144] S. Aberoumand, A. Jafarimoghaddam, Tungsten (III) oxide (WO3) – Silver/transformer oil hybrid nanofluid: Preparation, stability, thermal conductivity and dielectric strength, Alexandria Engineering Journal, 57(1) (2018) 169-174.

[145] A. Yasinskiy, J. Navas, T. Aguilar, R. Alcántara, J.J. Gallardo, A. Sánchez-Coronilla, E.I. Martín, D. De Los Santos, C. Fernández-Lorenzo, Dramatically enhanced thermal properties for TiO2-based nanofluids for being used as heat transfer fluids in concentrating solar power plants, Renewable Energy, 119 (2018) 809-819.

[146] A. Asadi, A guideline towards easing the decision-making process in selecting an effective nanofluid as a heat transfer fluid, Energy Conversion and Management, 175 (2018) 1-10.

[147] R. Gómez-Villarejo, P. Estellé, J. Navas, Boron nitride nanotubes-based nanofluids with enhanced thermal properties for use as heat transfer fluids in solar thermal applications, Solar Energy Materials and Solar Cells, 205 (2020) 110266.

[148] S. Al-Anssari, M. Arif, S. Wang, A. Barifcani, S. Iglauer, Stabilising nanofluids in saline environments, Journal of colloid and interface science, 508 (2017) 222-229.

[149] X. Yu, Y. Xuan, Investigation on thermo-optical properties of CuO/Ag plasmonic nanofluids, Solar Energy, 160 (2018) 200-207.

[150] N. Bouguerra, S. Poncet, S. Elkoun, Dispersion regimes in alumina/water-based nanofluids: Simultaneous measurements of thermal conductivity and dynamic viscosity, International Communications in Heat and Mass Transfer, 92 (2018) 51-55.

[151] S.H.A. Ahmad, R. Saidur, I.M. Mahbubul, F.A. Al-Sulaiman, Optical properties of various nanofluids used in solar collector: A review, Renewable and Sustainable Energy Reviews, 73 (2017) 1014-1030.

[152] S. Nabati Shoghl, J. Jamali, M. Keshavarz Moraveji, Electrical conductivity, viscosity, and density of different nanofluids: An experimental study, Experimental Thermal and Fluid Science, 74(Supplement C) (2016) 339-346.

[153] F. Jabbari, A. Rajabpour, S. Saedodin, Thermal conductivity and viscosity of nanofluids: A review of recent molecular dynamics studies, Chemical Engineering Science, 174(Supplement C) (2017) 67-81.

[154] F. Yu, Y. Chen, X. Liang, J. Xu, C. Lee, Q. Liang, P. Tao, T. Deng, Dispersion stability of thermal nanofluids, Progress in Natural Science: Materials International, 27(5) (2017) 531-542.

[155] Z. Sheng, J.D. Van Nostrand, J. Zhou, Y. Liu, Contradictory effects of silver nanoparticles on activated sludge wastewater treatment, Journal of Hazardous Materials, 341(Supplement C) (2018) 448-456.

[156] X. Wu, H.B. Wu, W. Xiong, Z. Le, F. Sun, F. Liu, J. Chen, Z. Zhu, Y. Lu, Robust iron nanoparticles with graphitic shells for high-performance Ni-Fe battery, Nano Energy, 30(Supplement C) (2016) 217-224.

[157] N. Kumar, K. Biswas, Cryomilling: an environment friendly approach of preparation large quantity ultra refined pure aluminium nanoparticles, Journal of Materials Research and Technology, (2017).

[158] J. Santhoshkumar, S. Rajeshkumar, S. Venkat Kumar, Phyto-assisted synthesis, characterization and applications of gold nanoparticles – A review, Biochemistry and Biophysics Reports, 11(Supplement C) (2017) 46-57.

[159] S. Chandrasekaran, A novel single step synthesis, high efficiency and cost effective photovoltaic applications of oxidized copper nano particles, Solar Energy Materials and Solar Cells, 109(Supplement C) (2013) 220-226.

[160] S.U. Ilyas, R. Pendyala, N. Marneni, Stability and Agglomeration of Alumina Nanoparticles in Ethanol-Water Mixtures, Procedia Engineering, 148(Supplement C) (2016) 290-297.

[161] Ç. Oruç, A. Altındal, Structural and dielectric properties of CuO nanoparticles, Ceramics International, 43(14) (2017) 10708-10714.

[162] Y. Wei, B. Han, X. Hu, Y. Lin, X. Wang, X. Deng, Synthesis of Fe3O4 Nanoparticles and their Magnetic Properties, Procedia Engineering, 27(Supplement C) (2012) 632-637.

[163] A.J. Haider, R.H. Al– Anbari, G.R. Kadhim, C.T. Salame, Exploring potential Environmental applications of TiO2 Nanoparticles, Energy Procedia, 119(Supplement C) (2017) 332-345.

[164] D.M. Constantinescu, D.A. Apostol, C.R. Picu, K. Krawczyk, M. Sieberer, Mechanical properties of epoxy nanocomposites reinforced with functionalized silica nanoparticles, Procedia Structural Integrity, 5(Supplement C) (2017) 647-652.

[165] R. Eldawud, A. Wagner, C. Dong, T.A. Stueckle, Y. Rojanasakul, C.Z. Dinu, Carbon nanotubes physicochemical properties influence the overall cellular behavior and fate, NanoImpact, 9(Supplement C) (2018) 72-84.

[166] S. Ravi, S. Vadukumpully, Sustainable carbon nanomaterials: recent advances and its applications in energy and environmental remediation, Journal of environmental chemical engineering, 4(1) (2016) 835-856.

[167] S. Iijima, Helical microtubules of graphitic carbon, Nature, 354 (1991) 56.

[168] S. Iijima, T. Ichihashi, Single-shell carbon nanotubes of 1-nm diameter, Nature, 363 (1993) 603.

[169] A. Arya, M.M. Sarafraz, S. Shahmiri, S.A.H. Madani, V. Nikkhah, S.M. Nakhjavani, Thermal performance analysis of a flat heat pipe working with carbon nanotube-water nanofluid for cooling of a high heat flux heater, Heat and Mass Transfer, 54(4) (2018) 985-997.

[170] M.M. Sarafraz, F. Hormozi, S.M. Peyghambarzadeh, Role of nanofluid fouling on thermal performance of a thermosyphon: Are nanofluids reliable working fluid?, Applied Thermal Engineering, 82 (2015) 212-224.

[171] M.M. Sarafraz, F. Hormozi, Experimental study on the thermal performance and efficiency of a copper made thermosyphon heat pipe charged with alumina–glycol based nanofluids, Powder Technology, 266 (2014) 378-387.

[172] M.M. Sarafraz, Z. Tian, I. Tlili, S. Kazi, M. Goodarzi, Thermal evaluation of a heat pipe working with n-pentane-acetone and n-pentane-methanol binary mixtures, Journal of Thermal Analysis and Calorimetry, (2019).

[173] S.M.S. Murshed, C.A.N. De Castro, Nanofluids : Synthesis, Properties, and Applications, Nova Science Publishers, Inc, New York, New York, 2014.

[174] R. Lenin, P.A. Joy, Role of base fluid on the thermal conductivity of oleic acid coated magnetite nanofluids, Colloids and Surfaces A: Physicochemical and Engineering Aspects, 529(Supplement C) (2017) 922-929.

[175] Y. Zhang, Nanofluids : Research, Development and Applications, Nova Science Publishers, Inc, Hauppauge, New York, 2013.

[176] D. Banerjee, Nanofluids and Applications to Energy Systems, in: M.A. Abraham (Ed.) Encyclopedia of Sustainable Technologies, Elsevier, Oxford, 2017, pp. 429-439.

[177] A.H. Elsheikh, S.W. Sharshir, M.E. Mostafa, F.A. Essa, M.K. Ahmed Ali, Applications of nanofluids in solar energy: A review of recent advances, Renewable and Sustainable Energy Reviews, 82 (2018) 3483-3502.

[178] N.A.C. Sidik, S. Samion, J. Ghaderian, M.N.A.W.M. Yazid, Recent progress on the application of nanofluids in minimum quantity lubrication machining: A review, International Journal of Heat and Mass Transfer, 108 (2017) 79-89.

[179] M.M. Tawfik, Experimental studies of nanofluid thermal conductivity enhancement and applications: A review, Renewable and Sustainable Energy Reviews, 75 (2017) 1239-1253.

[180] D.K. Devendiran, V.A. Amirtham, A review on preparation, characterization, properties and applications of nanofluids, Renewable and Sustainable Energy Reviews, 60 (2016) 21-40.

[181] G. Colangelo, E. Favale, M. Milanese, A. de Risi, D. Laforgia, Cooling of electronic devices: Nanofluids contribution, Applied Thermal Engineering, 127 (2017) 421-435.

[182] M. Raja, R. Vijayan, P. Dineshkumar, M. Venkatesan, Review on nanofluids characterization, heat transfer characteristics and applications, Renewable and Sustainable Energy Reviews, 64 (2016) 163-173.

[183] K.Y. Leong, H.C. Ong, N.H. Amer, M.J. Norazrina, M.S. Risby, K.Z. Ku Ahmad, An overview on current application of nanofluids in solar thermal collector and its challenges, Renewable and Sustainable Energy Reviews, 53 (2016) 1092-1105.

[184] V. Kumar, A.K. Tiwari, S.K. Ghosh, Application of nanofluids in plate heat exchanger: a review, Energy Conversion and Management, 105 (2015) 1017-1036.

[185] A. Bhattad, J. Sarkar, P. Ghosh, Improving the performance of refrigeration systems by using nanofluids: A comprehensive review, Renewable and Sustainable Energy Reviews, 82 (2018) 3656-3669.

[186] A. Kasaeian, A.T. Eshghi, M. Sameti, A review on the applications of nanofluids in solar energy systems, Renewable and Sustainable Energy Reviews, 43 (2015) 584-598.

[187] T.B. Gorji, A.A. Ranjbar, A review on optical properties and application of nanofluids in direct absorption solar collectors (DASCs), Renewable and Sustainable Energy Reviews, 72 (2017) 10-32.

[188] Y. Wang, H.A.I. Al-Saaidi, M. Kong, J.L. Alvarado, Thermophysical performance of graphene based aqueous nanofluids, International Journal of Heat and Mass Transfer, 119 (2018) 408-417.

[189] N. Hordy, D. Rabilloud, J.-L. Meunier, S. Coulombe, A Stable Carbon Nanotube Nanofluid for Latent Heat-Driven Volumetric Absorption Solar Heating Applications, Journal of Nanomaterials, 16(1) (2015) 1-6.

[190] M.M. Sarafraz, V. Nikkhah, M. Nakhjavani, A. Arya, Thermal performance of a heat sink microchannel working with biologically produced silver-water nanofluid: Experimental assessment, Experimental Thermal and Fluid Science, 91 (2018) 509-519.

[191] W. Chen, C. Zou, X. Li, H. Liang, Application of recoverable carbon nanotube nanofluids in solar desalination system: An experimental investigation, Desalination, 451 (2017) 92-101.

[192] S.U. Ilyas, R. Pendyala, M. Narahari, An experimental study on the natural convection heat transfer in rectangular enclosure using functionalized alumina-thermal oil-based nanofluids, Applied Thermal Engineering, 127 (2017) 765-775.

[193] X. Wang, Y. He, X. Liu, L. Shi, J. Zhu, Investigation of photothermal heating enabled by plasmonic nanofluids for direct solar steam generation, Solar Energy, 157 (2017) 35-46.

[194] J. Zeng, Y. Xuan, Enhanced solar thermal conversion and thermal conduction of MWCNT-SiO2/Ag binary nanofluids, Applied Energy, 212 (2018) 809-819.

[195] T. Aguilar, J. Navas, A. Sánchez-Coronilla, E.I. Martín, J.J. Gallardo, P. Martínez-Merino, R. Gómez-Villarejo, J.C. Piñero, R. Alcántara, C. Fernández-Lorenzo, Investigation of enhanced thermal properties in NiO-based nanofluids for concentrating solar power applications: A molecular dynamics and experimental analysis, Applied Energy, 211 (2018) 677-688.

[196] C. Qi, J. Hu, M. Liu, L. Guo, Z. Rao, Experimental study on thermo-hydraulic performances of CPU cooled by nanofluids, Energy Conversion and Management, 153 (2017) 557-565.

[197] A.A. Hawwash, A.K. Abdel Rahman, S.A. Nada, S. Ookawara, Numerical Investigation and Experimental Verification of Performance Enhancement of Flat Plate Solar Collector Using Nanofluids, Applied Thermal Engineering, 130 (2018) 363-374.

[198] H. Wang, W. Yang, L. Cheng, C. Guan, H. Yan, Chinese ink: High performance nanofluids for solar energy, Solar Energy Materials and Solar Cells, 176 (2018) 374-380.

[199] Y. Guo, T. Zhang, D. Zhang, Q. Wang, Experimental investigation of thermal and electrical conductivity of silicon oxide nanofluids in ethylene glycol/water mixture, International Journal of Heat and Mass Transfer, 117 (2018) 280-286.

[200] S. Ghasemi, A. Karimipour, Experimental investigation of the effects of temperature and mass fraction on the dynamic viscosity of CuO-paraffin nanofluid, Applied Thermal Engineering, 128 (2018) 189-197.

[201] A. Sánchez-Coronilla, E.I. Martín, J. Navas, T. Aguilar, R. Gómez-Villarejo, R. Alcántara, J.C. Piñero, C. Fernández-Lorenzo, Experimental and theoretical analysis of NiO nanofluids in presence of surfactants, Journal of Molecular Liquids, 252 (2018) 211-217.

[202] M.S.Y. Ebaid, A.M. Ghrair, M. Al-Busoul, Experimental investigation of cooling photovoltaic (PV) panels using (TiO2) nanofluid in water -polyethylene glycol mixture and (Al2O3) nanofluid in water- cetyltrimethylammonium bromide mixture, Energy Conversion and Management, 155 (2018) 324-343.

[203] G.M. Son, K.M. Kim, I.C. Bang, Chromia coating with nanofluid deposition and sputtering for accident tolerance, CHF enhancement, International Journal of Heat and Mass Transfer, 118 (2018) 890-899.

[204] S. Hoseinzadeh, Heyns, P. and Kariman, H., Numerical investigation of heat transfer of laminar and turbulent pulsating Al_2O_3/water nanofluid flow, International Journal of Numerical Methods for Heat & Fluid Flow, ahead-of-print (2019).

[205] Y. Khanjari, F. Pourfayaz, A. Kasaeian, Numerical investigation on using of nanofluid in a water-cooled photovoltaic thermal system, Energy Conversion and Management, 122 (2016) 263-278.

[206] M. Sardarabadi, M. Passandideh-Fard, Experimental and numerical study of metal-oxides/water nanofluids as coolant in photovoltaic thermal systems (PVT), Solar Energy Materials and Solar Cells, 157 (2016) 533-542.

[207] G.D. Nicola, F. Mandorli, G. Coccia, Design, Manufacturing, Testing, and Mathematical Modeling of Concentrating Solar Systems: a Study Applied to Prototypes of Parabolic Trough Collector and Solar Box cooker, Marche Polytechnic University, Italy, 2016.

[208] T. Yousefi, F. Veysi, E. Shojaeizadeh, S. Zinadini, An experimental investigation on the effect of Al2O3–H2O nanofluid on the efficiency of flat-plate solar collectors, Renewable Energy, 39(1) (2012) 293-298.

[209] J.J. Michael, S. Iniyan, R. Goic, Flat plate solar photovoltaic–thermal (PV/T) systems: a reference guide, Renewable and Sustainable Energy Reviews, 51 (2015) 62-88.

[210] Z. Said, M.A. Sabiha, R. Saidur, A. Hepbasli, N.A. Rahim, S. Mekhilef, T.A. Ward, Performance enhancement of a Flat Plate Solar collector using Titanium dioxide nanofluid and Polyethylene Glycol dispersant, Journal of Cleaner Production, 92 (2015) 343-353.

[211] S.K. Verma, A.K. Tiwari, D.S. Chauhan, Performance augmentation in flat plate solar collector using MgO/water nanofluid, Energy Conversion and Management, 124 (2016) 607-617.

[212] Z. Said, R. Saidur, N.A. Rahim, Energy and exergy analysis of a flat plate solar collector using different sizes of aluminium oxide based nanofluid, Journal of Cleaner Production, 133 (2016) 518-530.

[213] A.H. Al-Waeli, K. Sopian, H.A. Kazem, J.H. Yousif, M.T. Chaichan, A. Ibrahim, S. Mat, M.H. Ruslan, Comparison of prediction methods of PV/T nanofluid and nano-PCM system using a measured dataset and Artificial Neural Network, Solar Energy, 162 (2018) 378-396.

[214] G. Coccia, G. Latini, M. Sotte, Mathematical modeling of a prototype of parabolic trough solar collector, Journal of Renewable and sustainable energy, 4(2) (2012) 023110.

[215] M.N. Rashin, J. Hemalatha, A novel ultrasonic approach to determine thermal conductivity in CuO–ethylene glycol nanofluids, Journal of Molecular Liquids, 197 (2014) 257-262.

[216] B.A.J. Rose, H. Singh, N. Verma, S. Tassou, S. Suresh, N. Anantharaman, D. Mariotti, P. Maguire, Investigations into nanofluids as direct solar radiation collectors, Solar Energy, 147 (2017) 426-431.

[217] S. khosrojerdi, A.M. Lavasani, M. Vakili, Experimental study of photothermal specifications and stability of graphene oxide nanoplatelets nanofluid as working fluid for low-temperature Direct Absorption Solar Collectors (DASCs), Solar Energy Materials and Solar Cells, 164 (2017) 32-39.

[218] Suleiman Akilu, Aklilu Tesfamichael Baheta, Mior Azman M.Said, Alina Adriana Minea, K.V. Sharma, Properties of glycerol and ethylene glycol mixture based SiO2-CuO/C hybrid nanofluid for enhanced solar energy transport, Solar Energy Materials and Solar Cells, 179 (2018) 118-128.

[219] A. Kasaeian, R. Daneshazarian, R. Rezaei, F. Pourfayaz, G. Kasaeian, Experimental investigation on the thermal behavior of nanofluid direct absorption in a trough collector, Journal of Cleaner Production, 158 (2017) 276-284.

[220] SomayehToghyani, EhsanBaniasadi, EbrahimAfshari, Thermodynamic analysis and optimization of an integrated Rankine power cycle and nano-fluid based parabolic trough solar collector, Energy Conversion and Management, 121 (2016) 93-104.

[221] M.X. Ho, C. Pan, Experimental investigation of heat transfer performance of molten HITEC salt flow with alumina nanoparticles, International Journal of Heat and Mass Transfer, 107 (2017) 1094-1103.

[222] Yathin Krishna, R. Saidur, M. Faizal, Navid Aslfattahi, K.C. Ng, A. Arifutzzaman, Effect of Al_2O_3 dispersion on Enthalpy And Thermal Stability of Ternary Nitrate Eutectic Salt, International Jounal of Nanoelectronics and Materials, (2019).

[223] M. Chieruzzi, J. Kenny, A. Miliozzi, Studio e sviluppo di un mezzo di accumulo a calore latente a media temperatura (200-400 C) costituito da una miscela di sali e nanoparticelle, 2013.

[224] D. Shin, Molten salt nanomaterials for thermal energy storage and concentrated solar power applications, Texas A & M University, Texas, 2012.

[225] D. Shin, D. Banerjee, Enhanced specific heat capacity of molten salt-metal oxide nanofluid as heat transfer fluid for solar thermal applications, 0148-7191, SAE Technical Paper, 2010.

[226] D. Shin, D. Banerjee, Specific heat of nanofluids synthesized by dispersing alumina nanoparticles in alkali salt eutectic, International Journal of Heat and Mass Transfer, 74 (2014) 210-214.

[227] H. Tiznobaik, D. Banerjee, D. Shin, Effect of formation of “long range” secondary dendritic nanostructures in molten salt nanofluids on the values of specific heat capacity, International Journal of Heat and Mass Transfer, 91 (2015) 342-346.

[228] S. Jung, Numerical and experimental investigation of inorganic nanomaterials for thermal energy storage (TES) and concentrated solar power (CSP) applications, Texas A & M University, 2012.

[229] Bharath Dudda, Donghyun Shin, Effect of nanoparticle dispersion on specific heat capacity of a binary nitrate salt eutectic for concentrated solar power applications, International Journal of Thermal Sciences, 69 (2013) 37-42.

[230] J. Seo, D. Shin, Enhancement of specific heat of ternary nitrate (LiNO3-NaNO3-KNO3) salt by doping with SiO2 nanoparticles for solar thermal energy storage, Micro & Nano Letters, 9(11) (2014) 817-820.

[231] S. Changla, Experimental study of quaternary nitrate/nitrite molten salt as advanced heat transfer fluid and energy storage material in concentrated solar power plant, University of Texas Arlington, United States, 2015.

[232] V. Somani, Colloidal stability of magnetic nanoparticles in molten salts, Massachusetts Institute of Technology, Massachusetts, US, 2010.

[233] M.W. Thoms, Adsorption at the nanoparticle interface for increased thermal capacity in solar thermal systems, Massachusetts Institute of Technology, Massachusetts, US, 2012.

[234] Judith C. Gomez, Nicolas Calvet, Anne K. Starace, Greg C. Glatzmaier, Ca (NO3) 2—NaNO3—KNO3 Molten Salt Mixtures for Direct Thermal Energy Storage Systems in Parabolic Trough Plants, Journal of solar energy engineering, 135(2) (2013) 8.

[235] P. Gimenez, S. Fereres, Effect of Heating Rates and Composition on the Thermal Decomposition of Nitrate Based Molten Salts, Energy Procedia, 69 (2015) 654-662.

[236] D. Zhou, P. Eames, A study of a eutectic salt of lithium nitrate and sodium chloride (87–13%) for latent heat storage, Solar Energy Materials and Solar Cells, 167 (2017) 157-161.

[237] Y. Xiong, Z. Wang, P. Xu, C. Hongbing, Y. Wu, Experimental investigation into the thermos-physical properties by dispersing nanoparticles to the nitrates, Energy Procedia, 158 (2019) 5551-5556.

[238] R.I. Olivares, W. Edwards, LiNO3–NaNO3–KNO3 salt for thermal energy storage: Thermal stability evaluation in different atmospheres, Thermochimica Acta, 560 (2013) 34-42.

[239] P.K. Nagarajan, J. Subramani, S. Suyambazhahan, R. Sathyamurthy, Nanofluids for solar collector applications: A Review, in: The 6th International Conference on Applied Energy – ICAE2014, 2014, pp. 2416 – 2434.

[240] T.K. Tullius, Y. Bayazitoglu, Analysis of a hybrid nanofluid exposed to radiation, Numerical Heat Transfer, Part B: Fundamentals, 69(4) (2016) 271-286.

[241] N. Chen, H. Ma, Y. Li, J. Cheng, C. Zhang, D. Wu, H. Zhu, Complementary optical absorption and enhanced solar thermal conversion of CuO-ATO nanofluids, Solar Energy Materials and Solar Cells, 162 (2017) 83-92.

[242] J. Fang, Y. Xuan, Investigation of optical absorption and photothermal conversion characteristics of binary CuO/ZnO nanofluids, RSC Advances, 7(88) (2017) 56023-56033.

[243] P. Good, G. Zanganeh, G. Ambrosetti, M.C. Barbato, A. Pedretti, A. Steinfeld, Towards a Commercial Parabolic Trough CSP System Using Air as Heat Transfer Fluid, Energy Procedia, 49 (2014) 381-385.

[244] F.A. Al-Sulaiman, M.I. Zubair, M. Atif, P. Gandhidasan, S.A. Al-Dini, M.A. Antar, Humidification dehumidification desalination system using parabolic trough solar air collector, Applied Thermal Engineering, 75 (2015) 809-816.

[245] A. Energy, Ait-Baha CSP power plant, in, Biasca Switzerland, 2015.

[246] M. Biencinto, L. González, L. Valenzuela, E. Zarza, A new concept of solar thermal power plants with large-aperture parabolic-trough collectors and sCO2 as working fluid, Energy Conversion and Management, 199 (2019) 112030.

[247] M.K. Islam, M. Hasanuzzaman, N.A. Rahim, Modelling and analysis of the effect of different parameters on a parabolic-trough concentrating solar system, RSC Advances, 5(46) (2015) 36540-36546.

[248] R. Vutukuru, A.S. Pegallapati, R. Maddali, Suitability of various heat transfer fluids for high temperature solar thermal systems, Applied Thermal Engineering, 159 (2019) 113973.

[249] A. Fritsch, C. Frantz, R. Uhlig, Techno-economic analysis of solar thermal power plants using liquid sodium as heat transfer fluid, Solar Energy, 177 (2019) 155-162.

[250] J. Pacio, C. Singer, T. Wetzel, R. Uhlig, Thermodynamic evaluation of liquid metals as heat transfer fluids in concentrated solar power plants, Applied Thermal Engineering, 60(1) (2013) 295-302.

[251] M.M. Sarafraz, M. Arjomandi, Demonstration of plausible application of gallium nano-suspension in microchannel solar thermal receiver: Experimental assessment of thermo-hydraulic performance of microchannel, International Communications in Heat and Mass Transfer, 94 (2018) 39-46.

[252] M.M. Sarafraz, M. Arjomandi, Thermal performance analysis of a microchannel heat sink cooling with copper oxide-indium (CuO/In) nano-suspensions at high-temperatures, Applied Thermal Engineering, 137 (2018) 700-709.

[253] T.C. Paul, A.M. Morshed, J.A. Khan, Nanoparticle Enhanced Ionic Liquids (NEILS) as working fluid for the next generation solar collector, Procedia Engineering, 56 (2013) 631-636.

[254] G.F. Annat, Maria MacFarlane, Douglas R, Ionic Liquid Mixtures Variations in Physical Properties and Their Origins in Molecular Structure, The Journal of Physical Chemistry B, 116(28) (2012) 8251-8258.

[255] M. Zistler, P. Wachter, C. Schreiner, M. Fleischmann, D. Gerhard, P. Wasserscheid, A. Hinsch, H. Gores, Temperature dependent impedance analysis of binary ionic liquid electrolytes for dye-sensitized solar cells, Journal of The Electrochemical Society, 154(9) (2007) B925-B930.

[256] I. Mohammadpoor-Baltork, A.R. Khosropour, S.F. Hojati, A novel and chemoselective synthesis of 2-aryloxazolines and bis-oxazolines catalyzed by Bi (III) salts, Synlett, 2005(18) (2005) 2747-2750.

[257] A. Finotello, J.E. Bara, S. Narayan, D. Camper, R.D. Noble, Ideal gas solubilities and solubility selectivities in a binary mixture of room-temperature ionic liquids, The Journal of Physical Chemistry B, 112(8) (2008) 2335-2339.

[258] Q.Q. Baltazar, S.K. Leininger, J.L. Anderson, Binary ionic liquid mixtures as gas chromatography stationary phases for improving the separation selectivity of alcohols and aromatic compounds, Journal of Chromatography A, 1182(1) (2008) 119-127.

[259] M. Kunze, S. Jeong, E. Paillard, M. Winter, S. Passerini, Melting behavior of pyrrolidinium-based ionic liquids and their binary mixtures, The Journal of Physical Chemistry C, 114(28) (2010) 12364-12369.

[260] T.L. Greaves, D.F. Kennedy, A. Weerawardena, N.M. Tse, N. Kirby, C.J. Drummond, Nanostructured protic ionic liquids retain nanoscale features in aqueous solution while

precursor Brønsted acids and bases exhibit different behavior, The Journal of Physical Chemistry B, 115(9) (2011) 2055-2066.

[261] F. Llovell, E. Valente, O. Vilaseca, L. Vega, Modeling complex associating mixtures with [C n-mim][Tf2N] ionic liquids: Predictions from the soft-SAFT equation, The Journal of Physical Chemistry B, 115(15) (2011) 4387-4398.

[262] A. Stoppa, R. Buchner, G. Hefter, How ideal are binary mixtures of room-temperature ionic liquids?, Journal of Molecular Liquids, 153(1) (2010) 46-51.

[263] J.N. Canongia Lopes, T.C. Cordeiro, J.M. Esperança, H.J. Guedes, S. Huq, L.P. Rebelo, K.R. Seddon, Deviations from ideality in mixtures of two ionic liquids containing a common ion, The Journal of Physical Chemistry B, 109(8) (2005) 3519-3525.

[264] K.A. Fletcher, S.N. Baker, G.A. Baker, S. Pandey, Probing solute and solvent interactions within binary ionic liquid mixtures, New Journal of Chemistry, 27(12) (2003) 1706-1712.

[265] D. Xiao, J.R. Rajian, S. Li, R.A. Bartsch, E.L. Quitevis, Additivity in the optical Kerr effect spectra of binary ionic liquid mixtures: Implications for nanostructural organization, The Journal of Physical Chemistry B, 110(33) (2006) 16174-16178.

[266] B. Wu, R. Reddy, R. Rogers, Novel ionic liquid thermal storage for solar thermal electric power systems, in: Proceedings of Solar Forum 2001 Solar, 2001, pp. 445-452.

[267] L. Moens, D.M. Blake, Advanced heat transfer and thermal storage fluids, in: ASME 2005 International Solar Energy Conference, American Society of Mechanical Engineers Digital Collection, 2008, pp. 791-793.

[268] M. Eck, K. Hennecke, Heat transfer fluids for future parabolic trough solar thermal power plants, in: Proceedings of ISES World Congress 2007 (Vol. I–Vol. V), Springer, 2008, pp. 1806-1812.

[269] T.C. Paul, A. Morshed, E.B. Fox, J.A. Khan, Thermal performance of Al2O3 nanoparticle enhanced ionic liquids (NEILs) for concentrated solar power (CSP) applications, International Journal of Heat and Mass Transfer, 85 (2015) 585-594.

[270] N.J. Bridges, A.E. Visser, E.B. Fox, Potential of nanoparticle-enhanced ionic liquids (NEILs) as advanced heat-transfer fluids, Energy & Fuels, 25(10) (2011) 4862-4864.

[271] C. Nieto de Castro, M. Lourenço, A. Ribeiro, E. Langa, S. Vieira, P. Goodrich, C. Hardacre, Thermal properties of ionic liquids and ionanofluids of imidazolium and pyrrolidinium liquids, Journal of Chemical & Engineering Data, 55(2) (2009) 653-661.

[272] A. Wittmar, D. Ruiz-Abad, M. Ulbricht, Dispersions of silica nanoparticles in ionic liquids investigated with advanced rheology, Journal of Nanoparticle Research, 14(2) (2012) 651.

[273] B. Wang, X. Wang, W. Lou, J. Hao, Ionic liquid-based stable nanofluids containing gold nanoparticles, Journal of colloid and interface science, 362(1) (2011) 5-14.

[274] I. Perissi, U. Bardi, S. Caporali, A. Fossati, A. Lavacchi, Ionic liquids as diathermic fluids for solar trough collectors' technology: A corrosion study, Solar Energy Materials and Solar Cells, 92(4) (2008) 510-517.

[275] J. Liu, Z. Ye, L. Zhang, X. Fang, Z. Zhang, A combined numerical and experimental study on graphene/ionic liquid nanofluid based direct absorption solar collector, Solar Energy Materials and Solar Cells, 136 (2015) 177-186.

[276] L. Zhang, J. Liu, G. He, Z. Ye, X. Fang, Z. Zhang, Radiative properties of ionic liquid-based nanofluids for medium-to-high-temperature direct absorption solar collectors, Solar Energy Materials and Solar Cells, 130 (2014) 521-528.

[277] G. Pikra, A. Salim, B. Prawara, A.J. Purwanto, T. Admono, Z. Eddy, Development of Small Scale Concentrated Solar Power Plant Using Organic Rankine Cycle for Isolated Region in Indonesia, Energy Procedia, 32 (2013) 122-128.

[278] J.F. Hoffmann, G. Vaitilingom, J.F. Henry, M. Chirtoc, R. Olives, V. Goetz, X. Py, Temperature dependence of thermophysical and rheological properties of seven vegetable oils in view of their use as heat transfer fluids in concentrated solar plants, Solar Energy Materials and Solar Cells, 178 (2018) 129-138.

[279] C.E. Tyner, G.J. Kolb, M. Geyer, M. Romero, Concentrating solar power in 2001, An IEA/SolarPACES Summary of present status and future prospects. SolarPACES Task I: Electric Power Systems, (2001).

[280] G. Kolb, C. Tyner, Solar thermal electricity, in: IEA Workshop on the Mitigation of Greenhouse Gas Emissions, 1997, pp. 15-16.

[281] A. Riahi, A. Ben Haj Ali, A. Fadhel, A. Guizani, M. Balghouthi, Performance investigation of a concentrating photovoltaic thermal hybrid solar system combined with thermoelectric generators, Energy Conversion and Management, 205 (2020) 112377.

[282] C.J. Winter, R.L.Sizmann, L.L.V.-H. (Eds.), Solar Power plants, Springer-Verlag, Berlin, Germany, Germany, 1991.

[283] T. Wilberforce, A. Baroutaji, Z. El Hassan, J. Thompson, B. Soudan, A.G. Olabi, Prospects and challenges of concentrated solar photovoltaics and enhanced geothermal energy technologies, Science of The Total Environment, 659 (2019) 851-861.